An enhanced sensor-based approach for evaluation of a geriatric fall risk in non-ambulatory environments

Zur Erlangung des akademischen Grades eines

DOKTOR-INGENIEURS

von der Fakultät für
Elektrotechnik und Informationstechnik
des Karlsruher Institut für Technologie (KIT)
genehmigte

DISSERTATION

von

M.Sc. Tomislav Pozaić

geb. in: Zagreb, Kroatien

Tag der mündlichen Prüfung: 11. Mai 2017
Hauptreferent: Prof. Dr. rer. nat. Wilhelm Stork
Korreferent: Prof. Dr. med. Clemens Becker

Stuttgart, den 23. März, 2017

An enhanced sensor-based approach for evaluation of a geriatric fall risk in non-ambulatory environments

by
Tomislav Pozaić

Declaration

I hereby declare that I wrote my doctoral dissertation on my own and that I have followed the regulations relating to good scientific practice of the Karlsruhe Institute of Technology (KIT) in its latest form. I have not used any unacknowledged sources or means and I have marked all references I used literally or by content. This work has not previously been presented in an identical or similar form to any other university or examination board.

Stuttgart, 23rd March 2017

_____

Tomislav Pozaić

Abstract

One third of population aged over 65 experience falls each year. Falls are major cause of middle to severe injuries becoming an enormous burden for the healthcare system. Timely accurate assessment of the fall risk in a widely accepted and non-stigmatized manner has the ability to provide crucial changes in the fall prevention strategies, thus possibly reducing the number of fallers, as well as their fall rate. Current clinical evaluation of the fall risk is time consuming and subjective, whereas assessments in non-ambulatory settings are obtrusive or focused on singular periodical aspects of human movement.

The focus of this thesis is on investigation and definition of novel concepts targeting assessment of inter-limb coordination, gait and sit-to-stand transitions by means of inertial and environmental wrist-attached sensors. Time- and frequency-domain hand-crafted features were used for deriving support vector machine based models describing one's physical performance in terms of an objective (quantitative) fall risk assessment in noisy perturbation-prone home settings.

An exploratory study on 28 elderly participants in a controlled setting was conducted for observational purposes. On top of that, a large cross-sectional study on a cohort of 180 participants with a six months follow-up phase was performed for the validation of developed models.

The results have yielded a novel acute fall risk predictor. Additionally, the importance of an environmental context for understanding of one's motor performance was presented. An innovative real-time algorithm for fusion of a multi-sensor approach and movement-based filters was proposed and influence of the hand-side-dependence on its performance was investigated. Validation of developed models for all three domains against the ground truth has shown clinically relevant accuracy comparable, or even partially better than obtrusive state-of-the-art.

The study overcomes limitations of clinical tests and shows a reliable application of wrist bands in terms of both, highly acute and conventional six-months based fall risk assessment. Moreover, it reveals wrist as a potential assessment source in the geriatric population.

Kurzfassung

Jedes Jahr stürzt rund ein Drittel der über 65 Jährigen. Stürze sind die Hauptursache für mittlere bis schwere Verletzungen und damit eine enorme Belastung für das Gesundheitssystem. Eine zeitlich akkurate Sturzrisikobewertung in einer breit akzeptierten und nicht-stigmatisierenden Art und Weise kann zu signifikanten Veränderungen in der Strategie der Sturzprävention führen und damit dazu beitragen, die Anzahl der stürzenden Personen, sowie die Sturzrate zu reduzieren.

Die gegenwärtige klinische Evaluierung des Sturzrisikos ist zeitaufwendig und subjektiv. Folglich sind Bewertungen in stationärem Umfeld obstruktiv, oder fokussieren sich ausschließlich auf einmalige, periodische Merkmale der menschlichen Bewegung. Der Fokus dieser Arbeit liegt in der Erforschung und Definition neuer Konzepte zur Beurteilung der Koordination der Extremitäten, der Art des Gehens und der Aufstehvorgänge anhand von Signalen von am Handgelenk getragener Inertial- und Umgebungssensorik. Merkmale im Zeit- und Frequenzraum wurden händisch entwickelt, um daraus Support Vector Maschine -Modelle abzuleiten. Die Modelle beschreiben die physikalische Leistungsfähigkeit einer Person in Form einer objektiven (quantitativen) Sturzrisikobewertung in einem störungsanfälligen häuslichen Umfeld.

Für erste Untersuchungszwecke wurde eine Forschungsstudie mit 28 älteren Teilnehmern in einem kontrollierten Umfeld durchgeführt. Darauf aufsetzend wurde eine große Querschnittsstudie mit einer Kohorte von 180 Probanden durchgeführt. Eine sich der Messwoche anschließende sechsmonatige Nachverfolgungsphase wurde zur Validierung der Modelle in die Studie inkludiert. Die Ergebnisse haben einen neuen Prädiktor für akutes Sturzrisiko hervorgebracht. Zusätzlich konnte aufgezeigt werden, dass die Kenntnis der Umgebungsbedingungen relevant sind, um die menschlichen Bewegungen richtig bewerten zu können.

Ein innovativer Echtzeitalgorithmus wurde entwickelt, in dem Multi-Sensor-Ansätze fusioniert, sowie auf Bewegung basierende Filter integriert sind. Die Einflüsse der Hand-Abhängigkeit auf die Leistungsfähigkeit des Algorithmus konnten im Rahmen dieser Arbeit untersucht werden. Die Validierung der entwickelten Modelle in allen drei Domänen gegen die Grundwahrheit zeigt eine klinisch relevante Genauigkeit oder zumindest teilweise bessere Ergebnisse gegenüber dem Stand der Technik.

Die Studie zeigt die Möglichkeit auf, Einschränkungen klinischer Tests zu bewältigen, sowie in Armbändern integrierte Sensorik sowohl für eine akute, wie auch eine konventionelle Sechsmontasbewertung des Sturzrisikos verlässlich anzuwenden.

Content

List of figures

List of tables

List of abbreviations

FRA	Fall Risk Assessment
STST	Sit-To-Stand Transition
RBK	Robert-Bosch-Krankenhaus (Robert-Bosch-Hospital)
IC	Inter-limb Coordination index
YC	Ipsilateral Coordination index
CC	Contralateral Coordination index
SPV	Swing Phase Time Variability
STV	Step Time Variability
SVM	Support Vector Machine
RBF	Radial Basis Function kernel
ADL	Activities of Daily Living
FRAQ	Fall Risk Assessment Questionnaire
FRAT-up	Fall Risk Assessment Tool
SOMC	Short-Orientation-Memory-Concentration test
GDS	Geriatric Depression Scale
VT	Vertical (Superior-Inferior)
ML	Medial-Lateral
AP	Anterior-Posterior
TTFS	Time to First Swing
AFS	Amplitude of the First Swing
AS	Amount of applied Support
AO	Amount of Oscillation

RMS	Root Mean Square
SD	Standard Deviation
95% CI	95% Confidence Interval
ROC	Receiver Operating Curve
AUC	Area Under Curve
SEE	Standard Error of Estimation
ICC	Intra-class Correlation Coefficient
IH	Index of Harmonicity
FF	Fundamental Frequency
STW	Sit To Walk
STSP	Sit To Stand Passive
STSA	Sit To Stand Active
BLE	Bluetooth Low Energy
RTC	Real Time Clock
CV	Cross Validation
FP	False Positive
TP	True Positive
TN	True Negative
FN	False Negative
F1-score	A measure of model's accuracy
PPV	Positive Predictive Value
NPV	Negative Predictive Value
SM	Signal vector Magnitude

HS_R	Heel Strike Right
HS_L	Heel Strike Left
SWT	Swing Phase Time
STT	Stance Phase Time
FF_R	Flat Foot Right
FF_L	Flat Foot Left
PPA	Psychological Profile Approach
TUG	Timed-Up-And-Go test
PD	Parkinson's Disease
MEMS	Microelectromechanical Systems

Preface

Looking back, more than three years ago when I packed my things, sat in my father's car and took, now already well-known and always crowded highway to Stuttgart, I have never believed that this could be a start of such an amazing journey. However, this journey would have never been possible without two most important persons in my life – my parents, whose constant unconditional support has been always an inexhaustible spring of motivation for me in good and bad times. To them, I will never be able to be grateful enough.

In the past three years I have also met an incredible number of amazing people, of whom many became my good friends and colleagues. I won't mention them all here, since I could forget someone but they all know who they are so thank you guys for everything. Hence, one name I can't forget – Kathrin Graner, simply thank you for being always there for me.

On this journey, I think I have learnt a lot, not just about my complex research topics, but also about life. When talking about life, I would like to thank two persons that were and still are my role models – my university supervisor in Zagreb, Croatia and now my friend Prof. Dr. Ratko Magjarević and my company supervisor Dr. Ulrich Ladstätter. You marked my career path significantly. From the very beginning to the end of my journey constant support of my PhD supervisors, Prof. Dr. rer. nat. Wilhelm Stork and Prof. Dr. med. Clemens Becker, was a faithful and wise companion. Thank you!

In the end, before the thesis indeed starts, I would just like to quote a king of rock, Elvis Presley – let's rock!

Stuttgart, March 2017

Tomislav Pozaić

1 Introduction

1.1 Motivation

Back then, somewhere in 2004, Cuba was a beautiful country and Fidel Castro was only 78. He had just finished with one of his several hours long speeches when going down the staircase from the stage he missed one stair, fell forwards and broke his knee and arm. Just recently, former 70 years old USA president George H. W. Bush, has fallen again and stayed hospitalized this time despite his fair condition. A fall can fairly end fatally. In 2013, a 71 year old co-founder of the political party "Die Linken", Lothar Bisky, died after a fall in his own house. These prominent examples around the world, just few of countless of them, are targeting the core motivation of the thesis – falls: occurrence, source and finally, measures to predict them.

What do these three famous politicians have in common? They are carefully guarded by numerous security agents, their medical conditions are probably cautiously monitored by geriatricians but yet they all managed to injure themselves and caused additional costs for already overloaded healthcare systems. A moment of negligence together with slight incoordination of limbs or infinitesimally small perturbations in kinematics have led to the loss of balance and finally to a fall. A combination of latterly mentioned motor parameters or their solely influence on one's physical performance is critical to understand, in order to predict these situations.

Above mentioned gentlemen, despite their active lifestyle, can be classified as elderly. Falls in this vulnerable geriatric population are everyday life. Real life has shown that one in every three adults aged over 65 falls each year (Tinetti, 1988) and fall risk increases with age (Masud, 2001). Falls are major cause for moderate to severe injuries with almost 10% of them calling for a hospitalization and immediate medical attention.

Furthermore, they are the fifth leading cause of death right after cardiovascular diseases, cancer, stroke and respiratory diseases (Deandrea, 2010).

The given figures are even more astounding when considering the current population and trends that it follows. At the moment, 21.7% of population in Germany is aged over 65, whereas this trend of aging will continue moving forward significantly so the predictions for 2050 estimate 32.7% of population aged over 65 (DESA, 2013). For comparison, in 1950 only 9.6% of population was over this threshold.

From the economical perspective, each fall that ends with a hospitalization costs the healthcare system € 32000 on average (Stevens, 2006). Additionally to these direct costs, the burden that falls, i.e. fractures, and corresponding rehabilitation period cause not only to affected persons but also to their families and surroundings should be taken into consideration. Only for the geriatric population total healthcare costs in Germany in 2007 were € 117.5 billion (or 47.9% of total healthcare costs) (Federal Office of Statistics, 2007). Although the solely fall-related figures for Germany were not publicly available, these costs in USA in 2013 account for € 30.6 billion (CDC, 2015).

One half of all falls are recurrent (Tinetti, 2003), which is besides the injury and long-term mobility constraints terrifying for the affected people. Falls, especially recurrent ones, can additionally lead to reduced physical activity and consequently fear of falling (Hausdorff, 2001). Loss of self-confidence in own capabilities and fear of falling further cause depression and social isolation (Biderman, 2002). Health-related quality of life suffers significantly in these cases as well.

The enormous figures shown above, huge social influence and wide spread of these worryingly devastating events are more than needed for a motivation for a research work on this topic. Solutions for fall prevention exist and only a small piece of a puzzle is still missing. Namely, the number of fallers (people that have fallen), as well as the fall rate can be reduced significantly by applying different fall prevention strategies

(such as strength and balance trainings, drug modifications or environment corrections). The crucial step is the timely correct identifications of subjects at increased risk of falling. Developed clinical fall screening tools are rarely used spontaneously in hospitals and are rather just part of a bigger assessment process, so information about one's risk of falling is mostly hidden till the point of time when it is already too late. The need for clinically relevant assessment of the fall risk calls for an objective continuous evaluation of one's physical performance in personal home setting and in a highly unobtrusive non-stigmatized manner (i.e. at the wrist).

1.2 Research questions

Motivation summed up in the last paragraph of chapter 1.1 leads to three crucial research questions that will be answered within this thesis. When formulating these questions, state-of-the-art findings were taken into consideration in addition to desired user-motivated outcomes. By fusion of latter mentioned methods, it is possible to focus on highly relevant research results, without losing the focus of the user experience, a subjective matter that indeed enables real-life applications and suitable reliable use of the proposed novel approach.

The research questions in the thesis deal with concepts, implementation and validation of models for assessment of the fall risk in geriatric population during activities of daily living (ADL). Recent clinical findings about the fall risk from the epidemiological and observational studies (such as epidemiological study of Rapp, 2012) identified most significant fall risk factors in daily life. Many further studies (please refer to chapter 2 for more details) confirmed these findings in the controlled laboratory environment, but without actual translation into the home setting, particularly due to lack of algorithm robustness or inappropriate and inadequate system configuration.

The thesis creates and implements concepts for quantitative assessment of inter-limb coordination, gait and sit-to-stand transitions (STST) in

non-ambulatory settings and in terms of fall risk assessment (FRA) by using a synchronized multi-sensor approach. Thus, the first research question tangents existing approaches for assessment of these domains by challenging them in terms of the number of sensor nodes and their positions. More precisely, focus of the first step is on finding novel robust methods targeting these three research domains that could maintain high reliability and precision but with significantly reduced information flow (i.e. sensor reduction) and in the marginal performance (i.e. assessment of non-recurrent movements in ADL, such as STST, at the wrist).

The second question broadens the current perspective of assessment of one's physical performance by means of inertial sensors. It addresses the environmental context as an added value to the solely assessment of motor functioning and examines the advantages, as well as possible limitations of such approach. Investigation of possible limitations is crucial to understand also the possible further applications of environmental sensors in wearables for clinically relevant use cases, since current research mostly neglected this opportunity.

Finally, the third question focuses on fusion of the extracted quantitative information into models that could reliably identify subjects at risk of falling. The process includes an iterative selection of the best quantitative parameters for each of the three mentioned domains, investigation of the best combination of these parameters and finally finding the means that would relate selected parameters to the ground truth for each subject. The thesis addresses habitual, commonly defined, groups in the FRA (please refer to chapter 3 for more information), but it also broadens the spectrum to acute FRA, i.e. identification of distinguished subjects at high risk of falling (acute fallers). This enables on-the-spot comparison of different groups, and it can further potentially offer clinicians additional tool for addressing this acute problem.

1.3 Research approach

In the thesis, an abductive iterative research approach devoted to explanation of incomplete hypothesis in terms of quantitative measures was applied. Namely, since existing theory about one's physical performance in terms of the FRA reaches either to conventional clinically-based methods or methods relying on assessment of logical and meaningful points (e.g. centre of mass), there is a gap to acceptance of unconfirmed methods for this use case. Furthermore, it is not clear whether the same or similar approaches could be used in the proposed non-stigmatized manner.

Thus, the set hypotheses based on the conventional findings (explained in the chapter 1.2) were firstly confirmed in a cross-sectional exploratory study within the controlled environment (explained in the chapter 3). This step ensured an iterative evaluation and adaptation of methods that are mathematically described throughout the chapter 5. It is not an intention of this step to serve as a reference compilation of the FRA techniques, however an intensive effort has been made to include a comprehensive overview of possible methods for novel assessment of motor performance and their positioning among state-of-the-art findings.

Identified methods, i.e. quantitative parameters (features), were further validated on a large-scale data sets. For these purposes another independent cross-sectional study on a large geriatric cohort (chapter 3) was performed. Validation of extracted features for defined groups, as well as definition of comprehensive models in terms of FRA was conducted (chapter 6).

Experimental results are discussed in the chapter 7. The discussion is focused on the limitation of implemented methods and applied efforts in overcoming the constraints of the proposed system design (models). Performance evaluation measures which affect the usability of the system such as robustness and uniqueness are elaborated here as well. Scientific contribution and conclusion are given in chapters 8 and 9, respectively.

2 Related work

2.1 Falls in the elderly population

Falls in the elderly population appear as a dominant hazard due to their high incidence and susceptibility to injuries, especially increased with age and frailty. They are a leading cause for disabilities in older adults, despite the fact that up to 40% of them could have been prevented (Sherrington, 2008). As previously mentioned, one in every three adults aged over 65 falls each years. In the literature, people that have fallen are often referred to as fallers (Prudham, 1981). Even more concerning than the number of fallers is the fall rate, i.e. number of falls per year. Namely, half of these fallers above 65, fall more than once per year (also called recurrent fallers) (Blake, 1988 and Graafmans, 1996). Furthermore, persons in residential care and nursing homes fall two to three times more often than community-dwelling older adults (Luukinen, 1994 and Milat, 2011). An overview of fall rates (number of falls per 100.000 population) for 5-years intervals can be seen in the Figure 1.

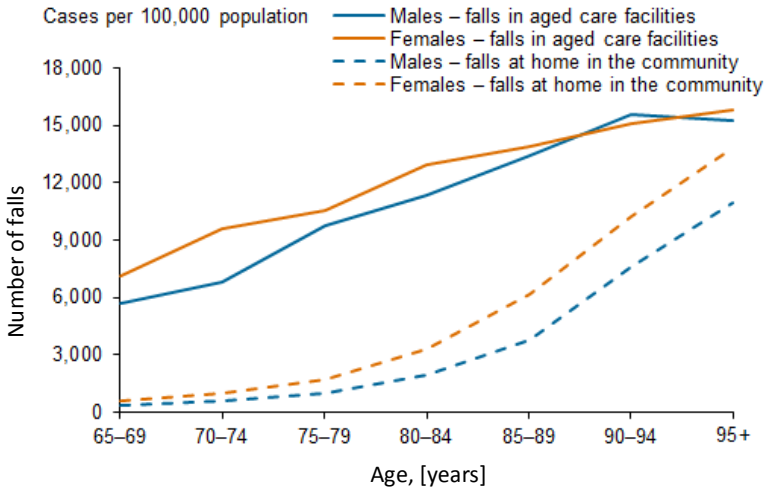

Source: Australian Institute of Health and Welfare, 2011

Figure 1 Fall rates in the elderly population

The definition of falls and their clinical relevance is a topic of many ongoing debates and varies throughout the literature. A general consensus about a definition of a fall is highly important as many studies fail to specify an operational definition, leaving room for interpretation to study participants and thus directly influencing the gold standard for the faller identification. Older people tend to describe a fall as a loss of balance, whereas health care professionals generally refer to events leading to injuries and ill health (Zecevic, 2006). In this thesis, a fall was defined as a non-intentional unexpected event in which one's body comes to rest on the ground, floor or lower level including events occurred by tripping over an obstacle or slipping due to various environmental conditions (indoor, as well as outdoor) (Hauer, 2006).

Devastating economical (rising costs in a continuously aging society), physical (middle to severe injuries such as hip fracture, bruises or head injuries) and physiological consequences (social isolation, depression, decline in physical activity) of falls were already addressed in the chapter 1.1. Falls-related injuries account for 40% of all injury deaths. Fall mortality rates vary depending on the country, age and sex (e.g. in USA they are 36.8 per 100.000 population aged above 65). In the Figure 2 the mortality rates are shown in a 5-years interval for men and women. The projected boost fall-related problems listed in this paragraph is expected to rise up to 100% by 2030 (Kannus, 2007).

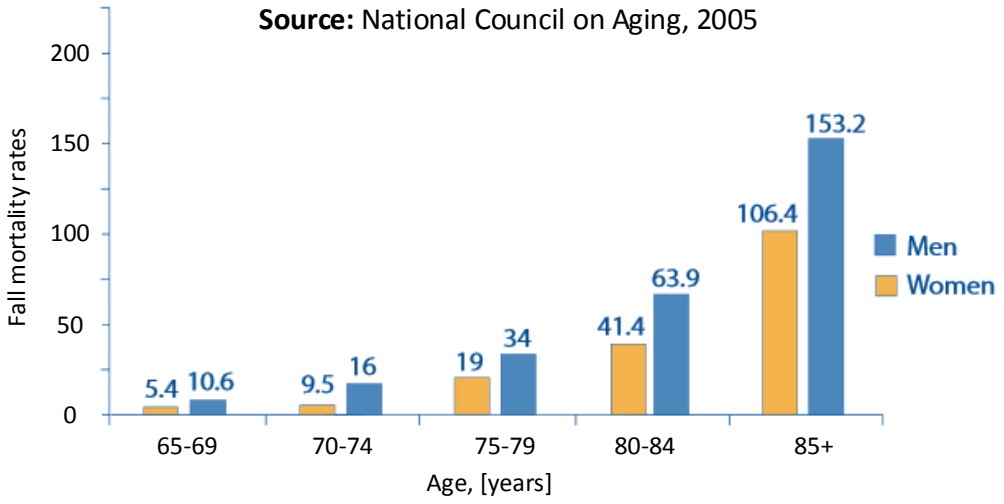

Figure 2 Fall mortality rates in the elderly population

2.2 Fall risk factors

Terrifying current and forecasted fall-related consequences have initiated numerous epidemiological studies in the past 50 years towards identification of most relevant risk factors for falls. More than 400 various risk factors were found, which in a complex interaction trigger a fall. Diversity of these factors and their interactions illustrate very well the multifactorial challenge for prevention of falls. Classification of risk factors differ, but two major directions can be formed. First classifies the risk factors into four categories: biological, behavioural, environmental and socioeconomic. Second direction is simpler and splits the risk factors in only two categories: intrinsic and extrinsic. The second classification will be further addressed in this chapter.

2.2.1 Intrinsic risk factors

Intrinsic risk factors are individual person-related factors that reflect one's physical performance, such as age, sex, balance and gait disturbances, muscle weakness, chronic diseases, cognitive disorders etc. With increasing age, the mentioned risk factors are accordingly getting more influential. Especially sensitive are the sense organs causing visual (e.g. by glaucoma or cataract) and hearing impairment (e.g. by natural aging loss) (Walther, 2008). Furthermore, adaptability of the eye to different luminance ratios and its accommodation capacity are decreasing leaving the vision out of focus (Pierobon, 2013). Cognitive perception disorders (e.g. dementia), as well as psychological diseases (e.g. fear of falling and depression) lead to increased fall risk. For example, a fall-induced fracture due to cognitive perception disorder is associated with 1.5 to 3 times increased risk (Shaw, 2002).

The balance, which is important for a stable body position and thus prevention of falls, is diminishing with age, mainly due to a reduction in a musculature and limited joint mobility. Therefore, degradation of the muscles and muscle pain results in decreased mobility and increased risk of falling (Moreland, 2004). This further leads to limited joint mo-

bility, which additionally emphasized with joint diseases, such as arthritis, rheumatism and osteoarthritis, cause joint stiffness (Pierobon, 2013). These factors cause morbidly altered gait and gait disturbances that are reflected throughout decrease in quantitative gait factors. Various changes in quantitative gait factors associated with increased fall risk were found (such as gait speed, swing phase time variability, stride length variability) (Verghese, 2009). Not just quality of daily life gait, but also its amount predicts falls in older adults. For example, it has been found that fallers walk significantly less in daily life, as well as duration of their gait bouts is shorter (Schooten, 2015).

Chronic diseases, such as Parkinson's disease (PD), diabetes mellitus, hypertension, multiple sclerosis and incontinence increase risk of falling. However, the most significant fall risk factor is PD, causing 6.6 times higher risk of falling in comparison to persons without PD (Deandrea, 2010). Another important risk factors are dizziness and syncope, having direct and extent influence on the balance (Walther, 2008). Coronary heart disease, functional disorders, postural hypotension, aorta stasis and insulin therapy can also lead due to the loss of consciousness to increased fall risk (Lipsitz, 1986). For example, postural hypotension that occurs due to rapid blood pressure reduction during a standing up process (e.g. rising from a chair) can lead to dizziness or even loss of consciousness. Postural hypotension is characteristic for persons with PD or diabetes (Rubenstein, 1996).

2.2.2 Extrinsic risk factors

Extrinsic risk factors are related to presence of various environmental hazards, intake of different medications and fall-prone activities or movements (e.g. sport and alcohol consummation). According to (Rubenstein, 1996), on average 41% of falls of the community-dwelling older adults belong to environmental factors. Hence, 16% of recorded falls occur due to environmental hazards in elderly population in nurs-

ing homes. These alarmingly high occurrences show that causes and frequencies of environmental (situational) falls should be further investigated.

A study on 414 community-dwelling older adults has shown that 56% of falls happen outside the home (in the garden, street, footpath or shops) (Lord, 2007). The second most common fall site was the level ground in different rooms of the household. In these cases, tripping over a carpet, on a slippery floor or on the object lying on the ground can be the cause of a fall (Figure 3). A large study on 1088 participants over 71 years was investigating location of falls (Gill, 2000). The most frequent falls with 21.9% happened outside home, followed by the living room and bedroom with 13.3% and 13.2%, respectively. Uneven ground like gravel, earthy ground with stones and roots or cobblestone pavement, as well as slippery ground due to rain, snow or ice increase the risk of falling outside home enormously. Contrary to the spontaneous assumption that in autumn and winter due to foliage, snow or ice an increased risk of falling would be present, a study from (Stalenhoef, 2002) has shown no significant difference between the fall rate in autumn/winter and spring/summer periods.

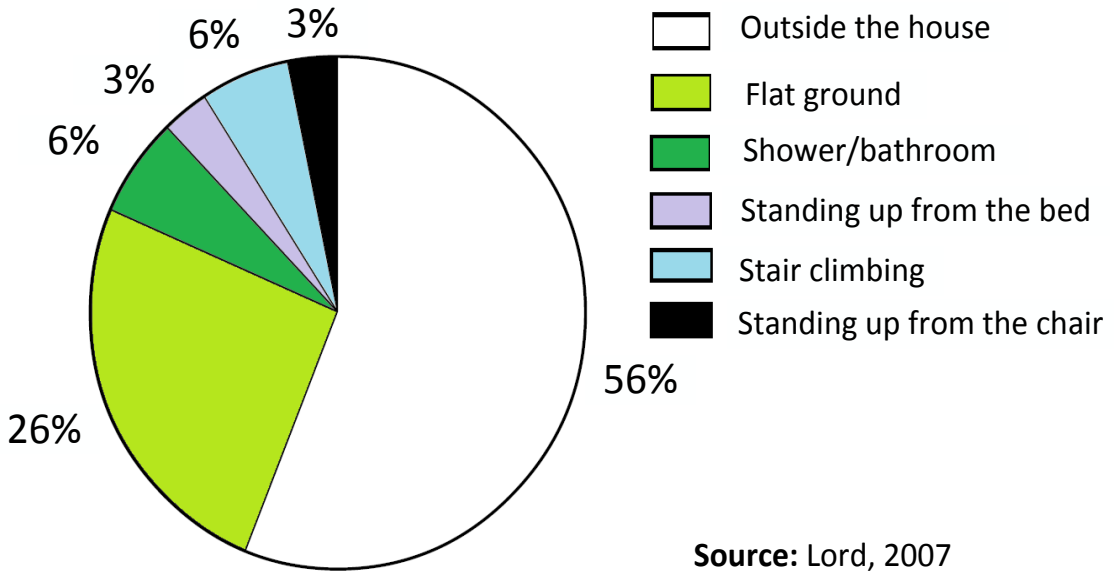

Figure 3 Location of falls in community-dwelling older adults

Different physical activities can lead to falls. Although stair climbing does not contribute to the falls in a large scale (only 10% of falls occurred at stairs), consequences due to these falls are very often fatal (Tinetti, 1995). A greater danger of falling is while walking downstairs than going upstairs (Handsaker, 2014). Getting out of the bed or standing up from a chair are threats to elderly population as well (Lord, 2007). More precisely, postural transfers are responsible for 41% of falls in the residents of nursing home (more than walking accounted for 36% of falls) (Rapp, 2012).

Another important risk of falling is the influence of medications, which due to various side effects, such as dizziness, increased postural hypotension or sedative effects, increase the fall risk. Especially good association has been found between fall risk and medications that target central nervous systems (such as sedatives, anti-epileptics, antidepressants and antipsychotics) (Deandrea, 2010). However, in a case of anti-epileptics it is difficult to determine which falls are caused by disease and which by medications. In addition, a weak correlation between cardiovascular medications and increased risk of falling has been found.

2.3 Fall prevention strategies

Once the risk factors have been identified, preventive measures can be taken in order to avoid a fall. A meta-analysis of fall prevention strategies performed in 159 different studies on 79.193 participants have shown a possible reduction of falls up to 40% (Gillespie, 2012). The prevention measures, that can significantly reduce not just the number of fallers, but also fall rates, are most often various training programs targeting balance (such as Tai Chi) and motor skills (e.g. by walking, group exercises or exercises at home). The most effective interventions are individually-designed training programs combining simultaneously, balance and strength trainings.

Since intake of medications can increase risk of falling, their dosage, indications, duration of ingestion and side effects should be regularly reviewed and alternatives, as well as individually-designed modifications should be recommended, when necessary (Becker, 2011). To identify individual medications' indications and side effects, a list of potential inadequate drugs for elderly population (PRISCUS list) together with alternatives was proposed (Holt, 2010). Nevertheless, some medications can reduce the risk of falling (e.g. deficiency of vitamin D can be significantly reduced by using its supplements and thus decrease the fall risk) (Gillespie, 2012).

Many falls occur because a potential source of danger has been overlooked. Therefore, visual impairments should be addressed as well (e.g. the removal of cataract by means of a surgical operation or adjustment of spectacles increasing the spatial perception) (Lord, 2007). Already a small modifications of footwear (e.g. using appropriate orthopaedic shoes) can reduce the risk of falling significantly (Balzer, 2012). Falls due to environmental hazards could be avoided by applying appropriate preventive measures, such as elimination of tripping obstacles, usage of non-slip carpets, sufficient lighting in individual rooms, particularly in corridors and on the stairs (Rubenstein, 1996).

2.4 Fall risk assessment

Main prerequisite for fall prevention strategies is an objective and reliable FRA to target the intervention. Objective assessment of the fall risk can imply crucial changes in the diverse number of fall prevention strategies, thus considerably reducing the number of fallers, as well as the fall rate. Current state-of-the-art solutions offer no widely acceptable solution. The FRA can be split into clinical (ambulatory) assessment and evaluation of the fall risk in ADL (non-ambulatory settings). In the following two sub-chapters these two approaches and latest achievements in the literature will be shown in details.

2.4.1 Ambulatory assessment

The FRA in a clinical setting is still considered to be the gold standard. These fall risk screenings are often part of larger examination and do not happen on a regular basis. Most common assessment for elderly above 65 years comprises of investigation of history of falls in the last 12 months, fear of falling and gait and balance disorders (Schooten, 2015). This solely questionnaire-based approach is above everything subjective, meaning susceptible to individual interpretation of falls, as well as influenced by fear of white coat in clinic and recalling of falls. Moreover, most often it investigates mainly intrinsic fall risk factors. Nevertheless, this subjective screening method can trigger further investigations towards FRA.

In case of a positive fall risk evaluation (especially in case of at least one fall in the last 12 months), an additional mobility screening, as an objective FRA test, should be conducted. These FRA tests comprises either of series of different tools (e.g. Psychological Profile Approach (PPA) (Lord, 2003) or Short Physical Performance Battery (Guralnik, 1994)), or of simple gait and balance tests (e.g. Timed-Up-And-Go (TUG) test (Shumway, 2000), Berg Balance Scale (Muir, 2008), Tinetti Balance Test (Raiche, 2000) or 5-times-sit-to-stand test (Whitney, 2005)).

The tests show numerous limitations, such as lack of cost-effectiveness, high time consumption for both, patients and professionals, or focus on singular aspects (e.g. time) of highly complex movements. Moreover, the tests have low capacity for adaption to persons with wide spectrum of physical performance, as well as they have poor to moderate (<75%) fall risk predictive values, especially for people at relatively good health (Hamacher, 2011).

2.4.2 Assessment in activities of daily living

Previously mentioned limitations of ambulatory FRA, motivated by the latest advantages in signal processing and sensor technology, have led to applications of wearable sensor-based devices in FRA. Several studies

were performed by integrating wearable devices with inertial sensors in functional tests to enhance their precision (Najafi, 2002 and Weiss, 2010). For example, waist-attached accelerometers were used to detect start and end points of the STST, eliminating the observer's response time (Najafi, 2002). The progress in sensor technology also induced translation of FRA from clinical to person's home setting (non-ambulatory environment). Therefore, recent studies have tried to perform objective and reliable FRA in a non-ambulatory environment by using unobtrusive systems containing inertial sensors (Rispens, 2015, Schooten, 2012, Ihlen, 2015 and Brodie, 2015).

Nowadays, wearable devices based on microelectromechanical systems (MEMS) measuring inertia (acceleration or angular rate) can be worn unobtrusively during ADL over longer periods of time, allowing reliable and clinically relevant assessment of fall risk. Moreover, advanced applications of MEMS (e.g. accelerometer or gyroscope) revealed differences in movement patterns between fallers and non-fallers during gait and sit-to-stand movements, which are invisible to human observer. Continuous assessment of walking quality and quantity throughout three or more days by waist-worn devices showed differences between fallers and non-fallers (Weiss, 2014). Similar findings were confirmed also for inertial sensors attached at the sternum (Brodie, 2015). Looking only at the macro perspective of the gait behavior acquired with a wearables attached at the lower back, a clear difference between fallers and non-fallers can be seen (Del Din, 2015). One study have addressed STST detected by waist-worn MEMS in ADL (Iluz, 2015), showing that features extracted from the multiple transitions recorded during daily living apparently reflect changes associated with aging and fall risk.

The MEMS have not only enabled continuous assessment of macro perspective of movement patterns in ADL, but they have also offered tools for capturing small perturbations in human kinematics. An application of a waist-attached sensor for investigation of local dynamic stability in over-ground walking has revealed more unstable gait patterns for participants at higher risk of falling (Schooten, 2012). Captured significant

differences in small perturbations in human kinematics, have led to findings that phase-dependent local dynamic stability in daily life walking can identify people at increased risk of falling (Ihlen, 2015).

Furthermore, these results were improved by combining sensor-based assessment with questionnaires (Schooten, 2014 and Rispens, 2015). However, sensor nodes in latter mentioned studies were mostly targeting different aspects of the gait in ADL. The focus on gait is justifiable, since gait parameters have been shown to be meaningful fall predictors (such as gait speed (Stone, 2015), step rate variability (Rispens, 2015) or local dynamic stability), but 41% of falls during postural transfer in elderly in nursing homes (Rapp, 2012) strongly suggest that more studies should address this problem in non-ambulatory environments. It is also reasonable to focus on singular periodical aspects of human movement (such as gait), since it is easier to distinguish them from other activities than non-recurrent movements (such as STST).

In addition, a sensor positioned close to one's center of mass (at lower back or even waist) captures more meaningful movement which is in direct connection with balance than sensor located at the wrist (at the extreme point of the body influenced by random movement). The MEMS at the wrist are affected by movements performed during the upper limb activities when the center of mass is in approximately motionless position (e.g. during sedentary activities such as standing, sitting or lying). Therefore, wrist bands, as the most unobtrusive and widely accepted devices for activity monitoring, have not been yet validated in terms of FRA in non-ambulatory environments. Moreover, this challenging position has shown low performance for activity classification (Mannini, 2013). However, analysis of the data acquired with wrist bands may reveal important information about physical performance in elderly during ADL that could have not been observed in clinical settings (e.g. different transfer strategies or walking patterns).

2.5 Overview of state-of-the-art limitations

Fall prevention strategies can reduce the number of fallers, as well as the fall rate. The main missing prerequisite for fall prevention strategies is an objective, reliable and cost-effective FRA. The FRA in a clinical setting is still considered to be the gold standard, but it is often time consuming, subjective, focused on singular aspects of highly complex daily life activities and unable to adopt to one's individual needs and physical performance. The latest advantages in sensor technologies have enabled continuous objective FRA in non-ambulatory environments by means of tiny MEMS integrated into wearables attached to human body. Initial sensor-based approaches are prevailingly focused on periodical movement patterns (e.g. gait) and use sensor positions close to one's center of mass (e.g. sternum or lower back). These choices are stigmatized and obtrusive for wearing sensor nodes during longer time intervals (one or more weeks). Further, they do not take into consideration the environmental context for the FRA (e.g. extrinsic risk factors) nor groups at high risk of falling (acute fallers).

The figures in fall-related injuries, their risk factors and limitations of state-of-the-art elaborated in previous subchapters and briefly listed in the paragraph above are main motivational aspects of this thesis. Therefore, the focus of this thesis was set on establishment of a reliable acute and habitual FRA in an unobtrusive setting (at home) and in highly non-stigmatized manner (at the wrist) based on quantitative assessment of three domains of human movement targeting both, recurrent and non-recurrent patterns: gait, inter-limb coordination and sit-to-stand transitions.

3 Clinical studies

3.1 Data acquisition

Data acquisition in this thesis was implemented in two basic steps. Firstly, a small pilot study designed as an exploratory cross-sectional study in a controlled environment was performed for the algorithm development purposes. More precisely, the data from this study was used for the iterative process of implementation of algorithms for inter-limb coordination, gait and sit-to-stand transition assessment. Since main focus of the thesis lies on the ADL, it was important to authentically simulate real-life situations already in the early stage of the process and adopt algorithms accordingly. Therefore, a true value of this video-recorded study was clearly visible.

Secondly, developed algorithms were validated in terms of acute and 6-months based FRA on a large cross-sectional study conducted in the participants' home environment. Focus was set on a clinically relevant number of participants, continuous long-term monitoring during all kinds of activities and conditions, as well as on acquisition of reliable reference and data protection. Exact fitting of data acquisition steps in the overall work progress can be seen in the Figure 4.

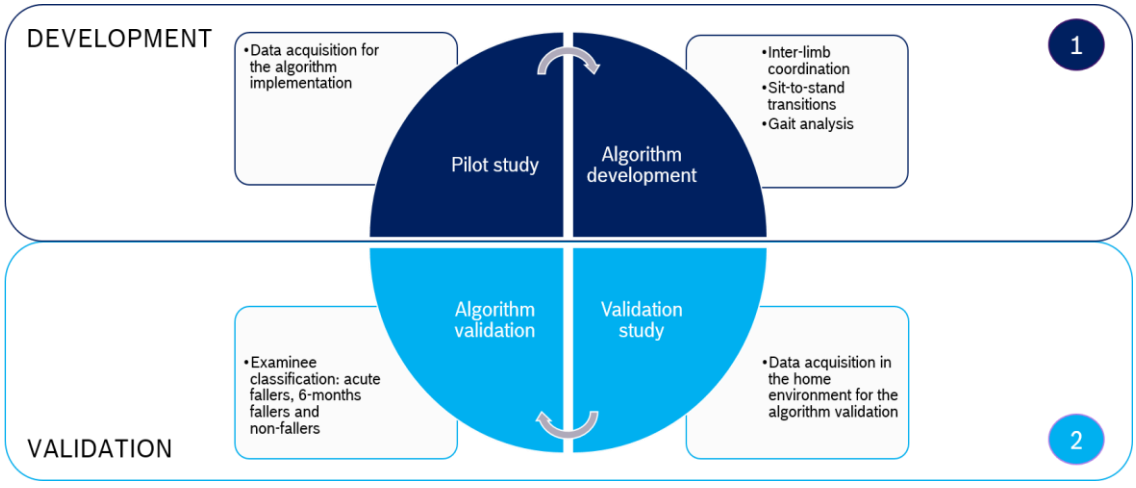

Figure 4 Procedure for implementation of reliable FRA on the wrist

3.1.1 Designing the pilot study

For the algorithm development purposes, as well as for the validation purposes, an exploratory cross-sectional pilot study in cooperation with the Clinic for Geriatric Rehabilitation at Robert-Bosch-Hospital, Stuttgart was designed and performed. In the pilot study 28 participants (23 females, 5 males) between 65 and 95 years with a wide range of physical performance (median habitual gait speed 0.88 m/s; range 0.25 m/s to 1.76 m/s) were recruited. Acquisition of participants' anthropometric measures in the pilot study was limited to age and side of the dominant hand.

The main focus of the study was simulation of home activities in a controlled environment (i.e. ambulatory setting). To enable a validation on both, structured and unstructured data, the study was split into a supervised and unsupervised part. The ground plan of the study environment is shown in the Figure 5. In the supervised part of the protocol participants were explicitly instructed what to do, while in the unsupervised part no spoken instructions were given and participants could move freely within the setting – guided by six written notes with general instructions to keep the unsupervised part of the measurement protocol in certain limits.

The supervised part of the protocol included walking on a straight line of the total length of eight meters with different paces: normal, slow and fast. Due to the wide range of the physical performance of participants, they interpreted the instructed pace in their own words. In case the participant was using a walking aid for walking in daily life, he or she was using it in the pilot study as well. Further, participants were instructed to perform five different sit-to-stand transitions: from the bed, from the chairs with and without armrests by using hands and without using hands. If possible, the participants had to climb up and down on four stairs, first with the dominant hand on the handrail and then with a non-dominant hand on the handrail.

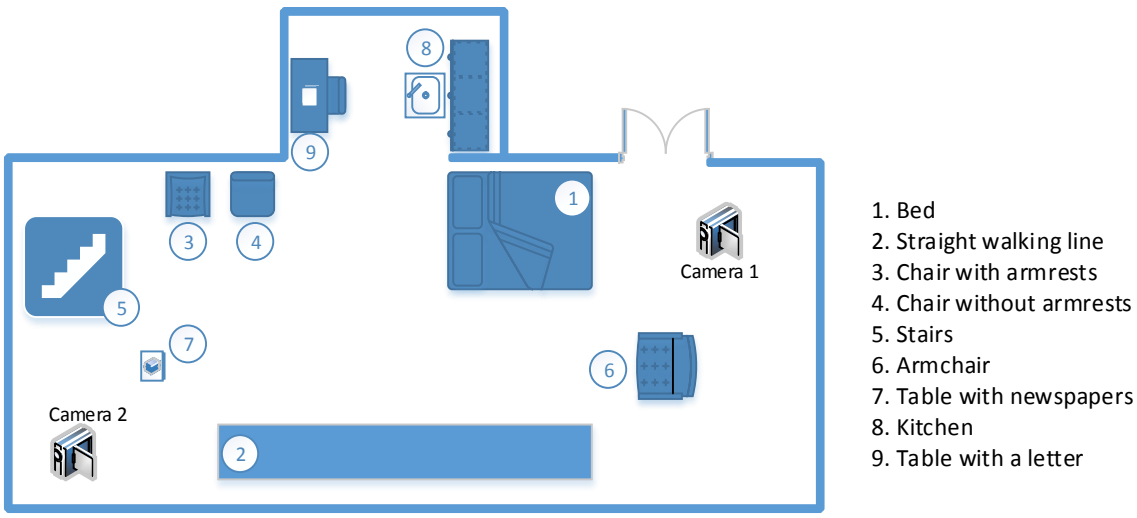

Figure 5 Ground plan of the pilot study

The unsupervised part of the protocol included execution of activities in self-interpretation that are characteristic for normal daily life routine (sit-to-stand transitions from the chair with and without armrests, as well as from the armchair and chair at the table, walking, lying, reading, cooking activities, carrying objects to specific place, searching for plate and bowl in the kitchen cupboards and writing a letter). An example of a written instruction used in the study is given by following steps:

- Walk from the sofa to the kitchen → locate a bottle of water and a glass → poor the water in the glass.

In this instruction, no strictly defined way was given, participant could chose pace and timing arbitrarily and searching for the glass and bottle in the kitchen additionally increased the variability of movement. Important to note for later thesis development, each participant performed eight different sit-to-stand transitions within this study (from the bed, from the armchair, from the chair with and without armrests by using and without using hands, instructed and not instructed transition) including supervised and unsupervised part of the protocol. The importance of the unsupervised part of the protocol is in the possibility of testing the developed algorithms in approximately similar setting as in

daily life but with advantage of having a partially controlled environment, which enable detail error analysis via video recordings.

3.1.1.1 Utilised hardware

The participants were wearing four sensor nodes, on both wrists and hips (i.e. on both side of the body). This approach allows detail analysis of the developed algorithms from perspective of both, dominant and non-dominant hand. Data was wirelessly transferred from the sensor node to a phone using Bluetooth Low Energy (BLE). Each sensor node comprises of 3-axial accelerometer, gyroscope and magnetometer with additional environmental sensors (pressure, temperature, humidity and luminance). Measurement ranges for the sensors were: ± 4 g, ± 500 °/s, ± 1000 μT, 300 - 1100 hPa, -40 - 85 °C, 0 - 100 %RH and 0 - 188000 Lux, respectively for sensor order mentioned in the latter sentence. The sensor resolution was set to 16 bit, whereas the sampling frequency was set to 100 Hz (with σ = 1 Hz).

3.1.1.2 Ground truth

The whole study protocol was monitored with two video cameras Samsung HMX-Q10TP with a video resolution SD 576/50p. The cameras were installed on diametrically opposite sides in respect to the monitored participants and were moved by trained supervisors when needed in order to capture movement of all parts of the body equipped with the sensors and register every single step, as well as sit-to-stand transition. It is also important to emphasize the importance of the data protection, so no participants were recorded above the shoulders and all data (including raw and processed sensor data, anthropometric measures and videos) was stored under randomly generated 3-digit pseudo identification number.

Acquired videos were used as a supplement for the detail error analysis as well as for video analysis of the sit-to-stand transitions and video labelling of activities and steps by using an in-house tool implemented in LabVIEW (Figure 6). Start and end of all sit-to-stand transitions and gait phases were labelled in the videos with a marker, which was then saved

as a part of the data stream with the same sampling frequency as the input sensor signal (frame rate of the recorded videos was up-sampled to the sampling frequency of the inertial signals). This enabled synchronous comparison of video labels and sensor data, which yielded a better understanding of the motor performance during particular movements.

The sit-to-stand transition was defined from the perspective of the body's centre of mass, where beginning is depicted with the start of the flexion phase and end is depicted with the end of stabilization phase. In case when a walking phase continues directly on the transition (i.e. absence of the stabilization phase is present), first heel strike is marker of the end of the transition. Different types of transitions performed in the supervised and unsupervised study parts were labelled accordingly based on the video observations. Although, focus of the thesis is on detection of sit-to-stand transitions from the wrist perspective, ground truth could not be generated in the corresponding fashion, since conventional postural transition definitions predominantly relate either to the participant's centre of mass (located around the fifth vertebrae in the lumbar spine) or to the upper part of the body.

Gait phase was defined as a block of three or more consecutive steps starting with a heel strike of the first step and ending with a heel strike of the last step of the corresponding gait phase. Last step of the corresponding gait phase was defined when a time difference (brake) between consecutive steps is longer than three seconds. In addition, average gait speed for each gait phase was calculated. The gait speed was used for labelling the phases into slow (0.0-0.6 m/s), normal (0.6-1.2 m/s) and fast walking (above 1.2 m/s). Stair climbing was not defined as walking, whereas turning was included in walking phases.

Figure 6 Comparison of the signals with the body movement in the video

3.1.2 Designing the FRA study

A cross-sectional FRA study that included in total 508 adults aged between 50 and 85 years was performed. In order to deliver consistent results with current literature findings (Schooten, 2015 and Rispens, 2015), the work in this thesis addressed only population aged above 65 years. The study was approved by the Ethical Committee of the Medical Faculty at the University Hospital of Tuebingen, Germany. The participants were recruited by a geriatric rehabilitation clinic at Robert-Bosch-Hospital and a health insurance company Bosch-Health-Insurance in Germany. All participants gave written informed consent according to the Declaration of Helsinki. In addition to the participant's age, exclusion criteria for participation in the study were impaired cognition (>10 points on the Short-Orientation-Memory-Concentration test (Katzman, 1983)), inability to walk and terminal diseases. Furthermore, 13 participants aged over 65 revoke their participation in the study, 26 participants had to be excluded due to complete sensor malfunction, while 2 participants haven't returned any fall diaries back. Therefore, in total 180 participants satisfying defined participation conditions were included in the further analysis in this thesis.

3.1.2.1 Data acquisition protocol

The data acquisition was performed from March 2015 till April 2016, including all seasons and weather conditions. Sensor data of physical activity from each participant was recorded for one week (seven consecutive days) during participant's daily living activities. The participants were wearing two sensor nodes attached at the wrist and ipsilateral hip. The date of the first day of the measurement week was manually noted by the trained supervisor. While wearing the sensor system, the participants were instructed to normally proceed with their daily obligations, so the recordings in extreme cases also included the vacation trips (e.g. skiing, camping, road trip) or flights. One week of data recording was chosen, since it reflects the person's behaviour during working hours (in case the participant is employed) as well as during leisure time (weekends). On the first day of measurement the participants could arbitrarily choose on which side the sensors were worn (dominant or non-dominant side) and continue wearing them there until the end of measurement. The sensors were attached in the morning and they were worn during normal daily routine. The sensors' batteries were charged overnight. The sensors were not waterproof so the participants were instructed not to wear them during the contact with water. Data corresponding to measurement over one day was stored in one file to ease the offline processing. During the measurement week the participants were further instructed to note for each day the times when they were wearing the sensor nodes.

On the first day of a measurement week the participant's characteristics were collected by a trained supervisor in the participant's home environment. Descriptive parameters included age, height, body mass, occupation and side of the dominant hand. A large number of participants in the study, orientation on the user satisfaction, as well as the different non-ambulatory settings in which the clinical test should have been performed influenced radically the choice of the tests that were implemented in the study. Both, trained supervisors and participants, have limited amount of time and patience thus the selected tests had to be low time consuming but still worthwhile for the defined purposes. For

example, the Berg Balance Scale which has been shown as an excellent tool for the fall risk assessment (Muir, 2008) could not be used since its duration of approximately 20 minutes per participant would result in the end with more than 300 additional hours of assessment. Additionally, some of the clinically relevant tests could not be implemented due to the limitations of the non-ambulatory environment (e.g. 10-meter walk test) or sensitivity of the questions and low user-friendly feedback from the previous studies (e.g. Geriatric Depression Scale, GDS).

As a result of discussion with clinicians, the following tests were chosen with the best trade-off between time consumption and clinical relevance:

- Short-Orientation-Memory-Concentration (SOMC) test;
- Habitual gait speed;
- Number of chair rises during 30 seconds.

The habitual gait speed was measured on a pathway no shorter than 3.5 meters. Walking pathway was variable due to various conditions in the participant's home environment (e.g. obstacles, small apartments). In cases when a participant used a walking aid for normal walking, the habitual gait speed was also assessed by walking with the corresponding walking aid. SOMC test was used for assessment of cognition. The prerequisites of the study were proper usage of the sensor system independently from the supervisor's presence and regular fulfilment of the fall diaries, which required certain level of cognitive functionality. The 30-seconds chair rise test was performed either from the chair with chair handles or without. Moreover, the participants could arbitrarily use their hands for support while standing up, which was then further noted.

Additionally, the participants answered a fall risk assessment questionnaire (FRAQ), investigating 18 most relevant fall risk factors identified in (Deandrea, 2010). The investigated factors together with their clinical significance on the fall risk are listed in the table below (Table 1). Risk factors were assessed with yes-no questions, except history of falls in the last 12 months and number of prescribed medications. History of

falls was graded with 0 for no reported falls, with 1 for one to two reported falls and with 2 for more than two reported falls. For more than two prescribed medications the answer was graded with 1, otherwise with 0. Other factors depending on their presence were graded either with 0 or 1. Total score of the FRAQ was defined as the sum score of the answers. Furthermore, anthropometric measures and FRAQ were used to determine the Fall Risk Assessment Tool (FRAT-up) score. This score for the FRA was previously developed and validated in (Catellani, 2015). Both measures, FRAQ and FRAT-up score, were used for further comparison with the study results.

Table 1 Investigated fall risk factors

Feature	**Statistical significance[2]**	**95% CI[1]**
Living situation	0.44	1.33 (1.21-1.45)
History of falls	0.04	3.46 (2.85-4.22)
Fear of falling	<0.01	2.51 (1.78-3.54)
Gait problems	<0.01	2.16 (1.47-3.19)
Number of medications	0.38	1.06 (1.04-1.08)
Urinary incontinence	0.10	1.67 (1.45-1.92)
Pain	0.80	1.60 (1.44-1.78)
Physical activity limitations	0.01	1.20 (1.04-1.38)
Physical disability	<0.01	2.42 (1.80-3.26)
Diabetes Mellitus	<0.01	2.04 (1.41-2.95)
Parkinson's Disease	0.50	1.57 (1.42-1.73)
History of stroke	0.17	1.28 (1.09-1.50)
Dizziness	0.56	2.84 (1.77-4.58)
Depression	0.52	1.79 (1.51-2.13)
Visual impairment	0.21	2.28 (1.90-2.75)
Hearing impairment	<0.01	1.86 (1.45-2.38)

[1]95% CI = 95% Confidence Interval; [2]Significant for $p < 0.05$

Starting with the first day of the measurement week, all participants filled out a fall diary for one year. Each day was marked either with 1 (in case of fall) or 0 (in case of no fall). Additionally, they were instructed to fill out a fall report consisting of the most important facts about the fall:

- Place of the fall (inside – outside);
- Activity directly before the fall;
- Triggers for the fall;
- Standing up after fall (yes/no; alone/only with help);
- Consequences of the fall.

The fall was defined as an activity where a person non-intentionally has fallen in the direction of the gravitation force, including situations where a person hits the wall or any other object (e.g. chair, stairs handle). A simplified analysis of the reported fall triggers was performed, which yielded two main groups of fallers. In case a person reported a fall during a fall-prone activity (sport activities, hiking) or during atypical activity for ADL (in the sea, under influence of alcoholic or other beverages that influence the balance), such person was not classified as a faller (despite the reported fall). Falls that were caused by different medical conditions (loss of balance, dizziness, blood pressure, problems with the cardiovascular system), during transitions (sit-to-stand, as well as stand-to-sit), walking (outdoor and indoor, including stairs up and stairs down), as well as falls caused by various different environmental conditions (slippery floor, in the bath, on the ice and other different terrain conditions) classified the person reporting the fall as a faller. In case a person has reported a fall caused by fall triggers from both groups (e.g. fall during bike ride due to the dizziness), the corresponding person was classified as a faller (i.e. more relevant fall trigger has a higher priority).

The fall diaries and reports were used as the reference method for splitting the participants into two groups: fallers (participants reporting one or more falls in the follow-up phase) and non-fallers (participants reporting no falls in the analysed period). Furthermore, the split was performed for two different durations of the follow-up phase: one month and six months. Participants classified as fallers based only on the first month of the follow-up phase were classified as acute fallers. Due to a slow recruitment process an acceptable number of participants required for the first reliable reference was available only after six months from the start of the study (for acute fall risk assessment) or almost after a year (for six months follow-up phase which is conventional in the literature for the clinical fall risk assessment), previously defined FRAQ and FRAT-up scores were used for preliminary analysis in the meantime. A timeline depicting points of investigation of each clinical measure is shown in the Figure 7.

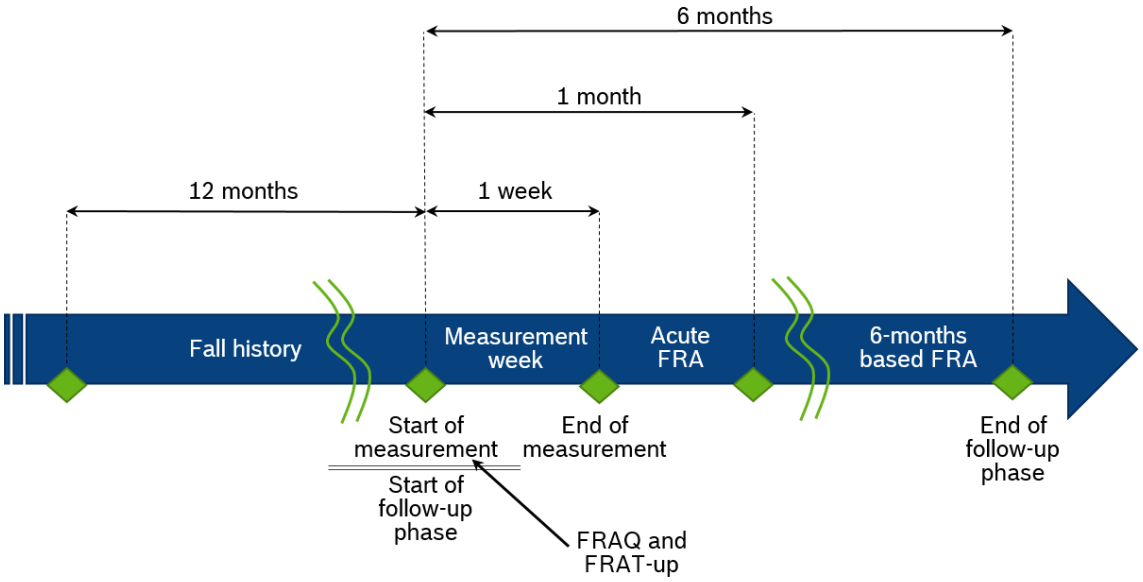

Figure 7 Explained fall risk assessment's milestones

3.1.2.2 Utilised hardware

Both sensor nodes attached at the participant had equal characteristics. Physical dimensions of the sensor nodes were 56 mm width, 46 mm length and 15 mm height (Figure 8). Sensor nodes consisted of inertial 3-axes sensors (accelerometer BMA280, gyroscope BMG160 and magnetometer BMC055), environmental sensor BME280 consisting of the pressure, temperature and humidity sensor and luminance sensor MAX44009. All sensors were produced by Bosch Sensortec GmbH, Reutlingen, Germany. Measurement range of each sensor is an important basis for further signal processing, but due to little previous experience with the wrist-worn devices, as well as further development of the project-related tasks and applications, the measurement ranges of the inertial sensors were changed two times within the study. Each time the measurement ranges were changed motivated by the fact that inertial sensors were getting to often into saturation due to the particular movement events. From participants satisfying the defined exclusion criteria and study conditions, 95 participants had the measurement ranges of the sensors set to ± 4 g, ± 500 °/s and ± 1000 µT. For 23 participants the measurement ranges were set to ± 4 g, ± 1000 °/s and ± 1000 µT, while for the last 62 participants the measurement ranges were set to ± 8 g,

± 2000 °/s and ± 1000 μT for the accelerometer, gyroscope and magnetometer, respectively. Measurement range of the environmental sensors was consistent throughout the whole study as follows: 300-1100 hPa, -40-85 °C, 0-100 %RH and 0-188000 Lux for the pressure, temperature, relative humidity and light sensor, respectively. Bit resolution of the accelerometer sensor was set to 14 bit, while gyroscope and magnetometer sensors had a 16 bit resolution. The resolution of the pressure sensor was 1 Pa, temperature 0.01 °C, humidity 0.01 %RH and light 1 Lux.

Figure 8 Wrist-worn sensor node used in the study together with the phone for data acquisition

The inertial data was sampled with 100 Hz, as this is the sampling frequency that by Nyquist-Shannon theorem should be able to cover 99% frequency components of the human daily movement (Karantonis, 2006). The environmental data was sampled with 1 Hz and later on in the preparation phase interpolated linearly to 100 Hz to ease the data analysis.

The energy friendly processing of the acquired sensor data was enabled via EFM32GG395 microcontroller based on the ARM Cortex-M3 high performance platform. Whole process was supported with the real-time operating system. The sensor nodes were supplied with a rechargeable lithium battery (170 mAh) which lasts for approximately eight hours of

continuous data acquisition. The sensor nodes were extended with another battery for the last 85 study participants, which enabled in case of the proper use 14 to 15 hours of continuous recording.

Since the sensor nodes did not have external flash for storage of bigger data volumes, two different approaches of data acquisition were implemented in the study. In the first revision, the sampled data was transmitted wirelessly as a package via a BLE connection to an Android phone (LG G2 mini, LG Electronics, Seoul, South Korea) attached to a belt around the waist. BLE packages are limited to 20 bytes and thus, the inertial data was sent in separate packages from the environmental data. Each package contained, additionally to the sampled data, the internal counter value at the time point when the data was sampled. The internal counter had to be limited to 22-bit due to the size of the BLE package, thus causing overflows every 1.16 hours. Arrival time of each BLE package was noted. Moreover, every minute the phone was sending a package to the sensor and it was waiting for its response. The round trip of that package between the phone and sensor was used later for the synchronization purposes. Two major effects were crucial for a decision to change the data acquisition protocol: data loss and phone time resets (see 3.1.2.3 and 3.1.2.4 for more details). The change to the second sensor system revision happened simultaneously with the second change of the measurement range of the inertial sensors.

In the second sensor system revision, the sampled data was stored on a micro SD card (SanDisk, 16 GB) integrated into the housing. This revision enabled a storage of data without losing any information. However, since the sensor nodes were not equipped with the real-time clock (RTC), a problem of distinguishing between the particular days of measurement was introduced.

The data corresponding to one day of measurement was stored in one file with a predefined filename structure:

BXXXX_YYYY_MM_DD_sensorPosition_sensor.type. (1)

Here, XXXX depicted a randomly four-digit generated pseudo ID assigned to each participant, YYYY was the year of measurement, MM is the month, DD is the day, sensorPosition noted where the sensor node was attached (wrist or waist) and sensor depicted either 9DOF for inertial sensors or ENV for environmental sensors. The file type where the data was saved corresponded to the sensor revision – a comma separated value file for the sensor revision with the smart phone or a text file for the sensor revision with the SD card. The particular days for the sensor system revision with SD card were determined based on the detection of charging of the sensor nodes, i.e. each time the sensor node was put to charge a new file on the SD card was generated. In order that this principle works, the main assumption is that participants were explicitly following the given instructions (i.e. sensor nodes were put to charge in the evening and taken from charging in the morning). Deviations from these instructions brought additional noise in the evaluation of the measurement data that was not able to be solved successfully within the scope of this study.

3.1.2.3 Data loss

Data loss was detected when the time difference between two consecutive BLE packages t_i and t_{i+1} in an arbitrarily chosen moment $i \in N_0$ (where i depicts ascending order of the BLE package within the measurement week) satisfied the following relation:

$$t_{i+1} - t_i > 1.5 * T_S \tag{2}$$

where T_S is the defined sampling period. Data loss was detected on a monotonously increasing time vector built from the mapping of the phone and sensor times. This approach allows to overcome the problem with counter overflow, as well as data loss over longer periods of time where whole counter cycles might have been lost (for example due to the BLE connection loss). Data loss happens when an obstacle appears between the sensor node and the acquisition unit (phone). An obstacle could be either part of the participants' environment or human body.

Although, one can only speculate what is the total influence of data loss on the final results of the study, their influence has been minimized with introduction of a valid flag. The valid flag denotes the parts of the signal that could be used for further processing. Three crucial conditions define the valid intervals of the signal:

- An interval between two consecutively acquired BLE packages is shorter than 250 milliseconds;
- An interval defined with a window size of one second has less than 30% data loss in total;
- An interval satisfying the two conditions above is longer than 10 seconds.

Additionally, the days with total data loss higher than 80% were excluded from further processing. The thresholds defined for the validity of data were set empirically based on the discussion between signal processing experts.

3.1.2.4 Phone time resets

The approach with mapping of the inertial counter of the sensor node with phone times showed also one weakness. Namely, the Data Privacy Concept V1.0 defines the data acquisition units without the possible connection to the Internet (i.e. without the GSM card). In cases when a back button of the phone was pressed continuously for 20 or more seconds, the time of the phone is reset to the last time setup. The absence of the Internet connection does not allow a phone to resynchronise, thus influencing the data acquisition that follows after the time reset.

The time resets in the acquired data were identified when a file name with the date earlier than the date of the sensor delivery to the study participants was detected. This affected in total 36 participants, whose acquired data was sorted by manually analysing and comparing the times when the participants were wearing the sensor nodes, phone time, as well as the counter values of both, inertial and environmental BLE packages.

3.1.2.5 Actual wearing times

Additional problem that influenced both sensor system revisions was the total actual time of wearing the sensor nodes. This occurrence can be either user- or system-influenced. Although, the participants were instructed to wear the sensor nodes during all daily life activities, except during the contact with water, from the various unknown reasons the sensor nodes were not continuously worn. System-influenced not wearing times were the consequence of improper sensor node charging. Namely, when the participants would let the sensor system to charge overnight, if the charging is not detected by the system, the data would be acquired also throughout the whole night. Not wearing times during the night were discarded by the implemented algorithms with detection of simple trigger events (i.e. sudden or periodical change in the acceleration signal), but these events during the day should not be disregarded since they may have direct influence on the one's performance (e.g. duration of sleep or sitting phases with dominant inactivity periods).

3.2 Data processing framework

Whole process of processing and analysing the data was implemented in MATLAB R2013b due to its user-friendly graphical interface, valuable API support in statistics and signal processing as well as matrix-orientated multi-thread programming. Acquisition and preprocessing of such large sets of acquired data could be a subject of different unexpected errors since they are performed by error-prone environment. Furthermore, analysis even when done in vectorized manner, on a dataset like the FRA study could take multiple days. These two factors implied a strong motivation for the development of a unique script that would handle structured data sets by having a reasonable contingency of actions in case of an error or boundary conditions.

Moreover, a lot of focus was set on reasonably time-efficient import of acquired data as well as on export of extracted features. Taking into account the time consumption for each step of the framework development, it was possible to reduce the import of acquired data from two

minutes to below 10 seconds for 126.7 MB of data (corresponding to eight hours of recording).

Since acquired data was saved as either CSV- or binary-files, its preprocessing was the most time consuming process. Therefore, it was important to limit this process to a minimal number of repetitions per participant and in further analysis use MAT-files that are based on the binary streams, which enables significantly faster import/export of data into MATLAB. The developed master script goes through all acquired data files, creates monotonously increasing time vectors, interpolates linearly the missing data (defined in 3.1.2.3), defines the validation flag, calibrates and scales acceleration and gyroscope data by using the BST Fusion library and finally derives the Euler angles from the quaternions. The preprocessed data is then stored in MAT-format for further analysis. In the following steps, only a uniquely processed data was accessed, without taking into consideration different measurement ranges, data loss or other effects mentioned in 3.1.1.

3.3 Analysis of participants characteristics

Participants' measures were analysed only for the FRA study, on which developed algorithms were validated. Collected participants' characteristics for this study are shown in the table below. The participants were split into four defined groups: non-fallers and fallers based on the 6-months FRA, as well as non-fallers and fallers based on the acute FRA (corresponding to one month follow-up phase) (Table 2). All measures in the table are shown as the mean value with the corresponding standard deviation. Additionally, a p-value derived from the Wilcoxon-Mann-Whitney test was applied in order to test the difference between each measure for 6-months based and acute FRA.

In total 180 participants were included in the acute FRA. If all reported (prospective) falls are taken into consideration, the analysis would yield 18 acute fallers and 162 non-fallers, whereas by the definition of a relevant fall in chapter 3.1.2.1 the ratio changes to 14 acute fallers (7.8%)

and 166 non-fallers. Four participants were reclassified because they reported falls during skiing, football and work in the garden. From the selected 14 acute fallers, seven have been identified as recurrent fallers in the 6-months follow-up phase (4.2 ± 2.6 falls per recurrent acute faller), whereas other seven reported only one fall (i.e. in the first month of the follow-up phase). Interestingly to note, the prospective number of falls was significantly higher ($p < 0.01$) than the retrospective ones indicating obvious problems in the fall-recalling. The prospective number of falls was also the only anthropometric measure that indicated the significant difference between the acute fallers and non-fallers or more precisely, acute fallers have reported more than six times more prospective falls than non-fallers in the following six months, whereas there was no significant difference in the fall history ($p = 0.17$). Moreover, acute fallers have reported significantly more falls than 6-months based fallers as well ($p < 0.01$). Traditional clinical tests conducted in the FRA study could not significantly distinguish acute fallers from non-fallers although the values were indicating in the previous findings in the literature ($p = 0.17$, $p = 0.83$ and p 0.33 for SOMC, habitual gait speed and 30-seconds chair rise test, respectively).

Within defined groups, ratio of female participants in the analysis is slightly higher but still negligibly different. Another inconsistency is the allocation of the sensor system on the dominant and non-dominant side during the measurement week. No further differences were found in the collected anthropometric measures for acute FRA (Table 2). To conclude, acute fallers are definitely a distinct group of participants with emphasized differences in the number of falls although they have shown some association with recurrent fallers known also in the available literature. Thus, a clear objective parameters that could reflect their motor performance in the ADL is definitely worth investigating and will be addressed in this work throughout the methods described in the following chapters.

For the 6-months based FRA in total 145 participants were analysed. Thereof, 98 (67.6%) participants have reported no prospective falls in

the 6-months long follow-up phase, whereas 47 (32.4%) participants reported one or more falls. When applying the definition of a fall (3.1.2.1), 12 participants were reordered to the group of non-fallers (i.e. only 35 participants or 24.4% were identified as fallers). Furthermore, 14 participants (9.7% of the total number of participants or 40.0% of fallers) reported two or more falls in this phase (3.8 ± 2.3 falls with maximum of 10 falls).

Again, no significant difference was found in any of the collected anthropometric measures, as well as in the performed clinical tests (Table 2). Prospective falls were significantly higher for fallers than for non-fallers ($p < 0.01$). Moreover, as for the acute FRA the number of prospective falls was significantly higher than the number of reported retrospective falls ($p < 0.01$). Additionally, the 30-seconds chair rise test have yielded significantly higher results ($p < 0.01$) for this group of fallers as for the acute fallers (11.9 ± 3.0 and 13.5 ± 3.7 for acute and 6-months based fallers, respectively).

The alternative reference measures, FRAT-up and FRAQ, have shown good linear correlation (Pearson's $r = 0.77$, $p < 0.01$) for 6-months based FRA. The references have shown even slightly better correlation for fallers than for non-fallers ($r = 0.84$ and $r = 0.74$ with $p < 0.001$ for fallers and non-fallers, respectively). On the other hand, the same measures have shown moderate correlation for acute FRA (Pearson's $r = 0.60$, $p < 0.01$). Acute fallers were represented again with considerably better correlation of these measures than non-fallers ($r = 0.71$ and $r = 0.58$ with $p < 0.01$ for acute fallers and non-fallers, respectively). The statistical tests have not shown any significant difference between these two measures for any of the defined groups, although both values were higher for the participants at risk of falling.

In addition to visualize the distribution of participants in different groups a figure below is presented (Figure 9). The figure does not include the participants that were excluded willingly from the study or that had to be excluded due to total sensor malfunction during the measurement week. Additionally, it has to be noted that a significant number

of participants were not included in the analysis because they were younger than 65 years, but could be interesting in the future work where the focus can be on identifying the fall risk either during the fall-prone activities (as sport) or in the population between 50 and 65 years old that due to various medical conditions affecting motor performance are at higher risk of falling.

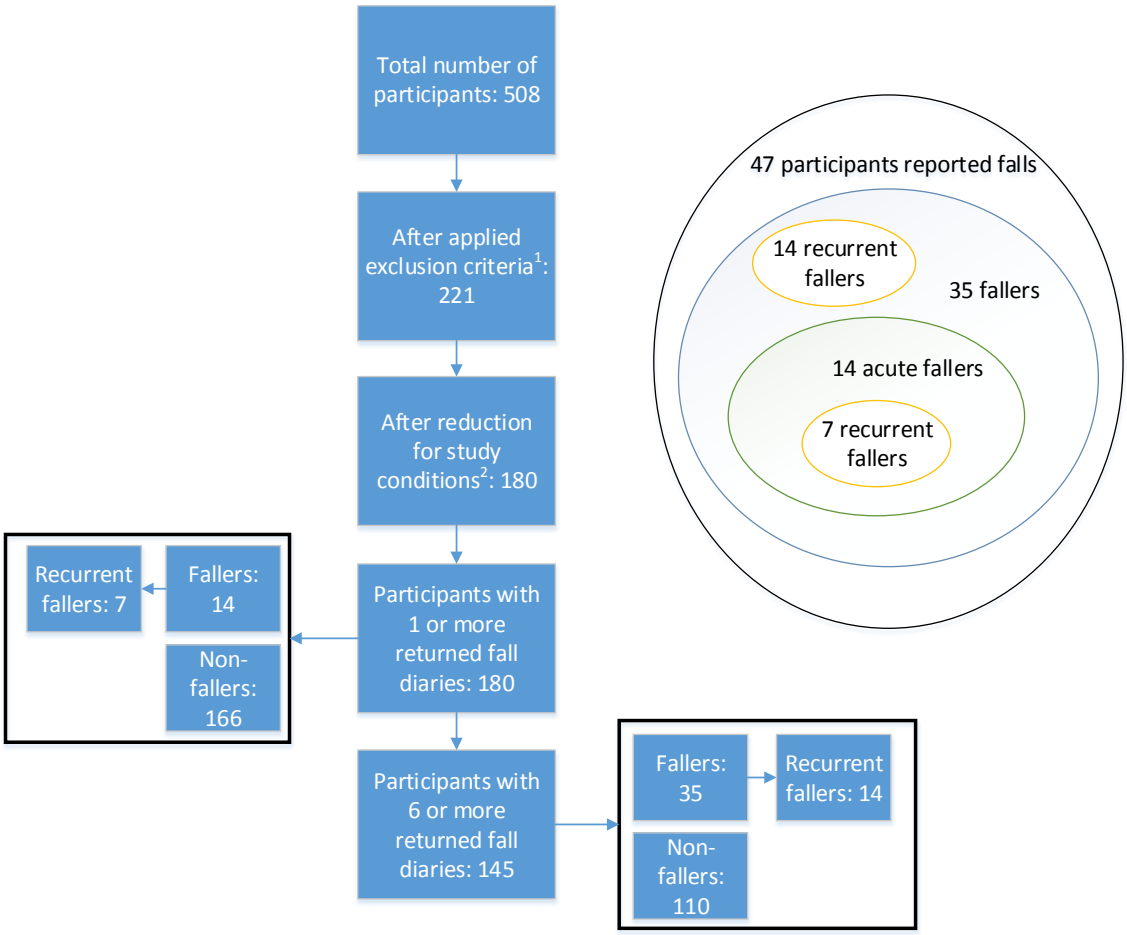

Figure 9 Distribution of participants in defined groups

Table 2 Participants' characteristics

	Acute FRA				6-months FRA			
Characteristic	All	Non-fallers	Acute fallers	p-values	All	Non-fallers	Fallers	p-values
N	180	166	14	-	145	110	35	-
Female, [%]	57.5	56.8	61.1	-	61.5	55.1	65.9	-
Sensor worn on dominant hand, [%]	49.4	48.7	55.6	-	46.9	44.9	51.1	-
Age, [years]	73.2±5.7	73.1±5.7	73.5±5.0	0.78	72.6±5.5	72.7±5.8	72.4±5.0	0.96
Height, [cm]	169.3±8.7	169.6±8.8	166.4±8.0	0.44	169.0±8.9	169.7±9.2	167.6±8.3	0.65
Weight, [kg]	73.7±13.8	73.7±14.0	73.9±11.9	0.83	73.6±14.4	73.4±13.7	73.8±15.9	0.91
[1]BMI, [kg/m²]	25.6±3.9	25.5±3.9	26.6±3.3	0.44	25.6±4.1	25.4±4.0	26.1±4.2	0.91
[2]SOMC [0-28]	3.0±3.2	2.8±3.1	4.7±3.7	0.17	2.9±3.1	2.7±3.0	3.2±3.2	0.96
Habitual gait speed, [m/s]	1.1±0.2	1.1±0.2	1.0±0.3	0.83	1.1±0.2	1.1±0.2	1.1±0.2	0.65
30 sec chair rise test, [n]	13.2±3.4	13.3±3.4	11.9±3.0	0.33	13.4±3.5	13.4±3.4	13.5±3.7	0.65
[3]FRAQ	3.5±2.7	3.4±2.5	4.3±3.5	0.63	3.4±2.4	3.3±2.4	3.5±2.6	0.96
[4]FRAT-up	0.3±0.1	0.3±0.1	0.3±0.1	0.38	0.3±0.1	0.3±0.1	0.3±0.1	0.72
Retrospective falls	0.3±0.5	0.3±0.4	0.5±0.5	0.17	0.3±0.4	0.2±0.4	0.3±0.5	0.65
Prospective falls	0.8±1.8	0.5±1.5	3.3±2.6	<0.01	0.8±1.9	0.3±1.7	2.1±2.0	<0.01

[1]BMI = Body Mass Index; [2]SOMC = Short-Orientation-Memory-Concentration test; [3]FRAQ = Fall Risk Assessment Questionnaire; [4]Fall Risk Assessment Tool

4 Preprocessing framework

Data acquired in clinical studies described in the chapter 3 was, in addition to conventional processing techniques (chapter 3.2), submitted to the process of wrist and waist sensor synchronization needed for the clock-precise inter-limb coordination assessment. A novel approach for clock synchronization of physically distant sensor nodes that cannot communicate with each other was described in this chapter. The sensor synchronization together with the video analysis of STST and transfer techniques (particularly from the wrist perspective) performed in the pilot study (chapter 3.1.1) compose a preprocessing framework for the algorithm development. The importance of these two steps is providing a solid evidence-based basis for algorithm development for STST detection in ADL, as well as support in a synchronized enhanced sensor-based approach for inter-limb coordination.

4.1 Clock synchronization of physically distant sensors

4.1.1 Implementation

In both studies, pilot and FRA, the human movement in terms of the FRA was observed with two physically distant sensor nodes, attached on the waist and wrist. As it was previously mentioned, the sensor nodes were not equipped with RTC or any other conventional method for data synchronization so alternative ways for precise clock synchronization of waist and wrist sensor data, especially acquired with sensor system revision equipped with the SD card, had to be found. The revision with SD card was even more critical since acquisition of data from utilised sensor nodes was started independently, whereas in the revision with a phone the start of acquisition was triggered by a start BLE package. More precisely, in the revision with SD card not even the starting mo-

ment for both sensor nodes was unique. End points in all revisions differed since they were depending on the sensor batteries' duration. In the thesis, the precise clock synchronization of waist and wrist data sets is critical for the inter-limb coordination assessment where a time delay between characteristic points in the arm swings and heel strikes was measured.

A method for synchronization of physically distant sensor nodes that cannot communicate with each other, nor with other devices or networks, was suggested in previous studies (O'Connor, 2013). The sensors were synchronized based on the correlation of the magnitude of the magnetometer signal, since the magnetic field within specific radius can be approximated as a constant. Although this method can be used for synchronization of sensor nodes that are distant up to one kilometre, in the environments with strong magnetic disturbances (e.g. caused by widely present electrical devices) the signal to noise ratio is significantly lower.

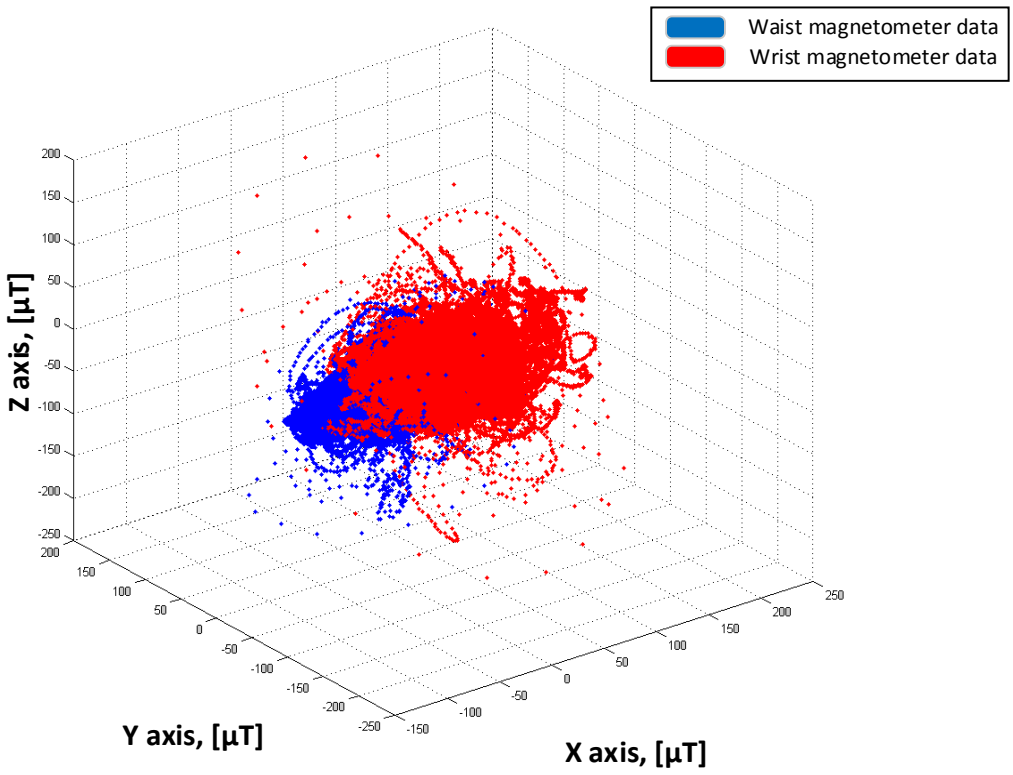

Figure 10 The 3-D plots of the magnetometer data acquired during eight hours of ADL

The effects of magnetic disturbances on the body-worn sensor nodes equipped with the magnetometer sensors can be seen in the Figure 10. The figure shows a three-dimensional plot of the three-axis magnetometer signals acquired at the waist and wrist during eight hours of continuous recording. In an ideal case the centre of these two signals should be in the centre of the coordinate system, while the signal samples should depict the sphere with constant radius, equal to the strength of the magnetic field (which varies between 25 and 70 μT depending on the geographical position). Moreover, the centre of each sphere is not just displaced in space with respect to the centre of the coordination system but they are also displaced with respect to each other indicating different sensor offsets due to different intensities of magnetic disturbances. Additional problem that was identified was high variability of the magnetometer magnitude caused by the sensor movement (e.g. in this particular use case when the sensors were attached on the body), as it can be seen in the figure below (Figure 11). Worth mentioning, despite temperature compensation of the magnetometer signal, its performance was dissatisfying for precise clock synchronization.

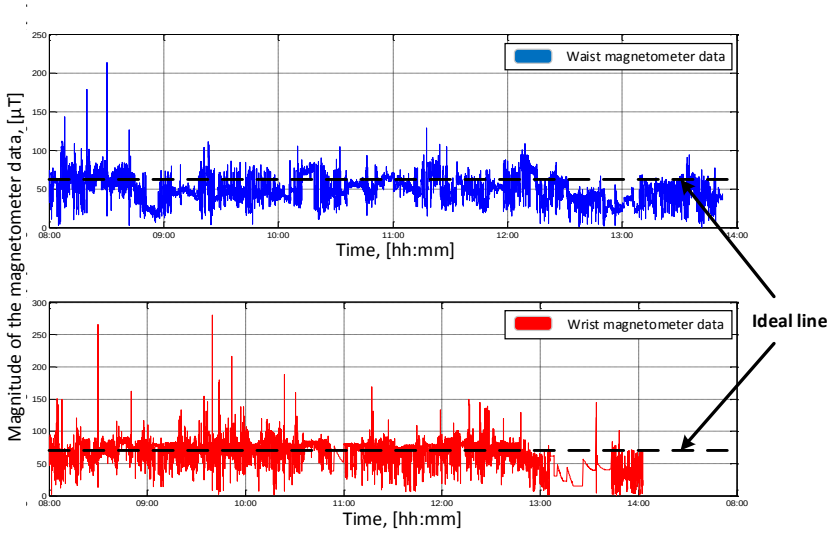

Figure 11 Variability of the magnitude of the magnetometer signal within a day of recording

Therefore, a strong motivation for an alternative approach for precise clock synchronization of two (or even more as in the case of the pilot study) physically distant sensor nodes attached at the human body was

identified. Pressure signals were considered for this purpose for multiple reasons. Firstly, pressure signals were temperature-compensated yielding small or no offset even during long-term measurements (e.g. during whole day of measurement). Secondly, the sensor placement spots on the human body were from the vertical perspective relatively close (up to one meter) and more importantly fixed so the offset in the pressure signals can be easily removed. Lastly, pressure signal was not affected by the human movement except in cases when a higher vertical differentiation was present, but even then the change was observed synchronously in all sensor nodes.

The proposed method can be split in the following six steps:

1. Two temperature-compensated pressure signals $p_{1,raw}$ and $p_{2,raw}$ are acquired from two sensor nodes with a sampling frequency of 1 Hz and then later on up-sampled, as it is currently done in both data collection studies described in chapter 3.1. Alternatively, they can be immediately acquired with a sampling frequency up to 100 Hz allowing signal alignment with resolution up to 10 milliseconds. The method is limited to body-worn sensors (human or animal) or in more general case on the devices that are with full body volume in the similar working (environmental) conditions. This means, all the sensor nodes equipped with the pressure sensors should be placed in the same room or in the environment with maximal vertical distance between sensor nodes (systems) of 10 meters. Additional specification is set here on the minimum time of the data acquisition. For the reliable sensor node synchronization the acquisition of the pressure signals should be no shorter than five minutes (equal to 300 samples at sampling frequency of 1 Hz or 30000 samples at sampling frequency of 100 Hz). Temperature-compensated pressure signals $p_{i,raw}$ contain measured pressure component $p_{i,ideal}$ multiplied by the sensor sensitivity S_i (for simplification in further text taken as $S_i = 1$), sensor offset $p_{i,offset}$ and noise n_i:

$$p_{i,raw} = S_i p_{i,ideal} + p_{i,offset} + n_i, \tag{3}$$

2. The acquired pressure signals should be up-sampled (interpolated) to the same sampling frequency of 100 Hz. This step also resolves a problem of possible data loss that can occur in cases of wireless data transmission or due to other sensor node errors. For the up-sampling process a linear interpolation was proposed although other methods can be used as well (e.g. polynomial interpolation or nearest neighbour method).
3. Since the air pressure changes with the height, to enable synchronization of the sensor nodes at different heights, the offset and influence of white (Gaussian) noise were removed (i.e. reduced) from (3) by the following equation:

$$p_{i,measured,k} = p_{i,raw,k} - \overline{p}_{i,raw,k}, i \in \{1,2\}, k \in \{1,2,...N\}, \quad (4)$$

   where N is the signal block length in samples, index i depicts particular pressure signal, while $\overline{p_{i,raw}}$ is the mean raw pressure value within defined signal block.
4. The cross-correlation signal *Acorr[n]* between the two discrete pressure signals is calculated as a function of delay:

$$Acorr[n] = \sum_{m=-\infty}^{\infty} p_{1,measured} * [m] p_{2,measured}[m+n]. \quad (5)$$

5. The delay (time displacement) L between these two signal is defined as a global maximum of the cross-correlation signal *Acorr[n]*:

$$L = \max(Acorr[n]). \quad (6)$$

6. Signals are aligned with respect to each other for the derived signal delay L.

The improvement that the proposed method delivers is visible in the figure below (Figure 12). The figure shows the cross-correlation signal of two magnetometer signals (blue line) and two pressure signals (red line) acquired during eight hours of continuous recording of daily life routine of an elderly person. The sensor nodes were attached on the wrist and waist. The significance in the global maximum of the cross-correlated pressure signals with respect to the global maximum of the cross-correlated magnetometer signals is clearly visible.

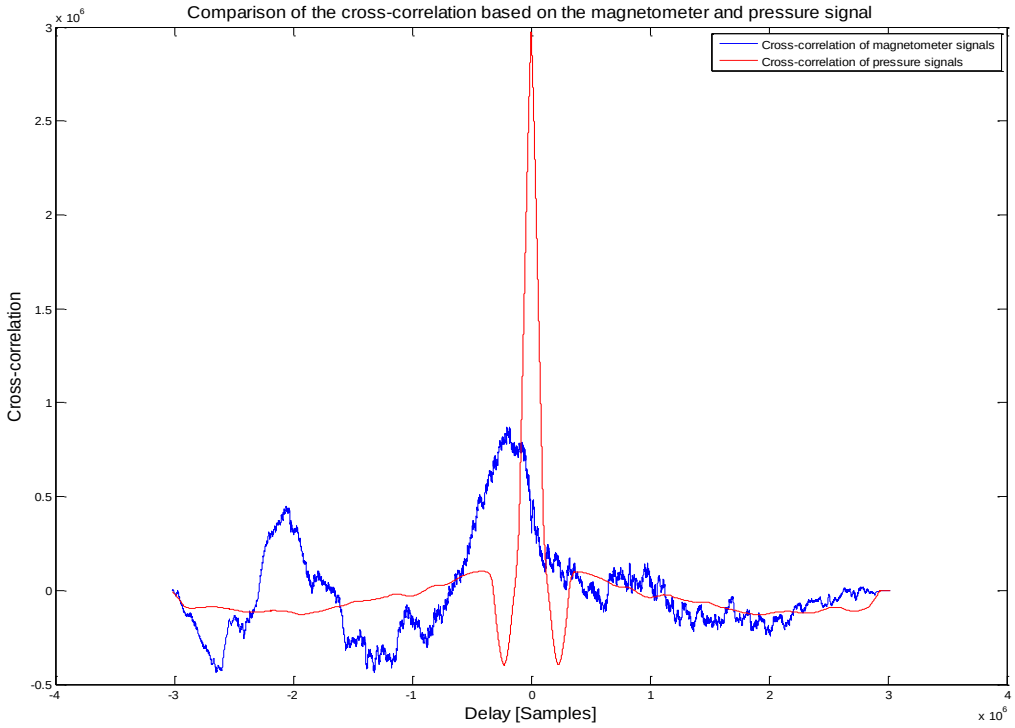

Figure 12 Cross-correlation based on the magnetometer and pressure signals

In comparison to other synchronization methods, the proposed method enables cheaper systems (no need for complex network synchronization or energy-consuming RTC), which is crucial especially for the wearables market. In addition to that it allows accurate synchronization (with resolution up to 10 milliseconds) which does not depend on the movement of the sensor (i.e. body where the sensor is attached) and magnetic disturbances. Moreover, to the best of the author's knowledge, this is the first method which uses pressure sensors for the clock synchronization. The method is suitable for both, real time synchronization (with a delay of minimum needed signal length) as well as for the offline synchronization of different sensor signals acquired with two or more physically distant sensor nodes.

4.1.2 Possible use cases

The proposed method is an important feature for the inter-limb coordination assessment where outputs of two physically distant sensor nodes

(one at the waist and one at the wrist) had to be synchronized in order to enable precise and reliable estimation of the time delays between arm swings and corresponding heel strikes. Furthermore, the method can be also used in numerous other medical and sport applications where the need for synchronous sensor approach is needed. Tracking of one's physical activity with multiple different sensors in ADL is one example. Often a disease progression (e.g. for neurodegenerative diseases) should be reliably monitored during longer time periods in order to determine effects of various drug treatments or apply additional interventions (Holford, 2006 & Ilg, 2009). Clinical assessments that currently rely on wireless network synchronization or synchronization over BLE (Mancini, 2016) are affected with disturbances in wireless connection, high network costs or complicated system configurations. Therefore the proposed method seems like a reasonable alternative choice.

Another intrinsic properties of wireless sensor networks such as limited resources of energy, storage, computational power and bandwidth combined with potentially high density of sensor nodes emphasize the advantages of the proposed approach above traditional synchronization methods. Synchronized sensor approach can also be potentially applied in studies on animal behaviour and movement. For example, an application for monitoring wildlife passages as suggested in (Garcia-Sanchez, 2010) could be further improved with the proposed approach since it can significantly prologue the sensor life time. Accurate time synchronization of the sensor nodes that assumes continuously connected nodes, as in the example of the wild rat movement observation (Landsiedel, 2006), can be easily improved with this method since no physical connection nor equal active time of all sensor nodes included in the network is needed. As already mentioned before, the application of this method can be further extended in the heavy industry and transportation where a lot of extrinsic disturbances are present. Even the conditions with high temperature changes are applicable since the pressure signals are temperature-compensated.

4.2 Video analysis

To support the idea of the implementation of the transition detection algorithm based on the wrist-acquired movement signals, a video analysis of the transitions recorded in the pilot study explained in 3.1.1 was performed. From the whole pilot study, 72 transitions (one third of all performed transitions) were randomly selected and analysed independently by the author of this text and another blind peer reviewer. Randomly selected transitions covered 12 different participants, from which seven were classified as non-fallers and five were classified as fallers. Recorded videos were analysed by using an in-house tool implemented in LabVIEW, which enables video frame-wise analysis. Results from both reviewers were compared and the differences were discussed in the meeting that followed the next day in order to meet the final decision.

All eight different types of transitions performed in the pilot study were analysed. For each transition five different parameters were analysed:

- Existence of the hand movement prior to the transition;
- Existence of the hand movement posterior to the transition;
- Usage of hands for support during transition;
- Existence of the rotation in the wrist during transition;
- Duration of the rotation in the wrist.

Although there is still no general consensus about the definition of STST, particularly in the unsupervised non-ambulatory environment, clinically every STST can be split into four main phases (Schenkman, 1990):

- Flexion (leaning forward);
- Momentum-transfer (seat-off);
- Extension (returning to upright position);
- Stabilization phase.

The transitions described by this definition are rather rare in the home environment, mainly because they are often followed by a walking phase. As suggested in (Iluz, 2015), most common transitions in normal

daily routine are sit-to-walk (STW) transitions, where walking continues directly after the extension phase, skipping the stabilization phase. In these cases the initialization of the first step takes place at the same time when centre of mass reaches the highest vertical point in the transition during extension. This movement requires very good coupling of both, upper and lower limbs. Weaker inter-limb coordination is characteristic for the elderly population at high risk of falling (Pozaic, 2015), thus these STW transitions are interesting for investigation in terms of FRA. The hereby exposed conventional definition of STST was used in the video analysis.

Transition duration (i.e. its starting and ending points) were defined from the perspective of one's centre of mass as explained in 3.1.1.2. Existence of the hand movement prior and posterior to the transition was graded positively when a movement unrelated to the corresponding transition happened within two seconds before the start of the flexion or after the end of the stabilization phase (i.e. with the first heel strike for STW). The results of the video analysis have shown that prior hand movements happened in 26.4% of transitions whereas posterior hand movements were present in 76.4% of transitions. In 22.2% of transitions both, prior and posterior hand movements were present. Prior hand movements mostly included repositioning of the body for the transfer or taking a swing for standing up, while posterior hand movements included broad spectrum of different activities (e.g. reaching for something, random arm swings, holding the balance, carrying or holding something in hands, starting directly to walk etc.). The analysis showed that fallers contributed to results for prior hand movements significantly more ($p < 0.01$) than non-fallers (i.e. prior hand movement was detected in 40.0% of performed transitions by fallers versus 16.7% by non-fallers). This suggests that triggers for prior hand movements should be looked for in the root causes for increased risk of falling. Contrary to prior hand movement, posterior hand movement did not reveal any significant difference between the groups. Fallers performed posterior hand movements in 80.0% of transitions, whereas non-fallers in

73.8%. Nevertheless, the exact reason for this behaviour remains unclear within the scope of this thesis, but it is definitely worth investigating in a prospective study.

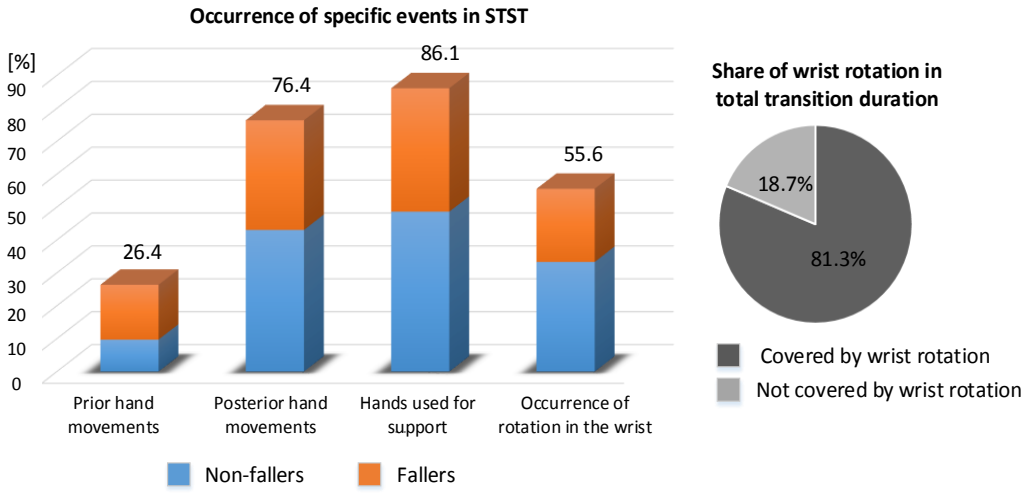

Figure 13 Occurrence of the specific empirically observed movement patterns in transitions

Despite the fact that participants in the study were explicitly instructed to use their hands for support during the transition in only two cases (25.0% of all transitions), video revealed that hands were used as a support during standing up in 86.1% of transitions. Participants were supporting themselves using armrests, thigh, chair, table or their personal walking aid (walking stick, walker or crutches). Fallers used their hands for support more frequent than non-fallers (90.0% versus 83.3%), which correlates with the previous findings in the literature regarding severe lower limb weakness and correspondingly adopted transfer techniques (Dolecka, 2015). Use of hands for support while standing up, especially in a population at higher risk of falling, indicates the need for further analysis of the standardized clinical test for fall risk assessment, such as 5-times-sit-to-stand (Buatois, 2008). Although this test shows good discrimination abilities in terms of the fall risk, it disregards the influence of the upper limbs in the overall performance.

During the transition, a rotation in the wrist that follows the movement of the centre of mass was present in 55.6% of cases. The rotation in the wrist was detected when the relative change around one of the axes of

the local coordination system of the wrist sensor exceeded 80°. Moreover, this rotation occurred around AP or VT body axis. Often a combination of these two rotations occurred. Further analysis has shown that from the temporal perspective, rotation in the wrist covers on average 81.3% of the actual corresponding transition (Figure 13).

Although fallers performed significantly slower transitions than the non-fallers ($p < 0.01$), which corresponds to previous literature findings (Zijlstra, 2014), no difference was found in the ration between duration wrist rotation and total transition ($p = 0.67$) for these two groups (Figure 14). These findings strongly support the thesis of possible implementation of the algorithm for the detection of sit-to-stand transition on the wrist, despite the distance from the centre of mass. Moreover, even slower transitions characteristic for the population at high risk of falling are well covered with a rotation in the wrist, thus enabling a reliable estimation.

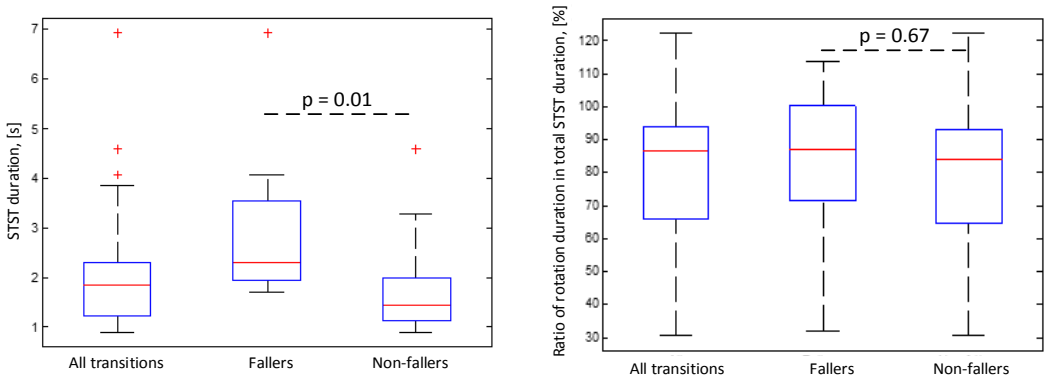

Figure 14 Ratio of the wrist rotation while standing up relative to the total STST duration

5 Algorithm development

The main focus of the thesis is algorithm development for assessment of the three main motor aspects of human movement: gait, inter-limb coordination and postural transfer. Postural stability, although very important for one's physical performance, and following that, for the assessment of risk of falling, was out of scope in the thesis. Multiple reasons justify this decision: prevailing number of falls happens during gait and transfer (Rapp, 2012) for which a good inter-limb coordination is necessary, clinical test that assess only gait can acceptably discriminate fallers from non-fallers (Barry, 2014), whereas assessment of balance (i.e. posture stability) far away from the centre of mass (at the wrist) has very little logical sense when focusing on the clinically relevant interpretations of results.

The following chapter describes different approaches for gait, inter-limb coordination and transfer assessment: from perspective of one sensor or by using the combination of sensors. While inter-limb coordination was assessed by combination of different time-series features targeting pace and asymmetry of one's movement, gait analysis was assessed by various non-linear measures (chapter 5.2). Inter-limb coordination assessment, divided into lower-limb and upper- to lower-limb coordination is described in the chapter 5.1. Additionally, enormous focus was given to analysis of the sit-to-stand movements. The transfer movement requires good coupling of both, upper and lower limbs, thus perfectly reflecting the inter-limb coordination assessment. The sit-to-stand transition assessment can be divided into sit-to-stand transition detection (5.3.1) and quantitative assessment of this movement (5.3.2). Most importantly, it is focused only on the wrist-attached sensor. Quantitative assessment of transitions was firstly addressed with the method that was translated directly from the waist-attached sensor (5.3.1.1) estimating their duration as a good fall predictor. Lastly, the assessment was improved with numerous features (5.3.2.1 and 5.3.2.2), including

the novel approach based on the amount of the applied support while standing up (5.3.2.3). Summary of these steps can be seen in Figure 15.

At the end of this chapter, models based on the support vector machine incorporating extracted time and frequency domain features were derived (chapter 5.4). The models were describing the non-linear relationship between acute fallers and non-fallers, as well as between 6-months based fallers and non-fallers.

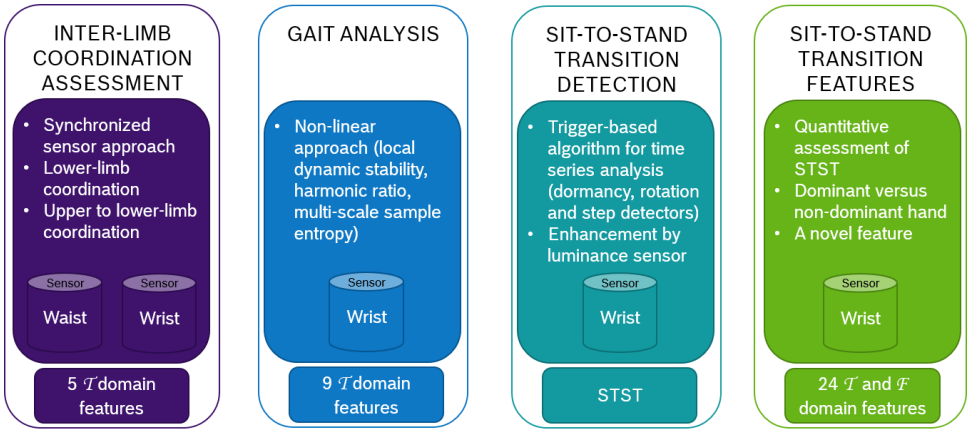

Figure 15 General approach in the algorithm development process

5.1 Inter-limb coordination assessment

The algorithm for the inter-limb coordination assessment comprises of the lower-limb and upper- to lower-limb coordination assessment. Lower-limb coordination assessment was performed only with the waist-attached sensor node, while upper- to lower-limb coordination was performed with the whole sensor system (waist and wrist sensor nodes). The flowchart of this algorithm is shown in the figure (Figure 16). In the first step the preprocessed synchronized wrist and waist acquired data is taken through the step and arm swing detectors after which the bout selection process started. Only selected gait bouts were used for the coordination assessment. As the final result, five features (step time variability, swing phase time variability, inter-limb coordination index, ipsilateral coordination index and contralateral coordination index) were chosen for the quantitative assessment of the inter-limb coordination.

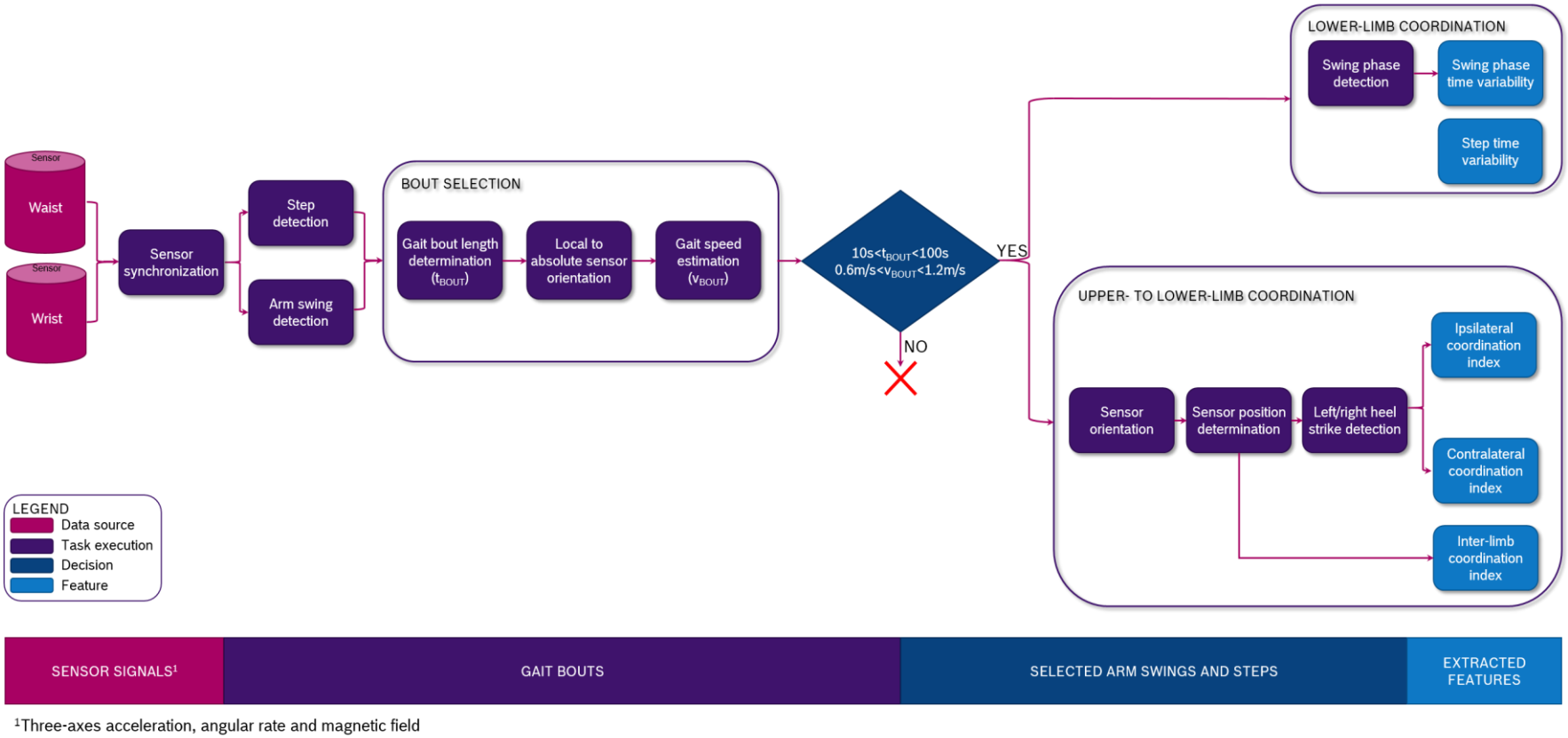

[1]Three-axes acceleration, angular rate and magnetic field

Figure 16 Inter-limb coordination assessment flowchart

5.1.1 Step detection

Step detection topic has been of interest for researchers and engineers for many years. Despite that, an optimal solution for the elderly population with a wide range of physical performance, as in the FRA study, has not been found yet. The most common trade-off is between the computational power (crucial for embedded systems) and adaptability (crucial for the elderly population). Furthermore, detection of steps using only a wrist-worn devices has shown in previous studies a poor consistence with the results from the waist in both, laboratory controlled environment and free-living conditions (Tudor-Locke, 2015). For the clinically relevant results that could lead to meaningful interpretation of the enclosed results, a reliable step detector has to be developed.

An analysis of three different algorithms (Pan-Tomkins, template matching method and peak detection based on combined dual-axial signals) in (Pan, 1985) has shown that peak detection algorithm provides the best performance and it can be easily written in the fixed-point arithmetic. Nevertheless, fluctuations in the signal can still yield with false detected steps, while self-adaptability is limited making recognition of variable walking intensities characteristic for the elderly population difficult. Thus, the need for a step detector with higher adaptability is still well expressed.

Step detector used in this study was implemented by using the Euclidean norm of the three-axial acceleration signal. To increase its adaptability, detection of steps was based on the consecutive detection of local maxima and minima points within defined time frame of the signal. Local maxima was detected when the signal was above the 50% of the signal dynamics, while local minima was detected in the time frame when the signal is below 50% of the signal dynamics (depicted with corresponding envelopes). The local maximum for the waist-worn device depicts the moment in the gait cycle that corresponds to the heel strike. This basic algorithm's principle was taken from (Pasolini, 2007). Since a single step can be characterized by several close peaks, there is a

mechanism that bans maxima for a certain time after maximum was found. The ban time is derived by the maximum step frequency that could be detected. Maximum step frequency was set empirically to 3 Hz, which enables detection of 3 steps/s for the waist-worn sensor or, taking into account average step length of 0.8 m, maximum detectable gait speed of 2.4 m/s (Peel, 2012). Additionally, derived minimum and maximum envelope of the whole signal were weighted by the delta-factor. For optimization purposes, the update of the envelope was empirically set to the decreased frequency of the input signal for factor four. The delta-factor defines the minimum needed distance between detected local maxima and minima after which they are considered as a part of the step. Since delta factor is dynamically shaping the amplitude of the signal envelope, it assures additional high adaptability to different gait intensities, as well as it increases algorithm's precision.

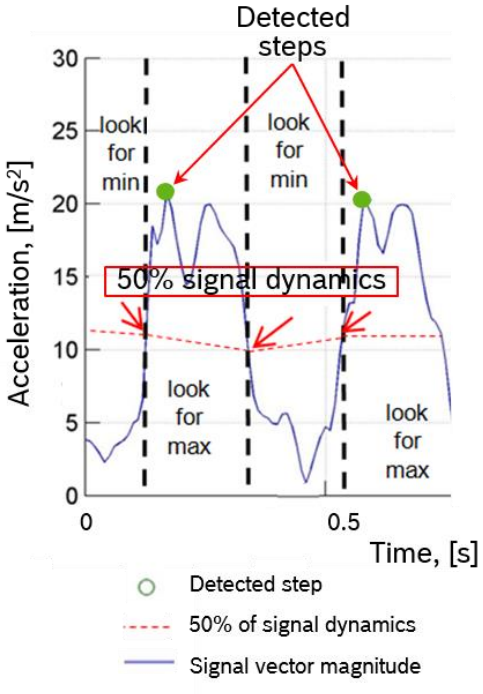

Figure 17 Step detection principle

Furthermore, high performance of the implemented step detector is based upon the definition of a walking flag (in addition to the validation flag defined in the chapter 3.1.2.3). Walking flag is set once the step detector's algorithm has detected three or more consecutive steps within

defined maximum time frame. Steps are defined as consecutive if the maximum time frame between them is lower than maximum allowed step duration set empirically to two second. As support for the definition of this constant, findings in (Hollman, 2011) can be used where it has been shown that average step duration in elderly population is 1.7 seconds for men and 1.9 seconds for women. Flow of the step detection algorithm explained in this paragraph can be followed also in the picture above (Figure 17). Whole processing in the step detector was based on the sliding window (sample-based processing), thus for the high performance it was implemented in C++ and then further used as a MEX-file in the MATLAB framework (3.2).

5.1.2 Gait bouts

A gait bout is defined as the time between start and end of walking. Start of walking is depicted with a rising edge on the walking flag (i.e. with at least three consecutively detected steps), while end of walking is depicted with a falling edge on the walking flag (i.e. no steps detected for maximum step duration time).

Walking in a non-ambulatory environment is often intersected by different other activities (e.g. standing or posture transfer). Previous study focused on analysis of human gait bout length in the daily life activities have shown that 60% of all gait bouts lasted 30 seconds or less (Orendurff, 2008). More precisely, 40% of all walking bouts were less than 12 steps in a row, and 75% were below 40 steps in a row. Eight weeks of remote monitoring of elderly adults has shown that step time variability follows a log-normal distribution, while its mode is significantly lower in non-fallers than in fallers (Brodie, 2015). Although, 50% of exposure to walk-related falls resulted from gait bouts shorter than 13.1 seconds, dropping the threshold for a gait bouts below six steps increases false positive errors. Proposal by (Brodie, 2015) was on analysis of gait quality on gait bouts of at least eight consecutive steps, offering a steady balance between number of gait bouts and low false positive error. Unfortunately, general consensus about the gait bout length despite these

findings has not been met yet. In studies from the Dutch group (Schooten, 2015) gait bouts longer than 10 seconds for analysis of the gait quality in terms of the fall risk assessment were used. On the other hand, research group in (Punt, 2015) analysed gait bouts above 30 seconds, whereas (Ihlen, 2015) focused on those above 60 seconds.

Motivated by the fact of prevailing small number of gait bouts longer than 30 seconds for elderly population, especially for those at risk of falling, further analysis of the inter-limb coordination was performed on gait bouts with length between 10 and 100 seconds. Upper threshold for the length of the gait bouts was defined in order to make the comparison between different lengths more consistent as proposed in (Brodie, 2015).

When analysing gait bouts from the ADL, one has to take into account a possible influence of different living conditions (house versus apartment), different walks indoors (uphill, downhill), as well as variability of different weather conditions (sun, rain, snow). For now, all these gait bouts were analysed equally.

5.1.3 Local to absolute orientation (Euler angles)

Inertial sensors (accelerometer, gyroscope and magnetometer) used in this study provide raw data in three perpendicular axes of their local coordination system. A 4-D vector of the inertial sensor data can be described as:

$$s_{\omega} = \begin{bmatrix} 0 & \omega_X & \omega_Y & \omega_Z \end{bmatrix}, \tag{7}$$

$$s_{a} = \begin{bmatrix} 0 & a_X & a_Y & a_Z \end{bmatrix}, \tag{8}$$

for the gyroscope and accelerometer data, respectively. In order to determine the absolute orientation of attached sensor nodes in the Earth's geodetic system, a transformation of raw acceleration data using well-known Euler angles was implemented. Namely, the relative change of the geodetic coordination system to the sensor system in a moment Δt

can be described as the quaternion product of the normalised sensor system and gyroscope vector (Madgwick, 2011):

$$q_{t_0+\Delta t} = \frac{1}{2} q_{t_0} \otimes s_{\omega} \tag{9}$$

where q_{t_0} is an initial guess of the quaternion vector $[q_1 \quad q_2 \quad q_3 \quad q_4]$. An error of estimation corrected by the step-size μ is calculated based on the gradient-descent algorithm as:

$$q_{t_0+\Delta t} = \frac{1}{2} q_{t_0} \otimes s_{\omega} - \mu \frac{\nabla f}{\|\nabla f\|} \tag{10}$$

where ∇f is a change of the object function f defined as quaternion product of the initial normalized guess $\hat{q}_{t_0}$, global orientation of the sensor $\hat{d}$ and normalized measured acceleration values s_a:

$$f = \hat{q}^* \otimes \hat{d} \otimes \hat{q} - s_a . \tag{11}$$

The change of the object function is defined with its Jacobian

$$J = \frac{df}{dx} = \begin{bmatrix} \frac{\partial f}{\partial q_1} & \frac{\partial f}{\partial q_2} & \frac{\partial f}{\partial q_3} & \frac{\partial f}{\partial q_4} \end{bmatrix} \tag{12}$$

via quaternions:

$$\nabla f = J^T f = \begin{bmatrix} -2q_3 & 2q_4 & -2q_1 & 2q_2 \\ 2q_2 & 2q_1 & 2q_4 & 2q_3 \\ 0 & -4q_2 & -4q_3 & 0 \end{bmatrix}^T \begin{bmatrix} 2(q_2 q_4 - q_1 q_3) - a_x \\ 2(q_1 q_2 + q_3 q_4) - a_y \\ 2(\frac{1}{2} - {q_2}^2 - {q_3}^2) - a_z \end{bmatrix}. \tag{13}$$

Finally, solving (10) with (13), the change of the quaternion values based on the inertial sensor data can be described with:

$$q_{t_0+\Delta t} = \frac{1}{2} q_{t_0} \otimes s_{\omega} - \mu \frac{J^T f}{\|J^T f\|} . \tag{14}$$

Furthermore, Euler angles (yaw ψ, pitch θ and roll φ) are then derived from quaternions as (Madgwick, 2012):

$$\begin{bmatrix} \phi \\ \theta \\ \psi \end{bmatrix} = \begin{bmatrix} \arctan \dfrac{2(q_1 q_2 + q_3 q_4)}{1 - 2({q_1}^2 + {q_2}^2)} \\ \arcsin(2(q_1 q_3 - q_4 q_2)) \\ \arctan \dfrac{2(q_1 q_4 + q_2 q_3)}{1 - 2({q_3}^2 + {q_4}^2)} \end{bmatrix}. \quad (15)$$

The Euler angles describe the orientation of the sensor's local system in relation to the geodetic coordination system. Interpretation of these angles is shown in the figure below. The yaw angle describes the orientation around the vertical global axis (X axis), roll is the angle around the horizontal axis (Y axis), while pitch angle is the angle from the XY plane.

The relation between geodetic coordination system and local system values measured by the attached sensor system is described with a Yaw-Pitch-Roll angle rotation matrix M_{YPR} defined by standard convention's ("x-convention") rotation order:

$$a_{t_0} = {M_{YPR}}^{-1} {a_{t_0}}', \quad (16)$$

where a'_{t_0} is one sensor sample at moment t_0, a_{t_0} is the corresponding sample in the geodetic coordination system and ${M_{YPR}}^{-1}$ is the inverse of the rotation matrix. M_{YPR} is defined as:

$$M_{YPR} = \begin{pmatrix} 1 & 0 & 0 \\ 0 & \cos\phi & \sin\phi \\ 0 & -\sin\phi & \cos\phi \end{pmatrix} \begin{pmatrix} \cos\theta & 0 & -\sin\theta \\ 0 & 1 & 0 \\ \sin\theta & 0 & \cos\theta \end{pmatrix} \begin{pmatrix} \cos\psi & \sin\psi & 0 \\ -\sin\psi & \cos\psi & 0 \\ 0 & 0 & 1 \end{pmatrix} \quad (17)$$

.

Although the extended derivation of quaternion from the inertial sensors is described also using the magnetometer sensor, only the simplified version with acceleration and gyroscope was used since empirically (chapter 4.1) it has been shown that magnetometer sensor is influenced significantly by the magnetic disturbances in the non-ambulatory environment of participants (e.g. from the mobile phone) and thus application without it can imply more consistent results than the application with it.

5.1.4 Gait speed estimation

Once the acceleration in global coordination system was calculated, it was possible to focus on determination of the real horizontal gait speed of the monitored participant. Only the horizontal acceleration was extracted for these purposes. The raw accelerometer output can be modelled as a_t:

$$a_t = a_g + a_d + n_a \tag{18}$$

where a_g is the gravitational vector, a_d is the acceleration disturbance and n_a is the white (Gaussian) noise of the accelerometer. In order to remove tilt (a_g) from the acceleration signal, a following filter proposed in (Moe-Nilssen, 2002) was applied:

$$a_{t_k,filt} = \frac{a_{t_k} - \bar{x}_a}{\cos(\arcsin(\bar{x}_a))} \tag{19}$$

where x_a is horizontal acceleration signal defined for *N* number of samples as:

$$x_a = \left[a_{t_0} \dots a_{t_k} \dots a_{t_N}\right]. \tag{20}$$

The a_{t_k} depicts the sample of the horizontal acceleration in moment *k*, while $a_{t_{k,filt}}$ is filtered sample in the same corresponding moment. Subtractor $\overline{x_a}$ in (18) is a mean value of the horizontal acceleration for the defined sliding window of length *N*. Additionally, to reduce the influence of the high frequency noise components in n_a, the signal was further filtered with a low pass FIR filter with a rectangular impulse response (i.e. moving average filter) defined as:

$$h[n] = \frac{1}{M}\sum_{k=0}^{M-1}\delta[n-k] \tag{21}$$

where *M* was empirically set to 51, defining a 50th order FIR filter.

Filtered acceleration signal was then integrated on the full length (Δt_x) of the gait bout deriving the velocity signal x_v as:

$$x_v = \Delta t_x \sum_{k=0}^{N-1} x_{a_{k,filt}} \ . \tag{22}$$

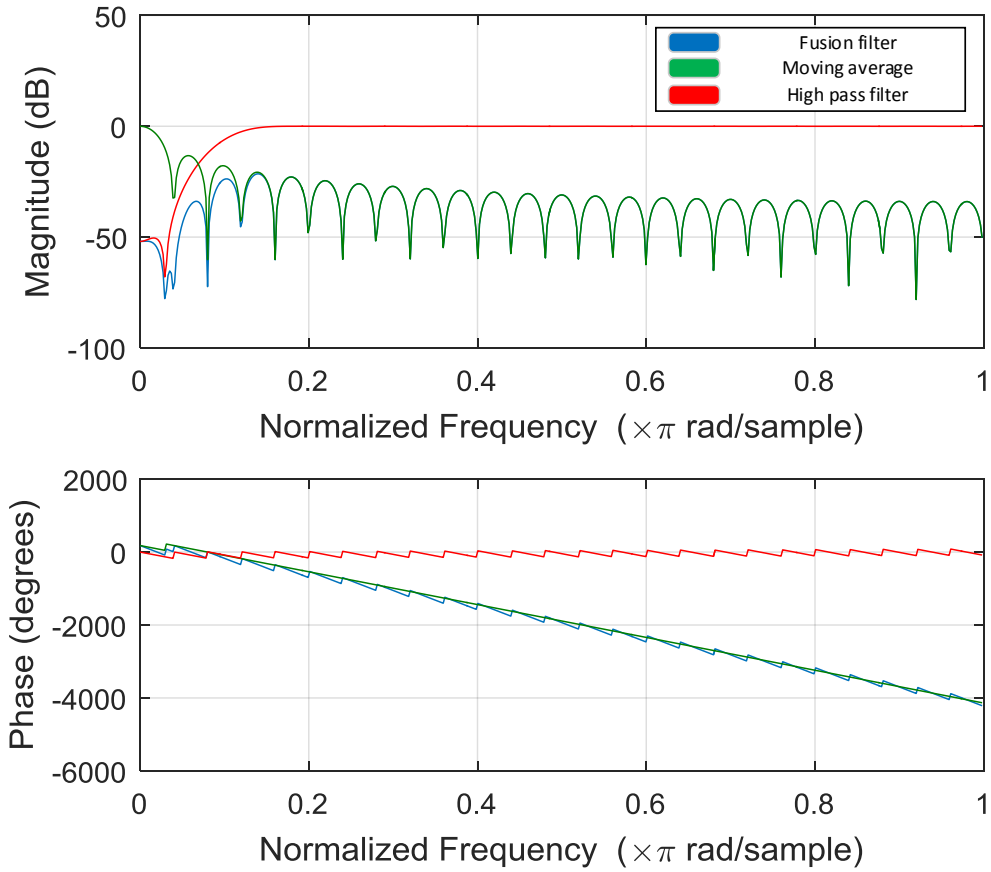

Figure 18 Frequency response of the applied filters

The frequency and phase response of the applied filters can be seen in the Figure 18. Their effects to the integrated acceleration signal compensated for the tilt and noise can be seen in the Figure 19. Since only gait bouts with duration between 10 and 100 seconds were used for the analysis of the inter-limb coordination, short possible brakes between particular steps in the gait bouts can, despite the applied filters, still induce significant signal drift during the integration process. Therefore, each point which corresponds to the moment in the gait cycle when a foot is on the ground (i.e. stance phase) was initialized to the gait velocity equals to 0 m/s. Furthermore, only the maximum relative change of velocity to this point in the following swing phase was noted. The analysed gait bouts were then approximated linearly with gait velocity which is equal to the mean value of calculated gait velocities for each

step in the integration process. Possible alternative to this solution of estimating the gait velocity from the acceleration signal could have been application of linear Kalman filter, which has shown good performance in previous studies (Grewal, 2001), but due to the higher computational power needed and questionable correction of the initialization error this approach has not been used nor validated.

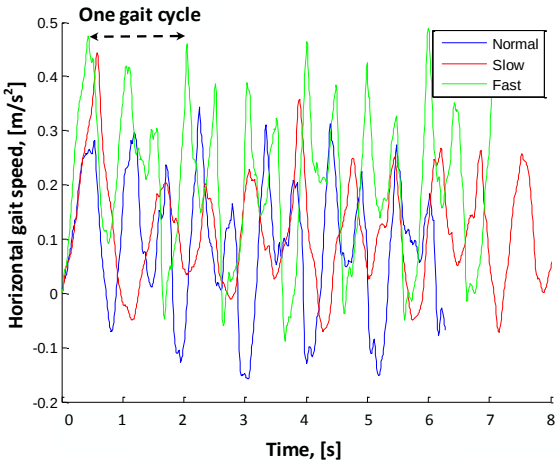

Figure 19 Horizontal gait speed derived from gait bouts performed at different paces

Previous systematic review of the gait velocity values for long term care residents, which are at higher risk of falling, has shown that mean gait velocity in clinical setting is 0.58 m/s (Kuys, 2014), as well as it is significantly lower than in community-dwelling older adults (Peel, 2012). Moreover, slow gait velocities have also been related to the higher risk of institutionalization and mortality. Thus, only gait bouts with mean gait velocity within corresponding bout between 0.6 m/s and 1.2 m/s were taken into further consideration.

5.1.5 Lower-limb coordination assessment

Gait cycle of human walking can be split into stance and swing phase, where swing phase starts with toe-off and ends with a heel strike. Since left and right swing phases (thus also swing times) are biomechanically independent, swing phase time variability (SPV) provides a measure of temporal left-right asymmetry (Yogev, 2007). Furthermore, and espe-

cially for walking while dual tasking, difference between swing time variability and step time variability is thus bigger since the stance time is increasing. From another side, step time variability (STV) is a feature that has been shown a remarkable performance in distinguishing between fallers and non-fallers in numerous studies (Toebes, 2012). Its value has been intriguing researchers also in ADL, where the most important undefined question is the minimum number of steps of a gait bout needed for reliable and clinically relevant assessment of step time variability.

Following this, lower-limb coordination was assessed with both features, STV and SPV. Step time is the time difference between two consecutively detected heel strikes. STV is defined as the variance of the step time duration t_{STV} within each gait bout with equation:

$$STV = \frac{\sum_{i=1}^{N}(t_{STV,i} - \overline{t_{STV}})^2}{N-1} \tag{23}$$

where $\overline{t_{STV}}$ is the mean step duration within particular gait bout and N is the number of detected steps in this bout. Heel strikes were detected from the acceleration signal acquired from the waist attached sensor by using the previously described step detector.

Swing time is defined as the time between the moment when the whole foot hits the ground (i.e. flat foot phase) and the moment when opposite leg does the heel strike. In normal human gait, swing time takes around 60% of total gait cycle, while for the elderly population this ratio is reduced (Plotnik, 2013). SPV is then defined as the variance of the swing phase duration t_{SPV} for each particular foot with the following equation:

$$SPV = \frac{\sum_{i=1}^{N}(t_{SPV,i} - \overline{t_{SPV}})^2}{N-1} \tag{24}$$

where $\overline{t_{SPV}}$ is the mean swing phase duration of particular gait bout and N is the number of detected steps in this bout. For detecting the swing phase in the gait cycle, the step detector was further extended so it meets the performance shown in the figure below (Figure 20). Once the

heel strike is detected, the step detector searches for the first local minimum in the AP acceleration signal, which depicts the moment when the whole foot is on the ground. This local minimum should happen within defined time interval from the heel strike (empirically set to 0.2 s) and it should be below the 50% of the value of the amplitude of the corresponding step.

This point in the signal depicts the start of the stance phase for one foot and start of the swing phase for another foot. End of the swing phase is depicted with the next detected heel strike. Moment between the heel strike and flat foot is moment of double support, more precisely moment when both feet are on the ground. In case when the next heel strike did not happen (end of gait bout) or was not detected (due to different interferences), the corresponding swing phase is not taken into calculation nor further analysis.

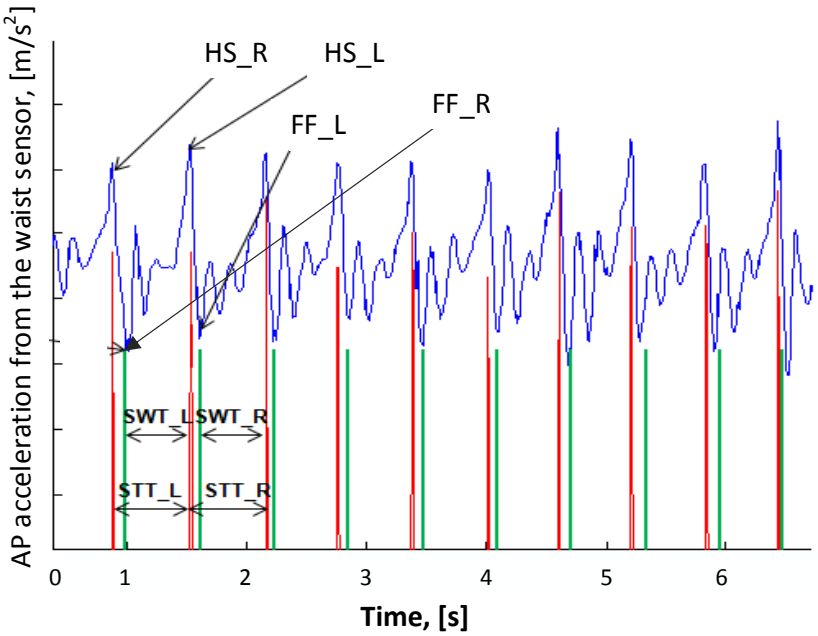

Figure 20 Swing phase detection from the waist-worn sensor node

Critical point in the reliable estimation of the swing phase duration is in correct determination of the AP acceleration. This was enabled throughout the determination of absolute orientation of the waist sensor in space by using the approach explained in 5.1.3.

It is important to emphasize that both features, STV and SPV, were calculated on all steps within one defined gait bout independently on whether this was a left or right step. Moreover, these features were extracted from the acceleration signal acquired at the waist since in terms of the inter-limb coordination this place of attachment reflects the real movement significantly better than the one at the wrist (Tudor-Locke, 2015).

5.1.6 Upper to lower-limb coordination assessment

Although, STV and especially SPV features have shown good performance in assessment of temporal step-to-step variations (i.e. coordination), there are two major problems identified in the literature. First problem is inability to distinguish between left and right foot performance, which can be especially interesting in patients with Parkinson's disease or post stroke population where one side of the body can be significantly altered in comparison to another and thus disregarded (or more precisely diminished) in the final evaluation. Second problem is in not taking the arm performance into consideration, which can also be influenced by different clinical conditions (e.g. tremor).

In order to overcome these two problems, an upper to lower-limb coordination assessment based on three different features was proposed. The features were as follows: inter-limb coordination index (IC), ipsilateral coordination index (YC), and contralateral coordination index (CC). IC was defined as the mean time delay between the highest points in the arm swing (t_{arm_swing}) and corresponding heel strikes (t_{heel_strike}) within one selected walking bout. In other words, the time delays were taken between highest backward arm swing and heel strike from the ipsilateral foot, as well as between highest forward arm swing and heel strike from the contralateral foot. Heel strikes were extracted from the waist-worn acceleration sensor, while arm swings were extracted from the wrist-worn acceleration sensor. Same principle that was used for detection of heel strikes was also used for detection of the characteristic points in the arm swings, with difference that for the arm swing only the

anterior-posterior acceleration axis was used. Forward arm swings were depicted with local maxima, while backward arm swings were depicted with local minima in the anterior-posterior acceleration signal.

In other words, IC can be defined with the following equation:

$$IC = \frac{1}{N}\sum_{k=1}^{N}\left(t_{heel\_strike,k} - t_{arm\_swing,k}\right) + \frac{1}{N}\sum_{k=1}^{N} n_k \ . \tag{25}$$

In this equation, n_k depicts the noise in the measurement caused by faulty arm or heel strike detection, as well as deviations in the sensor synchronization. One can assume the Gaussian (normal) distribution of this noise with the mean value equal to zero and variance N_S. Taking into consideration this distribution of possible time delays between upper and lower extremities, as it has been also shown in (Stephenson, 2009), one could also redefine equation (25) to the mean absolute time delay between the heel strike and corresponding arm swing, disregarding the fact of variations in consecutive order. Moreover, IC as well as other two indexes could be defined over the median values but in that case an influence of possible extreme values on the final result would have been reduced. Since the calculation of these indexes is already done on the walking bouts longer than 10 seconds, a certain degree of variability necessary for analysis of the coordination is still maintained by this choice.

YC was defined as the mean time delay between the highest points in the backward arm swings (t_{arm_bwd}) and the heel strikes of the ipsilateral foot (t_{heel_strike}). Following this definition and taking into consideration the assumption in (24), YC can be defined with the following equation:

$$YC = \frac{1}{N}\sum_{k=1}^{N}\left(t_{heel\_strike,k} - t_{arm\_bwd,k}\right), \begin{cases} t_{heel\_strike}, ipsilateral\_heel\_strike \\ 0, otherwise \end{cases} . \tag{26}$$

CC was defined as the mean time delay between the highest points in the forward arm swings (t_{arm_fwd}) and the heel strikes of the contralateral foot (t_{heel_strike}). CC can be defined with the following equation:

$$CC = \frac{1}{N}\sum_{k=1}^{N}\left(t_{heel\_strike,k} - t_{arm\_fwd,k}\right), \begin{cases} t_{heel\_strike}, contralateral\_heel\_strike \\ 0, otherwise \end{cases} \quad (27)$$

.

Calculation of CC and YC enables independent assessment of both sides of the body with only two sensor nodes. This can be especially important for stroke or PD patients, where one side can be more affected then another. Since these groups of examinees are already identified as high risk groups in terms of the FRA, the implementation of the above defined indexes is reasonable.

Critical point in the calculation of these two indexes is a reliable detection of left and right step. In previous solutions with multi-sensor systems, it was possible simply to use the corresponding ankle- or hip-attached sensor to distinguish between the consecutive heel strikes. In a system with only two sensors (one at the hip and one at the wrist), another solution was needed. Translation from the local coordination system of the sensor to the global coordination system helped in terms that it was possible to determine on which hip the sensor node was worn by only analysing the anterior-posterior acceleration axis or more precisely, its signature while being still (Figure 21). Dormancy phase was chosen here since it is the daily movement with the pattern that can be detected with highest reliability. In respect to the signature of this acceleration axis, if its values are predominantly positive (>90% of total number of samples within analysed signal block), the algorithm classified attachment of the sensor node on the right hip, while for the predominantly negative values it was classified on the left hip. Special case was when the examinees turn the sensor node upside-down, which was possible in extreme situation due to insufficiently robust system design. These cases were corrected by analysis of the superior-inferior acceleration axis, where the anterior-posterior axis was reflected over abscissa.

Once having the correct orientation of the sensor node, as well as reliable determination of the side of the body where the sensor node has been worn, it is possible to distinguish between left and right steps based on the gyroscope signal. Namely, information about the side of the body where the sensor node was worn reveals the movement of this hip.

Parallel observation of the videos and signals acquired in the pilot study has revealed the rotation in the hip that happens directly before the heel strike.

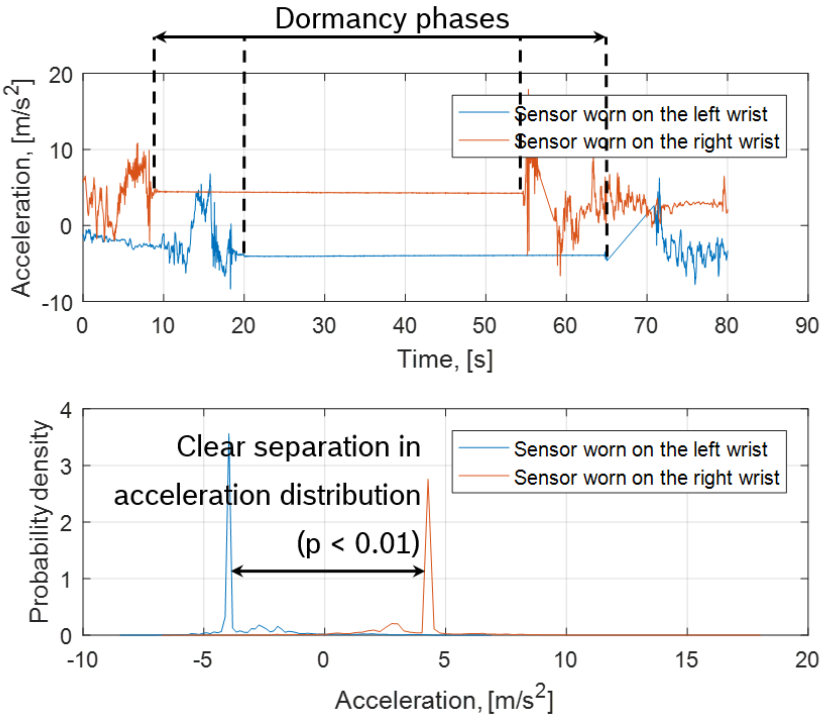

Figure 21 AP acceleration signal at left and right hip after correction

From the physiological perspective, this rotation in the hip happens after the toe-off phase and it is extended throughout the whole swing phase (Schultz, 2005 & Loudon, 2008). In the early swing phase, by normal gait, the hip extends to 10° and then flexes due to contraction of the iliopsoas muscle 20° with lateral rotation. In the mid-swing phase the hip flexes to 30°, while in the late swing phase hip flexes 25-30°. This characteristic movement is visible in the angular velocity around medial-lateral axis in the gyroscope signal (Figure 22). Lateral rotation of the hip is significantly dominant in the signal on the side where the sensor node was worn. By finding the local maxima in this rotation, it is further possible to classify the next heel strike as the heel strike of the ipsilateral foot. Logically, next consecutive heel strike is then classified as the heel strike of the contralateral foot. These three sequences are part of the gait cycle so from the algorithm point of view they have to happen within the three seconds time window.

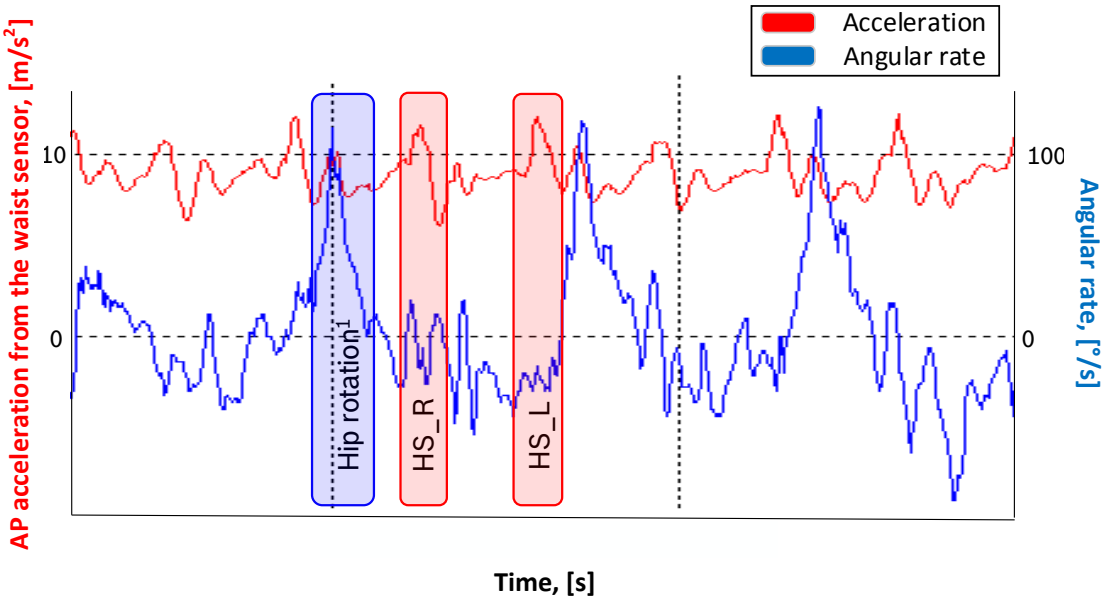

Figure 22 Hip rotation preceding the ipsilateral heel strike

This approach for distinguishing between left and right heel strike opens two questions. First is related to the design of the sensor system, where the waist-attached sensor is during the day slipping from the hip to pelvis (point opposite to the L5). In this case lateral rotations of both hips have similar interpretation in the gyroscope signal. Another question is in terms of the frailty of the elderly population. As it has been shown in numerous previous studies, frailty or more precisely lower-limb weakness is well correlated with the age, as well as with the fall risk. Moreover, this influences directly the hip rotation which is then reflected in the amplitude (i.e. angular velocity) during lateral rotation. Another special case that also fits in this group are examinees with walking aid like walking frame, where hip rotation is reduced due to absence of the arm swing (hands are tight to the walking aid).

In the figure below (Figure 23) it can be easily seen the variability of this hip rotation during walking in examinees from the pilot study. Each signal represent one step from another examinee, while the black line represent the mean value. The middle point (at two seconds) is the maximum lateral rotation of the hip. These two open questions were resolved by a trade-off solution. A threshold value for minimum necessary

lateral hip rotation was derived from the pilot study as the mean value of the examinees investigated within this study. Steps performed with smaller hip rotation were in the calculus of the CC and YC indexes rather ignored, since reliable recognition between left and right step was not possible. This approach introduced the trade-off between reliability of the detection of left and right step and smaller total number of analysed steps in the frail elderly population where hip rotation is not so dominant while walking.

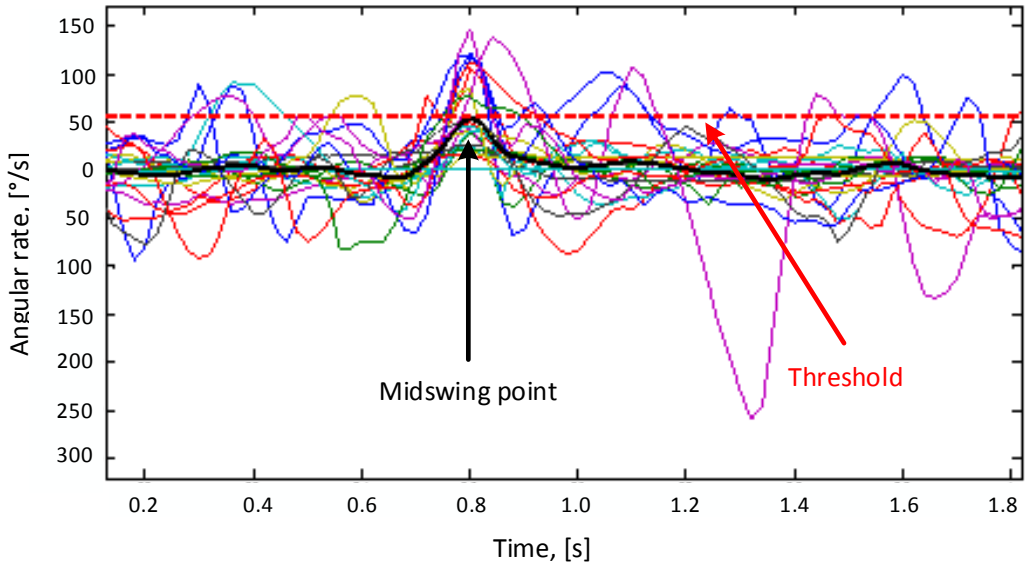

Figure 23 Hip rotation while taking the ipsilateral step (gyroscope signal)

Additional point important for all three indexes was an absence of the arm swing while walking or reduced arm swing due to the environmental factors. Although in scope of this thesis it was not enabled and further investigated the reduced arm swing due to different medical conditions (e.g. PD, stroke) and environmental factors (e.g. hands in the pocket, hands carrying something or holding for something), it is important to emphasize the difference between these two cases. Although in short terms (following few minutes or even seconds) both, medical conditions and absence of arm swings, could be significant for the FRA (i.e. can influence the gait so there is a similar change in index values), the medical history is dominantly more important in the long terms (for acute FRA,

as well as for 6-months based FRA) (Deandrea, 2010). The issue of absence of the arm swing, or more precisely the cases where no arm swing points in the wrist-attached acceleration sensor could be found for the corresponding heel strikes, was addressed by empirically defining the maximum time window in which the events should be detected.

5.2 Gait analysis in terms of the FRA on the wrist

The gait analysis from the perspective of the wrist, despite the widely present step counters (e.g. FitBit, iWatch), in the scientific community is still taken very critically. One of the problems here is also an issue addressed in this thesis in the chapter 5.1 regarding the upper- to lower-limb coordination. Additionally, an excessive occurrence of false positives for the wrist attached sensors is present in relation to the waist-worn devices (Tudor-Locker, 2015). Reliable step detection for further gait analysis is even more critical when one would like to derive clinically relevant information from it, as for example in the FRA. Thus, a need for robust gait features is emphasized as an issue in this chapter. Numerous features were addressed throughout this work but due to poor performance from most of them, only the best feature is elaborated in the following chapter. The feature assesses small perturbations in human kinematics by means of estimation of local dynamic stability.

5.2.1 Local dynamic stability

The Lyapunov exponent (λ_L) has shown in numerous previous studies an astonishing good performance for the gait analysis in terms of the FRA (Schooten, 2013, Rispens, 2015 and Ihlen, 2015). Generally, it is applied on the time series or discrete time signals where the unpredictability of the signal trajectories as a function of time is highly emphasized. What is interesting to observe in the signals of particularly human movement is with which speed, or more precisely how fast, do the closest trajectories or next points, so called nearest neighbours, that are at least in the time of one time period distant from each other move from or towards each other (i.e. to which quantity they converge or diverge).

In these terms, the Lyapunov exponent is a measure of the exponential divergence of the dynamic system. The fact that the trajectories in the time infinitesimally drift from each other is typical for cyclical periodical time series. The mean exponential value of this drifting of the trajectories describes the dynamical system (in the mathematical chaos theory defined with $Z(t)$) and it is defined as Lyapunov exponent as $|\delta Z(t)| \approx e^{\lambda t}|\delta Z_0|$, where δZ_0 is the trajectory's initial separation. Number of Lyapunov exponents is equal to the number of the state spaces in which the trajectories are constructed, but the final measure of the dynamic system is the maximal Lyapunov exponent (MLE).

The MLE was estimated in the literature either with the method proposed by (Rosenstein, 2013) or with the method proposed by (Wolf, 1985). Although the recent insights have suggested that the method by Wolf might be more suitable for data series influenced by noise as in daily-life accelerometry, the findings in (Schooten, 2013) have determined a high correlation between both estimation methods, with tendency of slightly better association of the Wolf's algorithm with the prospective falls. For the purposes of this thesis, only one implementation, the one from Rosenstein was used. Therefore, the Lyapunov exponent λ_L is defined with:

$$\lambda_{L,i} = \frac{1}{(T-1)\Delta t}\sum_{t=1}^{T-1}\log\left(\frac{d_i(t)}{d_0(t)}\right) \tag{28}$$

.

For this purpose a state space should be constructed with a time delay constant θ and dimension Δ. The state space from a time series $x(t)$ is then defined as:

$$X(t) = \left(x(t), x(t+\Theta), \ldots, x(t+(\Delta-1)\Theta\right). \tag{29}$$

The time delay constant θ is derived as the argument of the first minimum of the mean mutual-information from the time series $x(t)$ as defined in (Fraser, 1986). Time delay that shows the highest independence

between $x(t)$ and $x(t + \theta)$ is chosen. This approach allows by the transformation of the time series in the higher dimensional space the highest probability for finding the right nearest neighbour.

In (28) $d_0(t)$ is defined as the minimum Euclidean distance between two signal samples ($X(t)$ and $X(\tilde{t})$) that are in the time series at least one time period Δt distant: $d_0(t) = \min_{\tilde{t}} \left\| X(t) - X(\tilde{t}) \right\|$. Furthermore, $d_i(t)$ is the distance between the same points after i discrete steps, more precisely $d_i(t)$ defines the time distance between the two trajectories.

The number of state space dimensions was determined with the method false nearest neighbours proposed in (Hegger, 1999), which for each discrete step i finds the nearest neighbours on the trajectory distinct at least for one period Δt. For the chosen nearest neighbours the distance $d_i(t)$ is evaluated with a probability for the right nearest neighbour also in the next higher dimension. The number of state space dimension that has the highest percentage of the correct nearest neighbours is chosen for as dimension Δ.

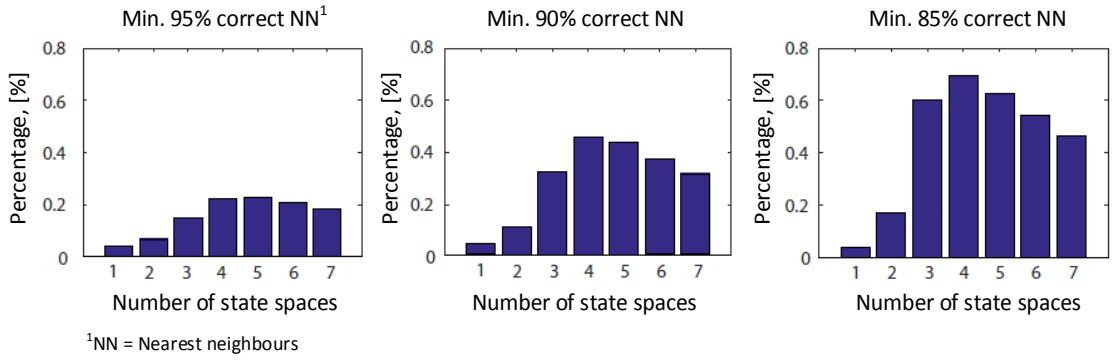

Figure 24 Percentage of correctly detected NN in relation to the number of state spaces

Lyapunov exponent was calculated only for the gait bouts with the duration between 10 and 100 seconds. This was chosen due to the suggestion in the literature, where a minimum number of steps or gait bout length for reliable gait analysis was analysed (Brodie, 2015). The choice was also consistent with the selection of gait bouts for the inter-limb coordination assessment (5.1). Additionally, although irrelevant for the importance of the results, the gait bout selection reduces significantly

the computational time of the algorithm. Gait bouts were determined based on the acceleration data acquired with the wrist-worn sensor node and by applying the arm swing detector defined in chapter 5.1.1. In addition to that, only the first 500 samples of each gait phase were analysed for determination of the time delay constant in order to reduce the computational time. These 500 samples cover approximately first five seconds of each gait bout (on average 4-6 steps), which anyways does not change a lot in the calculation since further steps in this case contain redundant information (Figure 25). The number of the state space dimensions (Δ) needed for signal reconstruction was firstly determined on the data from the pilot study and then only the Δ with the best performance was chosen. As it is seen in figure above (Figure 24), as well as in the Figure 25, four to six dimensions determine with the highest probability the correct nearest neighbour (i.e. the percentage of false nearest neighbours converges). This optimization has additionally improved the calculation time of the algorithm for the data from the FRA study.

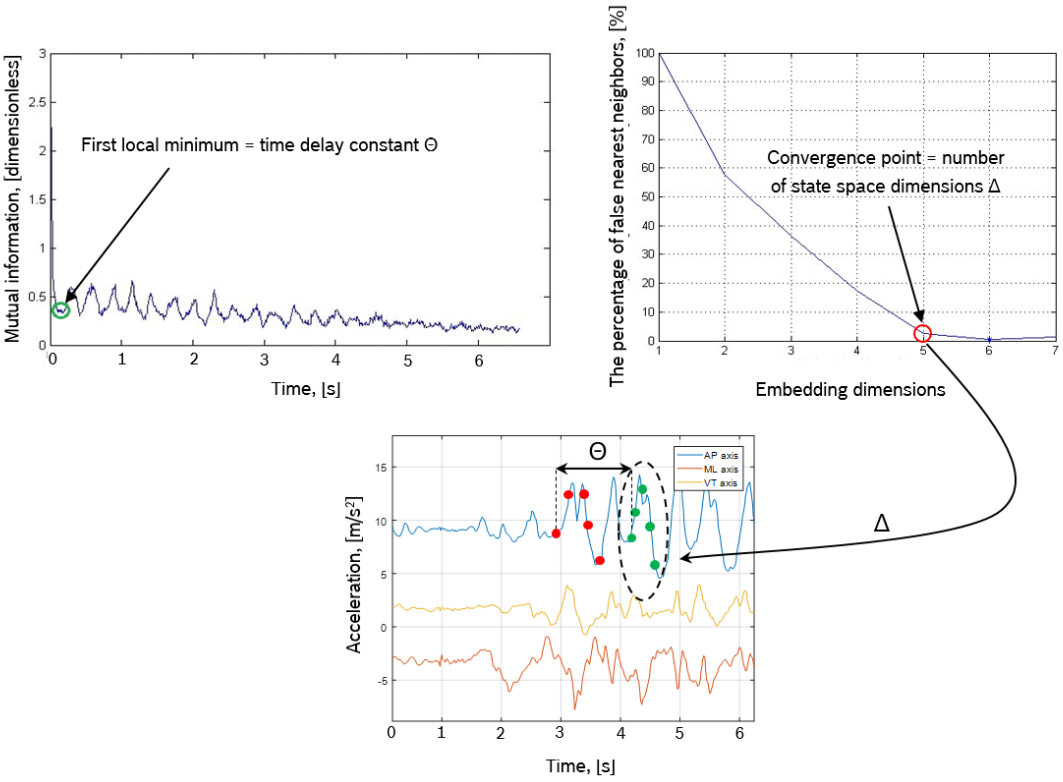

Figure 25 Parameter determination for estimation of MLE

There are three possible solutions for values of the MLE that will be separately addressed here. The negative Lyapunov exponent means that the trajectory attracts to a stable fixed point or stable periodic orbit. Such systems exhibit asymptotic stability, therefore a good example for them would be a critically damped oscillator that steers towards its equilibrium. For $\lambda = 0$ the trajectory is a neutral fixed point. An example would be two identical simple harmonic oscillators but with different amplitudes whose phase reconstruction is a pair of concentric circles. The human movement streams to the small positive values of the Lyapunov exponent ($0 < \lambda < 2$), which describes an unstable and chaotic system. Nearby points for these systems in the state space will diverge to any arbitrary separation.

5.3 Sit-to-stand transition

As described in (Rapp, 2012), transitions were quantitatively one of the major factors (triggers) for falls in the elderly population. Moreover, analysis of reported falls in the FRA study has further supported this conclusions. The thesis addresses this issue with two major blocks: sit-to-stand transitions (STST) detection and their quantitative assessment. Detection of the STST, a non-recurrent and highly variable movement in ADL, has shown relatively good performance on the waist (Zijlstra, 2012), as well as on the sternum (Zhang, 2012). Detection of STST in ADL with a wrist-attached sensor has not been yet successfully described in the literature. Thus, the first step in this direction was an attempt of transferring the algorithms developed for the waist-attached sensor to the wrist (5.3.1.1). This approach, although it has shown many disadvantages of the wrist, has also set the path for further development. In the second step key component of the algorithm development was the detailed video analysis of the STST, which identified most important points from the wrist perspective (described in the chapter 5.3.1.2). Added value for the STST detection algorithm was also found in the environmental context. Finally, quantitative assessment was performed with both, time- and frequency-domain based features (5.3.2).

5.3.1 Sit-to-stand transition detection

5.3.1.1 Waist to wrist algorithm transfer

In case of a direct transfer of current findings from the waist to the wrist sensor, a STST duration has been shown as a good quantitative fall predictor (Najafi, 2002). Therefore, first attempt was focused on the principles of estimation of the STST duration from the acceleration signal from both, wrist- and waist-worn devices. This does not include automatic segmentation of the signal (i.e. detection of STST in ADL), but rather only their quantitative assessment. Moreover, this approach was used to validate the possibility of a currently strong fall risk predictor in the new environment. Result of this approach enabled better steering of the further algorithm development for the non-recurrent movements in ADL and emphasize the need of diverse solutions for their evaluation.

For these purposes, a sample-based method for the estimation of the STST duration was proposed for both, wrist and waist acquired acceleration data. The method was based on the signal vector magnitude derived from the acceleration signal. In this way, an issue regarding the initial orientation of the sensor node immediately prior to the transition was overcomed (resultant vector has the same amplitude value, independently on the sensor orientation). Empirical evidence has shown that the STST from the waist sensor are depicted in a signal vector magnitude with a movement pattern that can be mathematically described with a biorthogonal wavelet with $N_r = 1$ and $N_d = 3$, where N_r is the order of the scaling function used for reconstruction and N_d is the order of the function used for decomposition (Figure 26).

Although the wavelets have already shown good performance in the activity classification, as well as good robustness, in above defined approach a simple sample-based method with empirically defined adoptive thresholds was given precedence. In the parallel analysis of the waist-acquired signals and recorded video from the pilot study, it has been noted that first local maximum depicts the seat-off moment, while local minimum depicts the moment when the one's centre of mass reaches vertically highest point (i.e. end of the leaning backward phase).

From this point of view, the STST movement pattern was described with three basic parameters as shown in the figure below (Figure 26):

- Minimum amplitude range;
- Defined time span between local extrema;
- Relative position of local extrema.

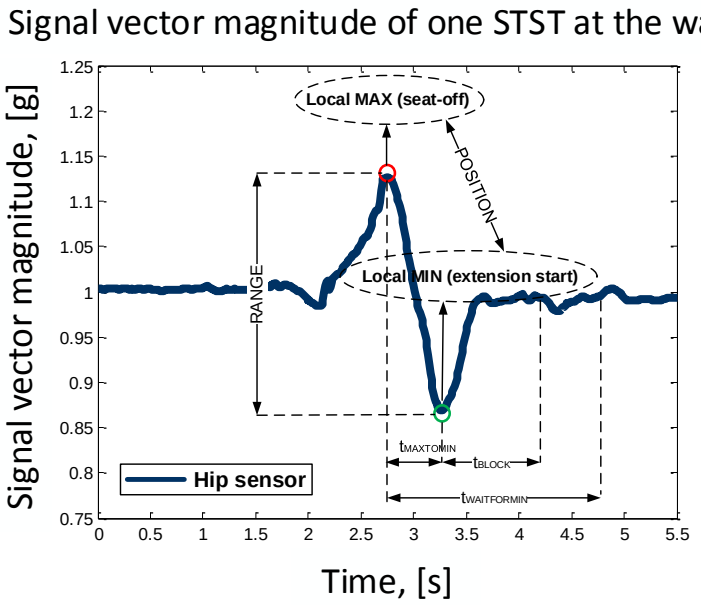

Figure 26 Transition pattern and its key points used for duration estimation

The proposed algorithm can be split into three major blocks (Figure 27):

- Detectable sit-to-stand transition phases;
- Extrema update;
- Parameter check.

First block is conceived as the finite state machine (FSM), which from the concept fits perfectly for the continuous signal evaluation. The start state is detection of the local maximum (i.e. seat-off moment), followed by the defined time span $t_{WAITFORMIN}$, which corresponds to the leaning backwards phase. This variable is defined within two thresholds:

$$0.25\ s < t_{WAITFORMIN} < 2\ s. \tag{30}$$

Assuming the plausibility between detected STST interval (local extrema) and its residual, STST duration can be estimated as a double span

between respective local extrema ($t_{MAXTOMIN}$). This approach was previously introduced in (Bidargaddi, 2007). Thus, the two defined thresholds enable detection of STST, whose duration spans in the interval from 0.5 to four seconds. As shown in the literature, the defined interval covers most of the STST performed by elderly. In the leaning backwards phase, once the local minimum is detected, one's centre of mass is in the highest point and final, stabilization phase starts. Extrema update block enables interruption of the FSM algorithm by the newly detected local extremum, fitting these characteristic points to their best fit. Once both characteristic points are found, a blocking time t_{BLOCK} for the next STST is set to action. This time is supported by logical conclusion that the next STST cannot happen in the following two seconds. By implementation of this blocking phase, posterior STST movements (present in more than four-fifths of all transitions performed by elderly as shown in the video analysis in 4.2) are filtered decreasing the FP rate of extrema detection. The parameter check block proves the above defined three parameters.

The time span between finally confirmed local extrema is then updated and defined as $t_{MAXTOMIN}$. The total STST duration was estimated as described in the literature, as well as with a best-fit linear relationship between the extrema span and total transition duration. The relationship was further described with linear, binomial, exponential and polynomial (third order) equations. The parameters for these equations were found based on the least square error method performed on the training data set and validated on an unseen data set. Both data sets were defined by the 10-fold cross validation method and mean absolute error of estimation was used for comparison of the results. The data sets had a corresponding reference values derived from the tagged videos and they were split separately on waist and wrist estimated values. Since the improvement of estimated STST durations was negligible in comparison to the conventionally proposed linear approach, they are not shown in the thesis. Nevertheless, performance of the proposed algorithm for both, waist and wrist sensor estimates, was tested and these findings were the basis for the next step in development of the STST transition detection algorithm for solely wrist-attached sensor nodes.

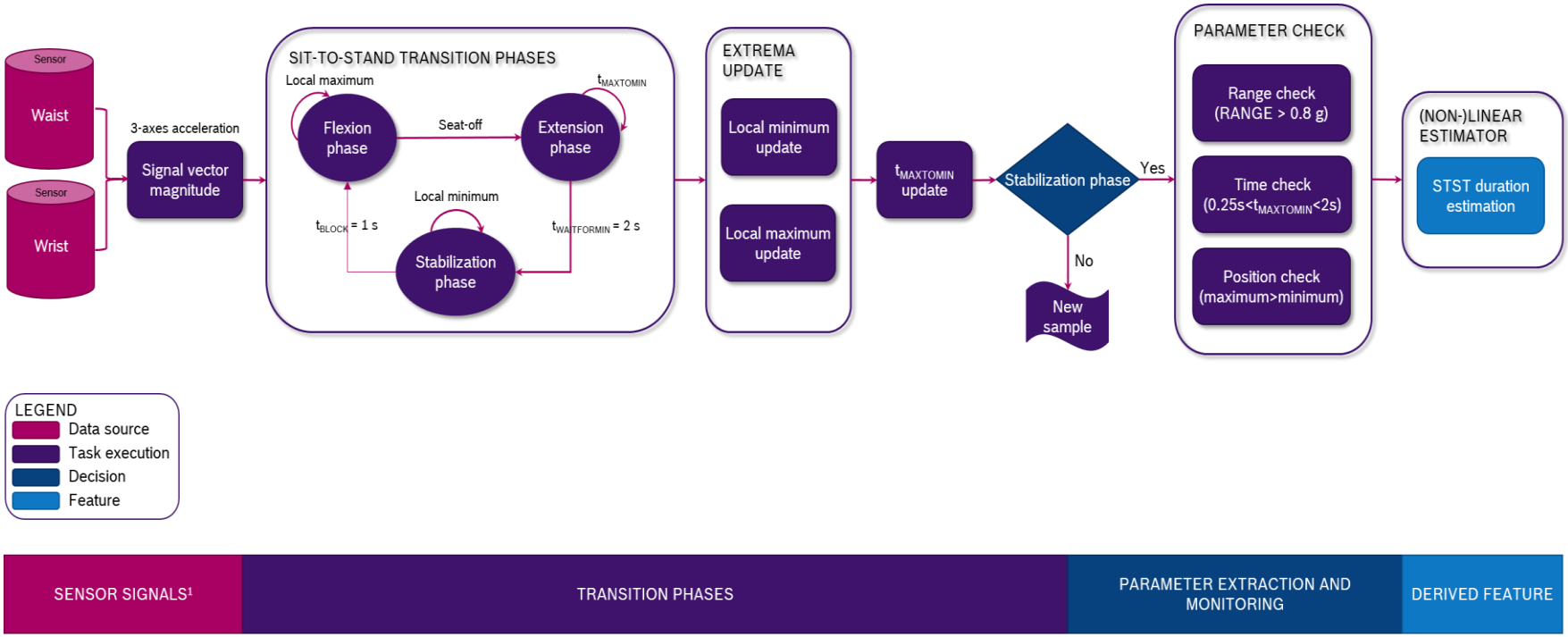

[1]Three-axes acceleration signal acquired at the wrist and waist

Figure 27 STST duration estimation algorithm based on the extrema detection

5.3.1.2 Wrist perspective

The analysis of STST in the previous chapter was not directly focused on their detection, but rather only on their quantitative evaluation, more precisely, on evaluation and validation of possibility of implementing the best fall risk predictor (STST duration) for the wrist-attached sensors. Next step steers into different direction in the algorithm development and proposes a method for STST detection, but with a clearer focus – optimisation of the approach only for wrist-attached sensors and based on the findings from the detailed video analysis described in 4.2.

While many previous studies have focused on the detection and assessment of the particular phases in order to reliably assess the performed transitions, the proposed method focuses on detection of particular trigger events (such as rotation of the wrist above a predefined threshold), as well as periodical or motionless situations after these events. There are multiple reasons justifying this approach. Movements of the hand prior to the transition can be described as chaotic movements contrarily to the body's centre of mass which is prevailing motionless during sitting or standing. From pure perspective of the STST, this means that there is not much connection between initial conditions (start of the transitions) and the outcomes (end of transitions). More precisely, STST can be seen as dynamic systems with widely diverging outcomes, rendering a robust detection fairly difficult in general.

The focus on dominant trigger events sets more emphasize on the algorithm's precision reducing possible false positives. The trade-off in this solution is loss in the algorithm's sensitivity, but since adults performed on average 50 or more STST during the day (Dall, 2010), this should not be a critical point. The Figure 28 shows an acceleration signal during eight hours of recording with a wrist- and waist-worn acceleration sensor. This example illustrates well the need for more robust algorithms (e.g. via trigger events) for the wrist since sitting, standing and lying movements are overlapped with significantly more (Spearman's $r = 0.05$, $p < 0.001$) chaotically signals (i.e. presence of significantly higher signal variability is obvious from the figure) compared against

the acceleration signals acquired with the waist-attached devices in previous studies (Zhang, 2012). As support for this hypothesis, the findings from previous study can be added (Ermes, 2008), where detection of especially sitting and standing classes has shown poor results for the wrist-attached sensor.

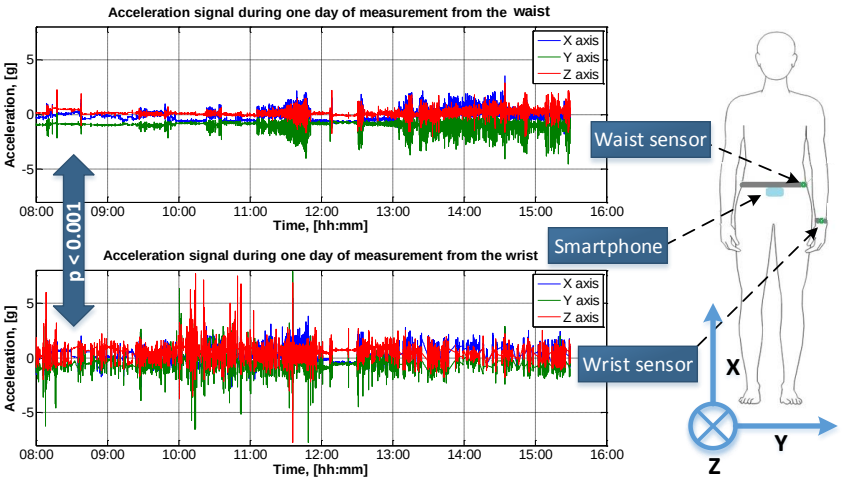

Figure 28 Typical movement patterns recorded with acceleration sensors

Moreover, as shown in the video analysis, the end of transition is dominantly affected with additional chaotic movements of the hands that do not necessary belong to the corresponding STST. Thus, focus on the periodical movements (i.e. walking) or dormancy phase (i.e. motionless situations), which is due to the relatively stable movement pattern trivial to detect on the wrist and which precedes or follows STST especially in the ADL (Kerr, 2007), can result in higher algorithm precision. Having maximized number of true positives events for the quantitative assessment is in the proposed method taken as a preferable solution in comparison to a solution with a high sensitivity rate.

Algorithm development was performed throughout three iterations:

- Trigger-based algorithm development based on the acceleration signal;
- Added values of other inertial (gyroscope, magnetometer) and environmental sensors (pressure, light);
- Hyper-parameter optimization.

The trigger-based part consists of a detection of the dormancy phase prior to the transition, detection of the rotation in the wrist together with the attached standing position within defined time frame and finally finding one of three possible end conditions of each STST (dormancy phase, gait bout or activity over predefined activity-count-based threshold). The main algorithm blocks and their representation in the time-series acceleration signal can be seen in the Figure 29.

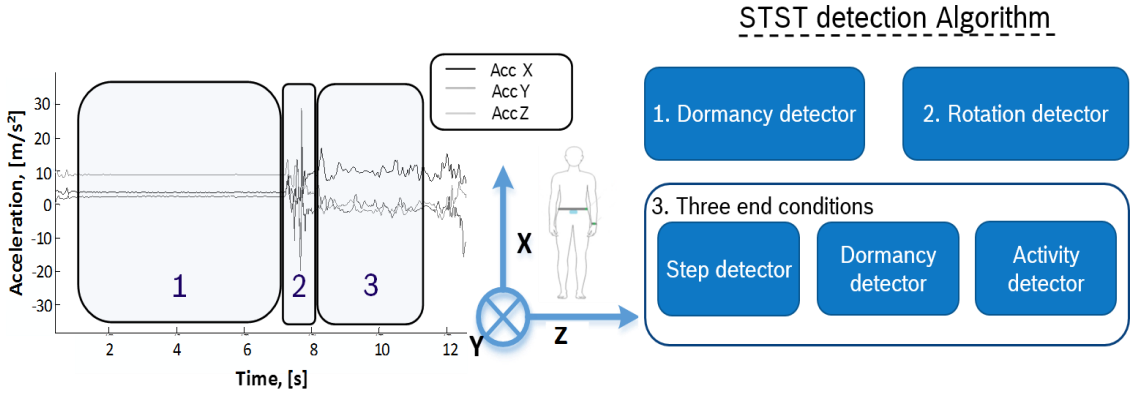

Figure 29 Implications of different detector on the acceleration signal of the STST

Acceleration signal was filtered with a low-pass Butterworth filter 50th order with a cut-off frequency at 20 Hz. This filtration has eliminated high frequency components that could have been misinterpreted as trigger events (i.e. rotation in the wrist). Moreover, the Butterworth filter has a maximally flat frequency response in the pass band, thus filtering the high frequency components but letting the rest of the signal go through without attenuation (i.e. preserving the realistic recorded human movement).

On such filtered acceleration signal an algorithm for local to global transformation of the axis as described in 5.1.3 was applied. Representation of the acceleration signal in the global coordination system was used for determination on which side of the body the wrist-sensor was worn. In contrary to the chapter 5.3.1.1, this time the side determination was done only on the wrist-based signals during walking by calculating the area under the curve for anterior-posterior acceleration axis.

Following the side determination, a dormancy detector was applied. This detector locates in the ADL a motionless situation with total duration of two seconds or more. From a macro perspective it works as a band-pass filter on the whole movement signal. The implementation is supported with findings in the chapter 4.2, as well as with a hypothesis that arises from these findings. Namely, right before the STST a characteristic motionless session is visible (in this case empirically set to minimally two seconds). The dormancy detector operates on the first derivation of the signal vector magnitude of the acceleration signal. This approach overcomes artefacts in the acceleration sensor described in chapter 3.1.1, as well as it evaluates the total movement of the wrist. The dormancy phase is detected once the derived signal is continuously within defined lower and upper limits described with parameters C_1 and C_2, respectively. The minimum duration of the dormancy phase is depicted with parameter C_3.

Once the dormancy phase is detected a search for a trigger event is activated. At the same time end of the dormancy phase is depicted as beginning of possible STST. Search for the trigger event is performed in the following four seconds with a rotation detector. Rotation detector is based on the detection of rotation around superior-inferior φ_X, anterior-posterior φ_Y sensor axis or they summation ($\sqrt{(\varphi_X{}^2 + \varphi_Y{}^2)}$). The total rotation φ_T should satisfy the following condition:

$$\forall \varphi_T \in \left\{ \varphi_X, \varphi_Y, \sqrt{\varphi_X{}^2 + \varphi_Y{}^2} \right\} : \varphi_T \geq C_4 \tag{31}$$

where C_4 is the parameter defining minimally needed rotation within defined time window with corresponding length C_5 for making the trigger event fulfilled. At the same time, φ_X and φ_Y are defined in the randomly selected point *k* with the following two equations, respectively:

$$\varphi_{X,k} = \left| arctg\left(\frac{a_{X,k}}{a_{Y,k}} \right) \right|, \tag{32}$$

$$\varphi_{Y,k} = \begin{cases} arctg\left(\frac{a_{X,k}}{a_{Z,k}}\right), sensor\_position = RIGHT \\ arctg\left(\frac{a_{Z,k}}{a_{X,k}}\right), sensor\_position = LEFT \end{cases}, \quad (33)$$

where $(a_{X,k} \quad a_{Y,k} \quad a_{Z,k})$ is a three-dimensional representation of the acceleration signal acquired from the wrist-attached sensor at the random point *k*. The orientation of the sensor axes is shown in the figure (Figure 29). Positive X axis shows in the direction of the shoulder, positive Y axis shows in the anterior-posterior direction, while positive Z axis shows in the medial-lateral direction. The calculated angle rotations describe the two most common wrist rotations during the STST identified in the video analysis (chapter 4.2).

The condition in (31) unlocks the second trigger event for the STST. The second trigger analyses the rest of the signal in the four second time window from the end of the dormancy phase and it determines whether the person is standing upright. Detection of the standing class with the acceleration sensor at lower back (Zijlstra, 2012), as well as at the sternum (Spain, 2012) has shown good performance in previous studies. Standing detection on the wrist is rather a challenging work since position of the hand for this sedentary class can be identical to sitting or even lying (e.g. while holding something in the hand in the upright position). The algorithm checks the inferior-superior axis, or more precisely the position of the hand in the Y-Z two-dimensional space, which fits to the situations when the hand is firmly attached to the body with additional allowed deviations. Standing detector is defined with an additional parameter C_6, defining the mean standing angle in the analysed time window (angle between the gravity vector and hand). From the macro perspective it can be also understood as the band-pass filter, removing the situations when the hands after rotation are not in the defined interval.

In order to analyse only the meaningful parts of the signal, or more precisely to define start and end of the STST for detection, the last step of the proposed algorithm defines three possible end conditions. For this purpose a step detector described in chapter 5.1.1 and above described

dormancy and rotation detectors were applied. If a dormancy phase is detected within four seconds from the trigger event, the corresponding transition is defined as sit-to-stand passive (STSP). In case when a walking phase is detected within the same time window, in the first detected arm swing the highest point which depicts the highest backward or forward arm swing defines the end of transition. Such transitions were classified as sit-to-walk (STW). If both conditions remain unfulfilled, the end of the transition is by default defined with a random activity following the transition and is assumed to last four seconds from the first trigger event. Such transitions were classified as sit-to-stand active (STSA). All eight different types of transitions together with their corresponding phases performed within the pilot study (chapter 3.1.1), as well as all transitions detected in the FRA study (chapter 3.1.2), were classified into these three groups (Figure 30). With definition of end conditions for the STST, the first iteration of the algorithm development for detection of transitions was concluded.

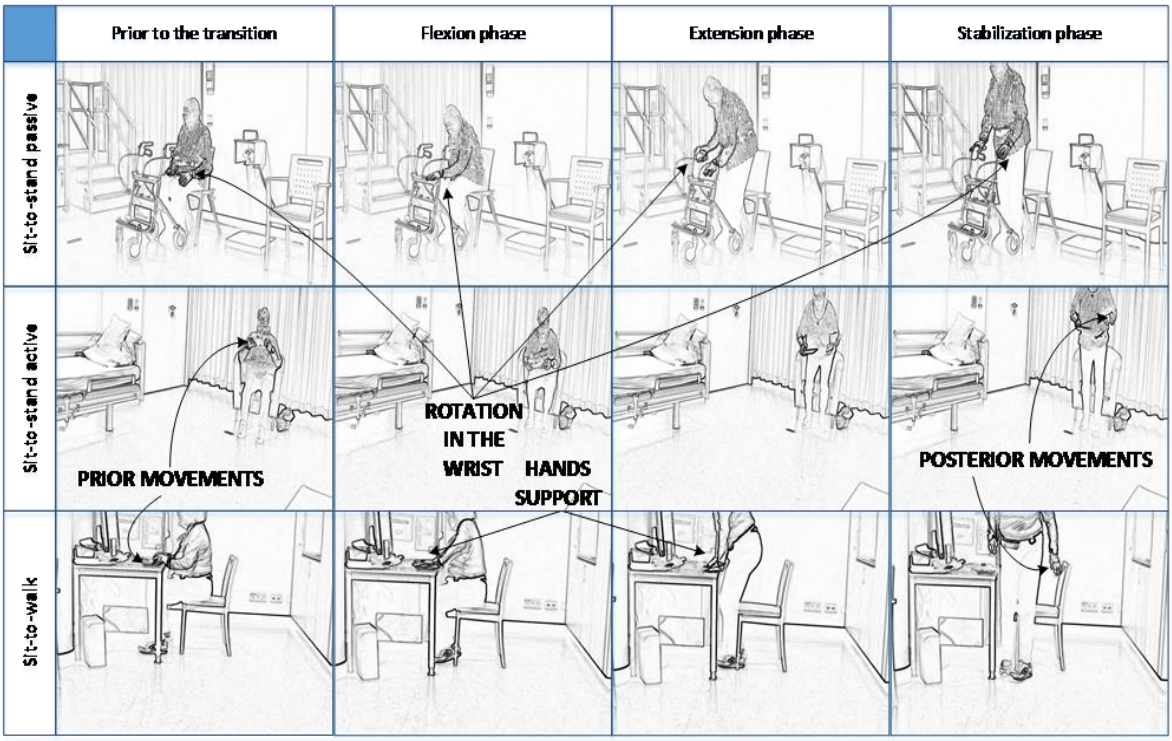

Figure 30 Transition phases depicted for the different types of transitions

Second iteration of the algorithm was further performed with a goal to increase its precision, also at a cost of lower sensitivity when needed. For that purpose a possible added value of other available inertial and environmental sensors was investigated. Previous studies have shown improved performance with the gyroscope (Najafi, 2002) and pressure sensors (Masse 2016), but not for the wrist-attached sensor nodes. The gyroscope has better signal-to-noise ratio and zero offset rate, but from another side has a high demand for the energy consumption in comparison to the accelerometer, as well as emphasized non-linear effects on the drift and sensitivity throughout temperature changes. When its application on a device on the wrist should be considered, with high demands for significant energy consumption optimization, gyroscope will certainly not be the first choice. The pressure sensors (or similar sensors for measurement of the altitude) are robust to the environmental noise (e.g. temperature changes), but one can argue whether there is any noticeable height change during the STST from the wrist perspective.

To make this clearer, acceleration and pressure signal acquired in the pilot study are shown in the figure below (Figure 31). The signals are showing different types of activities of daily living including eight STST. Each STST is labelled in the figure with a black rectangular signal. Relative changes in the pressure signal during these events are not significantly different from various other events during ADL, as well as they fit almost perfectly with the sensor's output noise and offset drift. Interesting, and specific only for the wrist-attached sensor, are the situations like reaching for something in comparison with the STST where the relative change in the pressure signal is even higher. After a careful reconsideration of elaborated disadvantages, the possible reasonable utilization of the pressure sensors as an added value in the detection of STST in ADL with a wrist-worn sensor device, as in the current state-of-the-art applications, is clearly not possible.

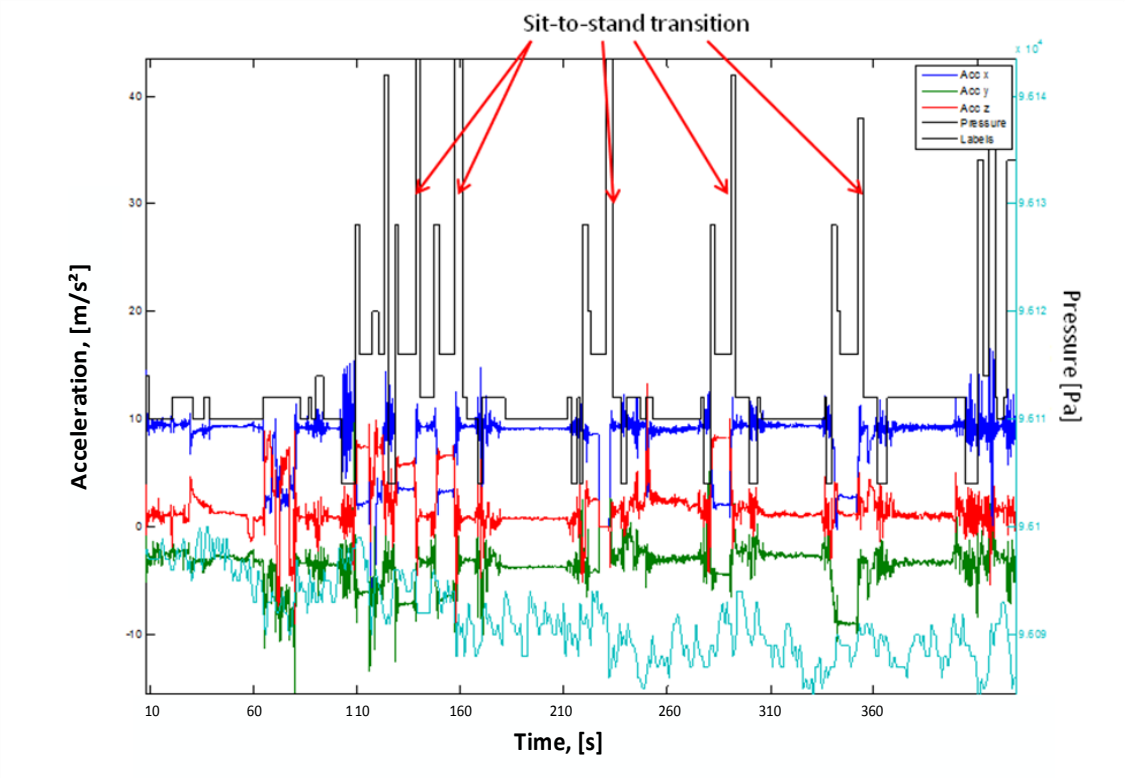

Figure 31 Disadvantage of the pressure sensor for the STST detection at wrist

The next hypothesis that arises considers the application of the light sensor (luminance) for improvement of the algorithm's precision. Three postulates are critical for this hypothesis:

- STST are in most cases performed in a closed setting (apartment, house, hospital, nursing home etc.);
- During each particular STST a constant source of light in the examinee's physically nearest environment can be assumed;
- The inclination angle between the source of light and light sensor changes during the STST.

The first postulate is based on the observation of behavioural patterns of elderly, more precisely on prevailingly sedentary life-style of the elderly population (Thibaud, 2012). Most recent findings have also shown that such a behaviour becomes even more present also in the young generations (Verburgh, 2013), but in the thesis these groups are out of the scope. This postulate is excluding transitions performed outside (e.g. in

the park, during sport activities or simply next to the window under direct contact from the sun). Second postulate has a strong basis in the total average duration of the STST. As most STST are performed within three seconds time window, or in the frail population within five seconds (Zijlstra, 2012), one can reliably conclude that the source of light in the setting defined with the first postulate will in most cases stay constant during the whole transition duration.

Third and the last postulate is supported with the findings in the video analysis (chapter 4.2). Since dominant rotation in the wrist happens in more than 50% of STST performed in ADL and since these rotations are mostly around anterior-posterior and superior-inferior axes, the angle between the constant source of light and the light sensor (receptor) attached on the sensor node changes significantly. By the cosine law, light at the measurement plane (photodiode of the light sensor) is proportional to the cosine of the angle at which the light incidents (ω):

$$E = \frac{I_V}{r^2} \cos \omega . \tag{34}$$

With rotation in the wrist, the angle between the source and receptor is getting bigger, thus reducing the total luminance (E) measured by the device. Luminance is a measure of visible energy falling upon the receptor and additionally depends on the square root of the distance between the receptor and light source. Due to the characteristic configuration of the sensor node, a small test was performed in order to investigate influence of the sum of extrinsic factors (inclination angle, light source distance, as well as plastic lid and housing itself) on the luminance detection.

The test was performed in a dark room where the sensor node used in the pilot and FRA study was exposed to the same source of light (I_v = constant) under different distances (0.02, 0.08, 0.24, 0.42, 0.62 m) and different inclination angles (-90°, -45°, 0°, 45°, 90°). The test have shown logarithmic association between the luminance measured by the light sensor and distance between the source and receptor (Figure 32). Furthermore, the inclination angle has shown the same relationship.

These findings support the hypothesis where a significant changes in the luminance can be detected only as a result of wrist rotation during standing up under given conditions independently on the distance from the light source (with assumption that the light source is at the distance bigger than 2 cm from the wrist). However, the integration of the receptor in the sensor node itself and influence of the housing and transparent plastic lid on the reflection of the incoming light should also not be disregarded.

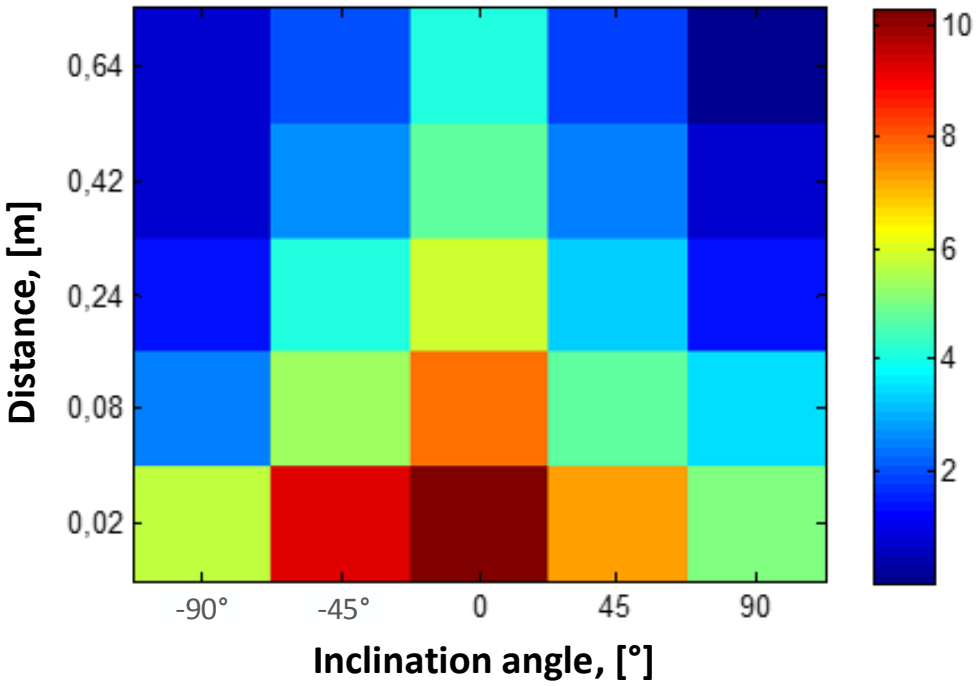

Figure 32 Association of inclination angle, distance and illumination

The relative change in the luminance measured by the light sensor was shown to be significant during transition movements in the pilot study as well (Figure 33), especially in comparison to other sensors such as gyroscope and pressure (Figure 31). The changes can be thus easily observed in the signal by analysing its first derivation. Minimum relative change in the defined time window needed for confirmation of detection of the STST is in the algorithm defined with the parameter C_7 as:

$$C_7 = \frac{d(E(t))}{d(t)}. \tag{35}$$

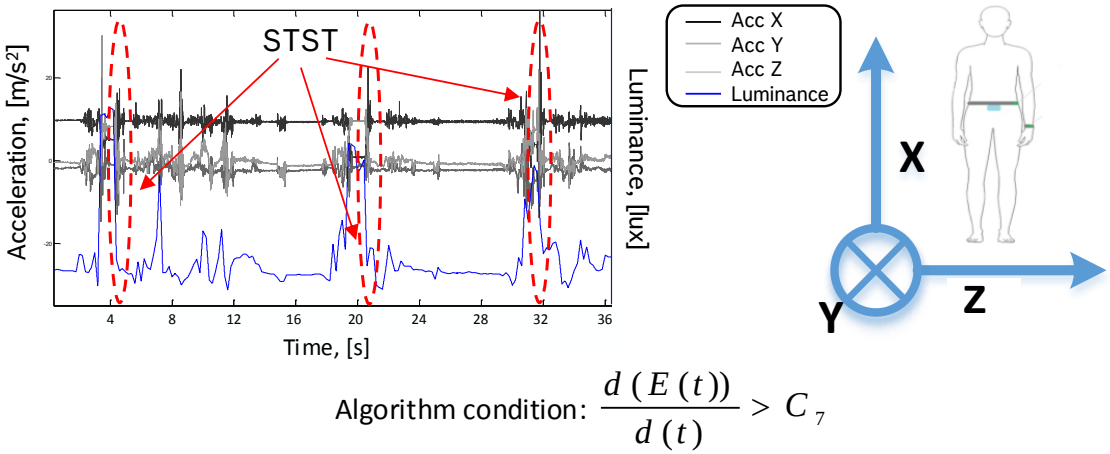

Figure 33 Changes in the luminance while standing up

The proposed approach does not work in cases when the sensor node (i.e. light sensor) is covered (e.g. with clothes, in the pocket or bag), as well as in the situations with reduced or no light (e.g. at night). Different intensities in the light source were addressed in the pre-study in a controlled setting, while for the purposes of the thesis an empirically defined value for the described parameter C_7 was chosen.

5.3.2 Sit-to-stand transition assessment

Quantitative STST assessment was performed by implementation of different features in the feature extraction process. All parts of the three-axis acceleration signal that were classified as STST with defined start and end point were used for their quantitative evaluation. An optimized feature extraction process allows significant dimensionality reduction (i.e. transformation of the existing signal into a higher dimensional space) (Zhu, 2001) and easier interpretation of the results for both, clinicians and engineers. The most significant sit-to-stand feature for distinguishing between fallers and non-fallers is its duration (Najafi, 2002), but as previously described (5.3.1.1), this feature shows a rather poor or limited performance for a wrist-attached sensor node due to the difficulties in correct determination of start and end points of transitions and therefore arisen loss of either flexion or stabilization phase parts. Moreover, the author of this text to the best of his knowledge could not identify other features in the literature that were

used for reliable assessment of the STST detected on the wrist in terms of FRA. This fact is important because the wrist is far from the centre of mass, thus a different behaviour during the transitions is captured with the sensors compared to sensors attached at the lower back or sternum. Furthermore, since the wrist-attached sensor is far from the centre of mass the movement it records is susceptible to different influences that do not need to have any contact points with one's balance and consequently with clinical relevance for the FRA.

5.3.2.1 Time domain

Following these statements, as part of this thesis 12 time domain features for quantitative assessment of the STST from the wrist data sets were introduced. All features were calculated for each particular STST by using only the three-axial acceleration signal. Time domain features were: peak value, root mean square (RMS), jerk, standard deviation (SD), median value, time to first arm swing (TTFS), amplitude of the first arm swing (AFS) and the amount of oscillation (AO). All time domain features, except the AO feature, were derived from the validated filtered signals. The AO feature was derived from the unfiltered signal since the oscillation spectrum is depicted with frequency components higher than the cut-off frequency of the applied filter. Peak value and amount of oscillation features were calculated for each particular acceleration axis, while all other time domain features were calculated only on the signal vector magnitude of the acceleration.

The peak value was calculated for all three axes of the acceleration signal as the maximum value during whole duration of the corresponding STST. It is commonly present at the seat-off moment and reflects the energy that a participant invests for pushing himself from the chair. Moreover, for the peak value at the lower back a good correlation with the sit-to-stand transition time has been shown (Weiss, 2011), therefore suggesting it also as a potential fall predictor worth investigating within the scope of this thesis.

The jerk $\overrightarrow{J_k}$ is defined as the mean change of acceleration between two consecutive samples *k* and *k-1* as $\overrightarrow{J_k} = \vec{a}_k - \vec{a}_{k-1}$. Main advantage of this

feature is easy cancelation of the gravitational component and therefore insensitivity on the sensor node orientation. Namely, since each acceleration sample can be decomposed as the sum of the current acceleration $\overrightarrow{a'_k}$ and gravitational component $\overrightarrow{g_k}$ as $\overrightarrow{a_k} = \overrightarrow{a'_k} + \overrightarrow{g_k}$. Since gravitational vector has constant intensity and direction on one spot on the Earth (i.e. $\overrightarrow{g_k} = \overrightarrow{g_{k-1}}$), the jerk value shows the change in acceleration independently on the current orientation of the hand. This feature has already shown some promising results for activity classification in previous studies (Hamalainen, 2011) and it has outperformed the traditional approach with the acceleration components. For each particular transition a mean value of the jerk was derived as a feature.

The RMS feature is defined on the whole transition as the square root of the arithmetic mean of the squares of the values with equation:

$$RMS_i = \sqrt{\frac{1}{N}\sum_{k=1}^{N} a_{SVM,k}{}^2} \tag{36}$$

where N is the number of samples for each particular transition i, and $a_{SVM,k}$ is the value of the signal vector magnitude at point k. Same approach was used for the SD and median features. While SD feature shows a deviation of the signal during the transition, median feature diminishes possible extreme values (e.g. sudden hand movements while standing up).

The TTFS feature corresponds to the feature time to walk introduced in (Kerr, 2007). Namely, it has been shown that fallers due to hesitation in the gait initiation need more time to perform the first step after the transition than non-fallers. This feature can also reveal the problem of freezing of gait characteristic for the patients with Parkinson's Disease (PD), where problems with gait initiation occurs also in the narrow or crowded places. The PD is also an important fall risk predictor (i.e. PD patients are at higher risk of falling, especially in the later stage (Deandrea, 2010)), but since the FRA study has very limited number of participants with PD, this problem was not addressed separately. The TTFS was defined as the time between the end of the rotation and first peak

in the anterior-posterior acceleration that depicts either highest backwards or forwards arm swing. First arm swing is in that case also first step in the gait bout, meaning that this feature was defined only for the STW transitions. In addition to this feature the AFS feature was introduced. This feature depicts the amplitude of the first detected arm swing.

The AO feature was derived as the variance of the change of the acceleration (jerk) independently for each acceleration axis. In other words, this feature for the particular transition *i* can be defined with the following equation:

$$AO_i = \frac{1}{N-1}\sum_{k=2}^{N}\left(\vec{j}_k - \mu^{(i)}{}_{AO}\right)^2 \tag{37}$$

where the mean jerk for this transition with length *N* depicting the number of samples is defined as:

$$\mu^{(i)}{}_{AO} = \frac{1}{N-1}\sum_{k=2}^{N}\vec{j}_k \,. \tag{38}$$

The AO feature is a novel proposed feature that combines two major previously described characteristics: independence on the sensor orientation and variability of the acceleration signal during the STST. With a measure of variability this feature also shows a complexity of the signal in the time domain. Therefore, higher values of this feature would reflect weakness in upper and lower limbs which further yields higher risk of falling, as previously shown in the literature (Lord, 2003).

5.3.2.2 Frequency domain

The frequency domain features were implemented on the sequence of the Fourier coefficients representing the amplitude and phase of each sample at the corresponding frequency. The frequency representation of the time series x was derived by implementing the Discrete Fourier Transform (DFT): $X(k) = F(x[n])$. The DFT was calculated in N = 512 points (Fourier coefficients) by using the Fast Fourier Transform (FFT) algorithm. The following eight features were derived: entropy, energy, fundamental frequency (FF), index of harmonicity (IH), energy of the

applied support in the oscillation spectrum (AS) and ratio between energy in the spectrum limited with minimum oscillation frequency and energy in the oscillation spectrum. All features except the latter two were calculated on the filtered signal for each particular axis independently.

The entropy *H(X)* of the signal *X(k)* with continuous probability density function (PDF) $p_X(x)$ is defined as (Shannon, 1948):

$$H(X) = -E_X\left[\log_2\left(p_X\right)\right] = -\int_{-\infty}^{\infty} p_X(x)\log_2 p_X(x)dx \tag{39}$$

or in case of the discrete signal it can be rewritten to:

$$H(X) = -\sum_{k=1}^{N} p(x_k)\log_2\left(p(x_k)\right) \tag{40}$$

where $p(x_k)$ is the probability of occurrence of the discrete value x_k in the signal *X*. The probability $p(x_k)$ was approximated by the difference of the spectrum component and the mean value $p(x_k) \cong |x[k] - \bar{x}|$.

The energy in the frequency spectrum was calculated as the squared sum of the harmonics lower or equal to the cut-off frequency of the low-pass filter applied in chapter 5.3.1.2 and higher than $f = \frac{2\pi}{N}$ Hz. Unlike the dominant frequency that is often used for quantifying the periodical movements like walking, for quantitative assessment of the STST, a FF was applied as a feature. FF is defined as the smallest frequency in the power spectrum having a peak (Riva, 2013).

The IH feature for the *i*-th transition was calculated as the ratio of the power of the fundamental harmonic P_0 and sum of the power of the following five (oscillating) harmonics as:

$$IH_i = \frac{P_0}{\sum_{k=1}^{5} P_k}. \tag{41}$$

The feature quantifies the contribution of the fundamental frequency of the transition pattern to the signal power relatively to the higher harmonics (Riva, 2013).

5.3.2.3 Novel feature

In addition to the currently available and implemented features, a novel feature for the assessment of the transition performance was proposed. The feature quantifies the energy of the applied support in the oscillation spectrum (AS) for the quantitative assessment of the STST. Elderly people often use hands for support while standing up as shown in the previous studies (Dolecka, 2015 & Mazza, 2004), as well as in the video analysis of the STST (chapter 4.2). This was a motivation for energy estimation in the frequency spectrum (7-40 Hz) of the human physiological tremor (oscillation spectrum). Despite the debate regarding the right bandwidth of the oscillation spectrum, a definition from (Mayston, 2001) was used for the proposed feature since it covers high frequency components of one's hand movement. The hypothesis is that people at higher risk of falling will have less energy in the oscillation spectrum, and since, due to the lower and upper limb weakness they apply less force for support during standing up activities. Moreover, weakness in the upper and lower limbs has been shown as a good fall risk predictor (Stephenson, 2009), thus assessing it throughout this feature can also show significant differences between fallers and non-fallers.

Signal energy E_S for a time signal *x(t)* is defined as its integral:

$$E_S = \int_{-\infty}^{\infty} |x(t)|^2 \, dt \tag{42}$$

or rewritten for a discrete signal *x[n]* as the sum of all signal components:

$$E_S = \sum_{n=-\infty}^{\infty} |x[n]|^2 . \tag{43}$$

By applying the Parseval's theorem on the equation (43), the signal energy defined in the frequency spectrum can be derived as:

$$E_S = \frac{1}{N} \sum_{k=0}^{N-1} |X[k]|^2 . \tag{44}$$

The equation (44) applied only on the defined oscillation spectrum could then be used for calculation of the AS feature for each particular transition *i* as a function of oscillation spectrum frequency components:

$$AS_i(f_L, f_H) = \frac{1}{\left(\frac{f_H - f_L}{F_S/2} * N\right)} \sum_{k=\frac{f_L}{F_S/2}*N}^{\frac{f_H}{F_S/2}*N} |X[k]|^2 \quad (45)$$

where F_S is the sampling frequency and oscillation spectrum is defined on the interval $[f_L \quad f_H]$.

Further investigation of the above defined hypothesis was performed with additional feature, ratio between the energy in the pre-oscillation spectrum (0-7 Hz) and energy in the oscillation spectrum (i.e. AS feature). Using (44), this feature can be defined as:

$$Ratio_i(f_L) = \frac{AS_i(0, f_L)}{AS_i(f_L, f_H)} \quad (46)$$

This feature should reveal the smoothness of the movement while standing up. The hypothesis is that in the non-fallers group the smoothness of the movement will be higher, thus this feature will tend to higher values. In other words, for a perfectly smooth postural transfer that can be described with sine function with frequency spectrum equal to $\delta(f)$, $f < f_L$, this feature would be indefinite. This hypothesis is supported also with the lower and upper limb weakness basis.

5.4 Statistical analysis

5.4.1 Feature analysis

Statistical analysis of the extracted features was performed in MATLAB R2013b. For each participant all validated parts of the acquired signals were submitted to the feature extraction process. For the quantitative assessment of the inter-limb coordination and gait, walking bouts satisfying the inclusion criteria defined in 5.1 were submitted to the feature extraction process, whereas for the sit-to-stand transition assessment

all parts of the acquired signals identified as transitions using the algorithm described in 5.3.1.2 were used. Once the corresponding features were extracted, a mean value (μ) as well as 95% confidence interval (95% CI) were calculated for each feature. The mean was used since it considers the influence of extreme values that might have occurred by gait bouts or transitions in a fall-prone environment.

The one sample Kolmogorov-Smirnov test was used to test the distribution of the values for each extracted features. Due to the non-parametric distribution of the features, a Wilcoxon-Mann-Whitney test was applied to analyse the differences between the defined groups (for acute FRA between acute fallers and non-fallers, whereas for the 6-months based FRA between corresponding fallers and non-fallers). The likelihood of the statistical type I error was addressed by using the Benjamini-Hochberg correction for multiple comparison. Intra-class correlation coefficient (ICC) was used for testing the reliability of implemented features throughout the measured week (i.e. test-retest reliability of implemented measures between the days).

As a novel approach for the sit-to-stand transitions (wrist-based assessment) the extracted features were additionally separately tested for the participants that wore sensors on their dominant and non-dominant hand. This analysis tests the side-dependence of the fall risk assessment at the wrist, as well as the solely performance (i.e. robustness) of the proposed algorithm.

Important to add, a hyper-parameter optimization (C_1-C_6) for the sit-to-stand detection algorithm was performed by using the robust, but time consuming grid-search method. Hyper-parameter optimization can be seen as a formal outer loop in the learning process (i.e. prior to the feature extraction and classification steps), where the main problem is to optimize the function (algorithm) over a graph-structured configuration space (in terms of the algorithm's precision). Although some previous studies have suggested other optimization methods (such as random search), in which the fitness function is not costly to evaluate, a

grid-search method applied in the sequential model-based optimization performs well.

5.4.2 Classification

Classification of the participants in the FRA study was performed using the machine learning approach. The approach applied on clinically relevant number of participants allows development of the robust models for the FRA based on the extracted features. Basically, machine learning in the literature is defined as a method for data analysis that automates building of the analytical models in an iterative learning process from provided large amount of data without knowing at the beginning of the process where exactly to look at. This iterative aspect of the proposed approach enables independent adaption of the model to data which is of essential importance in the field of activity monitoring of elderly population where a high variability of extracted features is present.

There are four machine learning methods: unsupervised, supervised, semi-supervised and reinforcement learning. Supervised and unsupervised learning methods are the most common approaches currently used in the literature. While unsupervised learning is used against data that has no reference labels (i.e. the model is not told the right answer), supervised learning is focused on the labelled data. In other words, the difference in these two methods is in their causal structure, i.e. in unsupervised learning all outputs are assumed to be caused by a set of latent variables, while in supervised learning one set of variables (inputs) is assumed to be the cause of another set of variables (outputs). Since in the terms of the FRA an actual reference (labels) for each participant are well-known as described in chapter 3.1.1, supervised learning method seems as an reasonable choice. Nevertheless, unsupervised learning could theoretically be able to yield different clusters and find possible different meaningful connections between extracted features in order to distinguish between two defined groups, but this is currently out of scope in this thesis. Moreover, main benefit of the unsupervised learning, fast adaption to more complex structures with deep hierarchies,

does less sense for building a model on finite small number of features as in the case of inter-limb coordination assessment and assessment of the sit-to-stand transitions in terms of the FRA.

In case of a supervised machine learning methods a four main issues while training a model should be addressed: complexity and amount of training data, dimensionality of the input space, noise in the output variables and trade-off between the bias and variance. Furthermore, the algorithms can be divided into two main categories: classification and regression algorithms. While regression algorithms (e.g. linear regression) are used for continuous variables, the classification algorithms (e.g. support vector machine, decision trees, Naïve Bayes) are used for categorical variables, where the data can be separated into specific clusters. Again here, the classification algorithms seems as a reasonable choice for the FRA since the final goal of the study is to develop a model able to distinguish between two clusters of elderly population – fallers and non-fallers, based on the extracted feature sets.

When talking about the choice of the optimal classification algorithm, multiple choices might be possible. In respect to the dimensionality of the input space (i.e. number of available features), as well as the complexity of the training data (i.e. margin functions that describe them), support vector machine (SVM) was chosen for classification of participants. The basic idea of the SVM is in finding an optimal hyperplane (or in case of only two dimensional space an optimal line) that separates two clusters of data.

Between two clusters of data lots of possible solutions for the hyperplane are possible. SVM can find the optimal hyperplane by using the optimization techniques (Lagrange multipliers) and maximizing the margin around the separating hyperplanes. Any hyperplane can be written as:

$$\vec{w} * \vec{x} + b = 0 \tag{47}$$

where $\frac{-b}{\|\vec{w}\|}$ is its offset. The linearly separable data can be bounded with two hyperplanes $\vec{w} * \vec{x} = c$ and $\vec{w} * \vec{x} = -c$, $c > 0$, where the distance between them can be expressed as $\frac{2c}{\|\vec{w}\|}$. This description for the defined hyperplanes can be further rewritten for each point *i* as $\vec{w} * \overrightarrow{x_i} + b \geq c$, for $y_i = 1$ and $\vec{w} * \overrightarrow{x_i} + b \leq -c$, for $y_i = -1$. More precisely, each point has to satisfy the relation:

$$y_i(\vec{w} * \vec{x}_i + b) \geq 1, \text{ where } 1 \leq i \leq N . \tag{48}$$

Contrary to the linear regression or Naïve Bayes, where all points influence the optimal margin between two clusters, in the SVM only the so called difficult points (close to the decision boundary) influence the margin optimization process. Points that lie close to this decision boundary are called support vectors. This means that movement of the support vectors will shift the decision boundary while movement of other points far away from the margin will not influence the boundary. Thus, support vectors are defined as points in the space of the training set that change the position of the margin.

The goal of the whole learning process is to maximize the margin, or more precisely, maximize the distance $\frac{2c}{\|\vec{w}\|}$ between the two defined hyperplanes that linearly separate two data clusters. In order to do so, $\|\vec{w}\|$ should be minimized by solving a quadratic programming problem. Namely, this mathematical optimization problem is used for minimizing quadratic functions of two or more variables which are linearly constrained. More precisely, a minimum of *f(x)* should be found such that *g(x) = 0* where these two functions are defined as:

$$f(x) := \frac{1}{2}\|w\|^2, \tag{49}$$

$$g(x) := y_i(x_i * w + b) = 1. \tag{50}$$

The constrained optimization problem of these two functions can be solved by using the Lagrange multiplier method. In this case, Lagrangian *L(x, λ)* is defined as:

$$L(x,\lambda) = f(x) - \lambda g(x) = f(x) - \sum_i \lambda_i g_i(x) \tag{51}$$

and its partial derivatives should be equal to zero (i.e. $\nabla_{x,\lambda} L(x,\lambda) = 0$). By applying (49) and (50) into (51) the formulation of Lagrangian becomes as follows:

$$L(x,\lambda) = \frac{1}{2}\|w\|^2 - \sum_i \lambda_i \left[y_i (x_i * w + b) - 1 \right] \tag{52}$$

or further rewritten as:

$$L(x,\lambda) = \frac{1}{2}\|w\|^2 - \sum_i \lambda_i y_i (x_i * w + b) + \sum_i \lambda_i \,. \tag{53}$$

The prerequisite on the partial derivatives yields the following:

$$\vec{w} = \sum_i \lambda_i y_i \vec{x}_i \,, \tag{54}$$

$$\sum_i \lambda_i y_i = 0 \,. \tag{55}$$

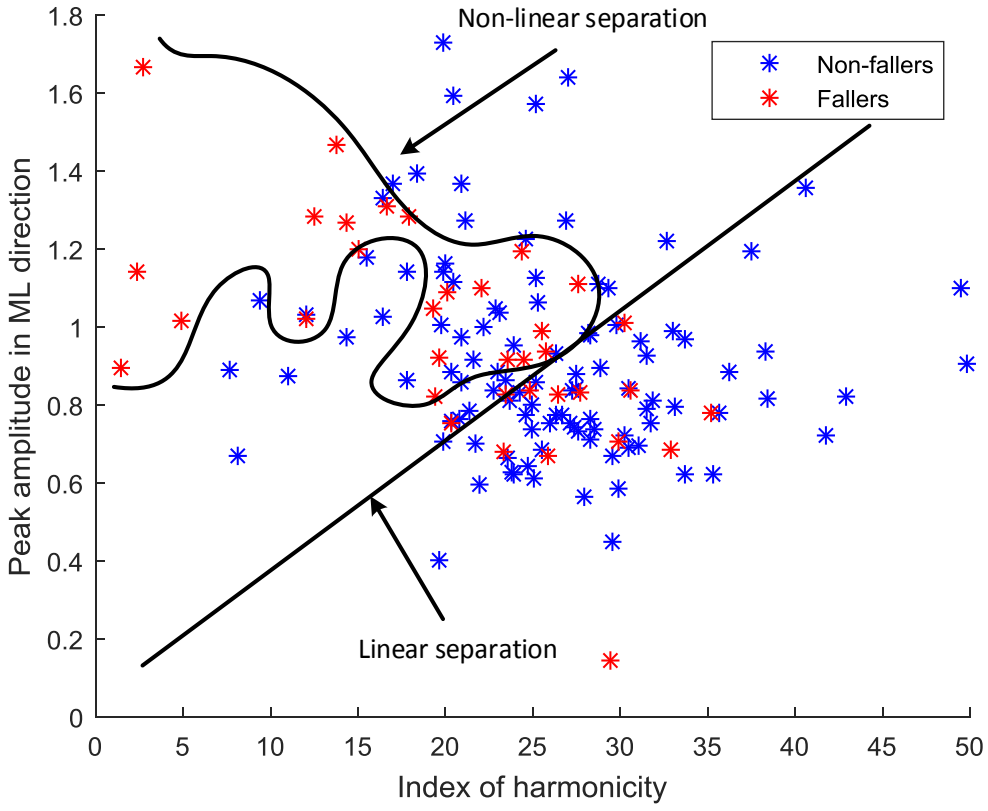

Figure 34 Two-dimensional projection of STST features

The task for training the data is to maximize the function $f(\lambda_1, \lambda_2, \ldots \lambda_n)$ defined by:

$$f(\lambda_1,\ldots\lambda_n) = \sum_i \lambda_i - \frac{1}{2}\sum_i\sum_j x_i x_j \lambda_i \lambda_j \tag{56}$$

as subject to the equations given in (54) and (55). The given solution fits for linearly separable data, but as previously mentioned, the sit-to-stand and inter-limb features, as well as gait features are difficult to separate linearly for the given classes. An example of this problem can be seen clearly in the figure above (Figure 34), where a two dimensional projection of the sit-to-stand features for 145 participants in the 6-months based FRA analysis is shown. The training set in this case is not linearly separable, however an imaginary non-linear function could separate these two classes. Thus the idea is to simply map the existing data into a higher dimensional space by using functions whose exact definition is not even necessary. This approach is called the kernel trick.

Namely, the dot product of x_i and x_j that should be optimized in equation (56) can be then replaced with a dot product of function ϕ that maps initial dataset into higher dimensional space. The kernel function is defined as $K(x_i, x_j) = \Phi(x_i) * \Phi(x_j)$. Applying the kernel trick for optimisation in the equation (56) yields following:

$$f(\lambda_1,\ldots\lambda_n) = \sum_i \lambda_i - \frac{1}{2}\sum_i\sum_j \lambda_i \lambda_j K(x_i, x_j), \tag{57}$$

$$f(\lambda_1,\ldots\lambda_n) = \sum_i \lambda_i - \frac{1}{2}\sum_i\sum_j \lambda_i \lambda_j \Phi(x_i)\Phi(x_j). \tag{58}$$

The most popular kernel function in the SVM classification method is radial basis function (RBF) kernel. The function its popularity mostly owns to its wide robustness in separating linearly not separable data. The RBK kernel function is defined as:

$$K(x_i, x_j) = B\exp(-\gamma\left\|\vec{x}_i - \vec{x}_j\right\|^2), \text{ for } \gamma > 0. \tag{59}$$

The parameter γ defines how far the influence of a single training sample can reach. Standard choice for this parameter is the inverse of a standard deviation of samples depicted as support vector or in other

words $\gamma = \frac{1}{2\sigma^2}$. The *B* parameter makes a trade-off between the misclassification of the training data and simplicity of the decision surface. The low value of this parameter would mean a smooth decision surface, while high value would classify correctly as much training data as possible giving the model freedom to select more data samples as support vectors. Selection of this parameter can thus easily lead to overfitting by making the decision surface to sensible. An example of a RBF kernel with conventional parameters (*B = 1*) derived from (58) would look like:

$$K(x_i, x_j) = \exp\left(-\frac{\left\|\vec{x}_i - \vec{x}_j\right\|^2}{2\sigma^2}\right). \tag{60}$$

Nevertheless, for purposes of this study, parameters *γ* and *B* were varied throughout the training process and optimised values for the SVM model were used. Furthermore, for the non-linear separation of data, a function $C(y, y')$ that penalizes the deviation between the real class y and estimated class $y' = e(x)$ can be defined. Empirical risk $R(e)$ is the decision strategy used in SVM that minimizes the total loss so that the data on the wrong side of the margin have their output values proportional to the distance from the margin. The optimization problem of the empirical risk $R(e) = \sum C(y, e(x))$ is then given with equation:

$$\hat{e} = \arg\min_{e \in E} R(e). \tag{61}$$

The classifier defined with a RBF kernel function in (60), optimization problem of the dataset mapped in the multidimensional space in (56) and penalization function in (61) were used for the non-linear classification of the study participants based on the features extracted only from the wrist (sit-to-stand and gait features) and features extracted from the combination of the waist and wrist attached sensor nodes (inter-limb coordination features).

The issue while training a model addressed in the further paragraphs is regarding the overfitting, or more precisely finding an optimal robust model able to classify correctly new (unseen) data. Overfitting of the model parameters as well as training the model on only particular, statistical most appropriate data occurs when a model rather adopts to the

noise in the data set (so called outliners) than on the exact clusters. The problem is especially important when addressing the elderly population in the non-ambulatory environment where a high influence of noise is expected. Models affected with overfitting have poor predictive performance since they exaggerate even minor fluctuations in the data.

Overfitting can be avoided by using the model validation techniques that assess how the analytical model will perform on an independent data set. Two most popular techniques are leave-one-out (LOO) and k-fold cross-validation (CV), but due to its time effectiveness (i.e. lower computational demanding) the latter one was chosen for the purposes of this study. Simple solution for the problem raised already in the early 1930s by (Larson, 1931) starts from a remark that testing the defined model on new data yields a good estimate of its performance.

The basic idea of the k-fold CV is in splitting the limited available data into *k* clusters. Thereby, it was important to ensure that data (i.e. all extracted features) of a particular participant belong to the same cluster. These clusters were iterated in k-number of loops, where *k-1* clusters were used for the training, while the remaining *k*-th cluster was used for model validation purposes (i.e. evaluation of the model performance). A single iteration with divided data yields a validation estimate of the risk, while averaging it over k splits yields a cross-validation estimate. Robustness of the CV method lies in the assumption that the data distribution is identical, as well as that the training and validation clusters are independent. Numerous previous studies have used for these purposes a 10-fold CV (Schooten, 2015), so due to the consistency purposes the same number of iterations was used in this thesis too.

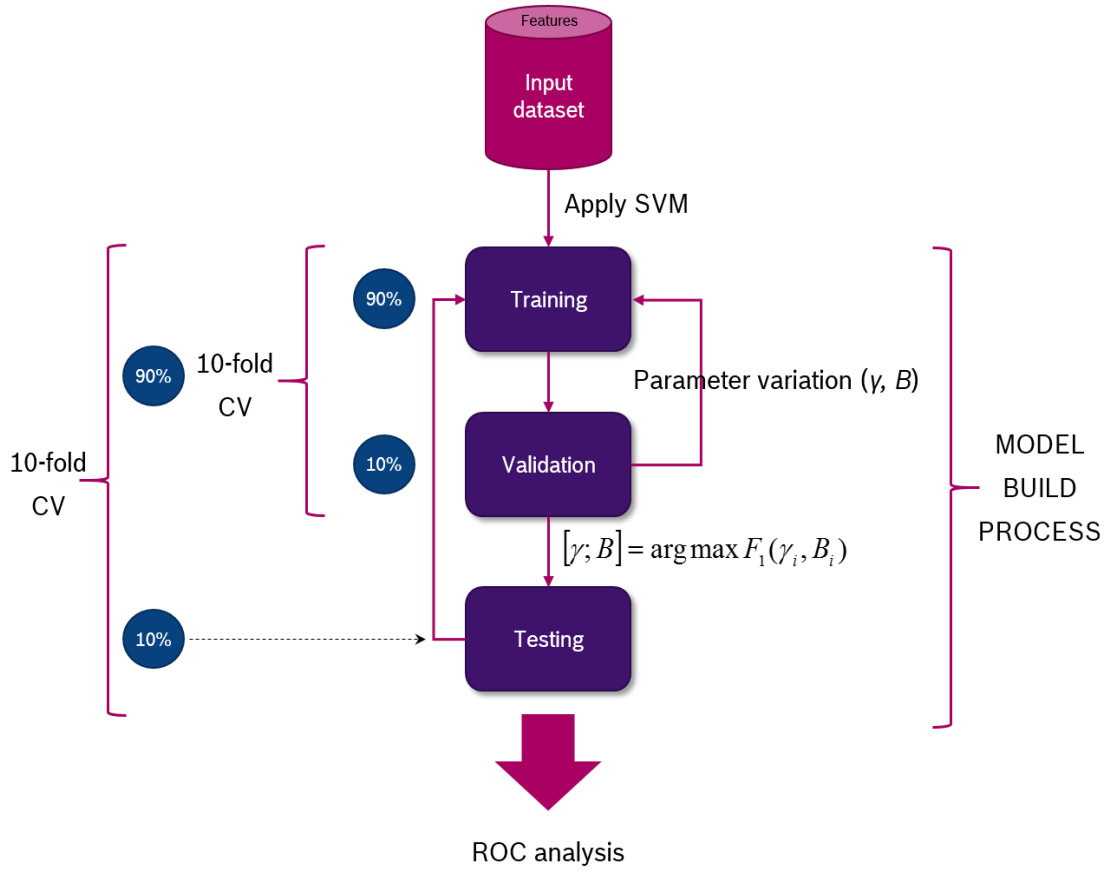

Figure 35 Training of the SVM model for the fall risk classification

The whole process of training a model based on the SVM that can distinguish between fallers and non-fallers is shown in the flowchart (Figure 35). It is split into three steps – training of the model, its validation and final testing. First two steps are used for the parameter selection for the RBF kernel and each time a new parameter set is tested on an unknown dataset. The best parameter set was chosen based on the maximum F_1-measure:

$$[\gamma; B] = \arg\max F_1(\gamma_i, B_i). \tag{62}$$

The F_1-measure for the *i*-th parameter set is defined as:

$$F_{1,i}(\gamma, B) = 2\frac{p_i s_i}{p_i + s_i}. \tag{63}$$

In the equation (62), the $p(\gamma, B)$ depicts the model's precision and $s(\gamma, B)$ depicts the model's sensitivity. Each output of the equation (61) was then further tested on the new dataset where for the each data point

(participant) a probability of correct classification was given. This output was then averaged throughout the 10-fold CV and finally a receiver operating curve (ROC) was calculated. ROC curve shows the algorithm performance in the way that it opposes false positive and true positive rates. A measure of the model accuracy is then given with the area under the curve (AUC). This approach was also previously used in the numerous other studies (Ihlen, 2015 and Schooten, 2015) so it additionally allows easy comparison of the results with the state-of-the-art literature findings. The AUC value at 0.5 and lower represents a worthless test, while the value 1 represents a perfect test.

5.5 Summary

In this chapter a trustworthy simulation of ADL in a controlled setting has yielded a solid basis for identification of inter-limb, gait and sit-to-stand features, as well as for the development of methods that could be used for their reliable extraction from inertial and environmental sensor signals acquired with the waist- and wrist-worn devices. The final steps of proposed methods offer novel approaches for understanding of the fall risk in a geriatric population from a highly non-stigmatized perspective – wrist.

Chapter 5.1 shows a noticeable reduction of the number of sensor nodes needed for assessment of the inter-limb coordination. Despite the existing methods for estimation of the gait speed from the acceleration signal, the proposed multi-model filter approach in chapter 5.1.4 leads to more accurate assessment in longer gait bouts since influence of the noise components is significantly reduced. Added value of the gyroscope signal (5.1.6) for discrimination between contralateral and ipsilateral heel strikes (or more precisely alternating hip rotations) in fusion with acceleration signal transformed into global coordination system (5.1.3) shows the importance of understanding of the model of human movement for direct implementation of reliable algorithms. Highly accurate step detector based on the adaptive multi-threshold approach (5.1.1)

and correct selection of clinically relevant gait bouts (5.1.2) have shown their further true value in the following chapter.

Implementation of the feature that assesses small perturbations in human kinematics throughout the measure of the maximal Lyapunov exponent (5.2) has broaden already wide spectrum of its possible applications. Approach with short Lyapunov exponent on specific gait bouts by means of minimum numbers of state spaces needed for trajectory reconstruction (determined by percentage of false nearest neighbours) and time delay constant (determined by the convergence of mutual information in the signal) have been shown as computationally less demanding than more reliable method proposed in (Schooten, 2012). Nevertheless, it satisfies rigorous requirements typical for the wrist-worn devices and possible clinical applications.

Direct transfer of the waist-based algorithms for STST detection to the wrist (5.3.1.1) has shown poor performance but it paved the way for further development. The chapter 5.3.1.2 has shown a simple sample-based algorithm highly optimized in terms of its precision for detection of non-recurrent movements in ADL (such as STST). The whole development process origins from the empirical evidence of the video analysis and its fundamentals were grounded in using various activity detectors as band-pass filters in specific phases of the transitions. Novel approach was additionally improved by adding the environmental context (i.e. detection of the change in luminance) to algorithm flow, which opens a completely new perspective in assessment and understanding of human physical performance.

Quantitative evaluation of extracted signals that correspond to transitions (5.3.2.1 and 5.3.2.2) was also radically different than in conventional methods found in the literature by means it was focused on finding vigorous robust features capable of assessing only chunks of the actual movement captured far from the centre of balance rather than unreliably taking into account extreme points. The need for that was simply inspired by intensive prevailing dynamics in transition's poste-

riori wrist movements, as noted in the previous observations. The chapter 5.3.2.3 investigates oscillation frequency spectrum in terms of an innovative quantitative measure for assessment of transitions. The hypothesis has shown clear difference between two groups in preliminary investigation, but feature robustness will be shown in the following chapter.

Statistical analysis inter alia proposes an approach for understanding the influence of both, dominant and non-dominant hand on the feature performance in terms of FRA (5.4.1). To round the quantitative assessment, a non-linear SVM-based algorithm with radial basis kernel function was introduced (5.4.2) for separating the defined groups of participants. This well-known kernel trick maps the hand-crafted non-linearly separable feature space into higher dimensional space, where it is possible to find a separating hyperplanes. The overfitting problem was addressed by cross-validating defined models, which utility for clinically relevant applications will be shown in the upcoming chapter.

6 Results

6.1 Inter-limb coordination assessment

In this chapter the results for the inter-limb coordination assessment in terms of acute and 6-months based FRA are shown. The analysis is separated in quantitative and feature analysis. Quantitative analysis evaluates amount of recording time, number of walking bouts, their duration and average speed. It is performed independently for acute and 6-months based fallers and non-fallers. Feature analysis includes evaluation of five proposed features (chapter 5.1) assessing lower-limb and upper- to lower-limb coordination: STV, SPV, IC, YC and CC.

6.1.1 Quantitative analysis

6.1.1.1 Acute FRA

For the acute FRA 9514.2 hours of validated recording were analysed, from which 799.3 hours (8.4%) belonged to acute fallers and 8714.9 hours (91.6%) to non-fallers. On average, the participants at no risk of falling generated slightly more data (52.2 h versus 44.4 h per participant). The total number of walking bouts that were satisfying the exclusion criteria explained in chapter 5.1.2 for acute FRA is 21618 (116.8 walking bouts per participant). For non-fallers 20115 walking bouts (120.0 walking bouts per participant per week) were detected, while for acute fallers in total 1503 walking bouts (83.5 walking bouts per participant per week) were identified. For the selected gait bout length for the non-fallers this choice included 37.6% of the total number of detected walking bouts, while for the fallers this included only 26.7%. The distribution of the walking bout length per participant is shown in Figure 36.

The upper subplot shows distribution of walking bout independently of the gait speed, while the lower subplot shows only the bouts satisfying the gait speed criteria from chapter 5.1.4. All values were normalized for the length of the validated recording time for these two groups in order

to avoid misinterpretation of the results. The number of walking bouts on average per participant is slightly higher ($p = 0.17$) in the acute fallers group than in non-fallers group, with emphasized difference for walking bouts shorter than 30 seconds ($p < 0.01$). Taking into consideration the defined average gait speed these results remain consistent ($p = 0.15$ and $p < 0.01$ for all and gait bouts shorter than 30 seconds).

Looking at the difference in average walking bout duration per participant for non-fallers and acute fallers, independently on the gait speed, significantly shorter bouts ($p = 0.02$) were found for acute fallers ($\mu = 20.3 \pm 15.7$ versus $\mu = 21.3 \pm 16.0$ for fallers and non-fallers, respectively). However, no difference in average walking bout duration between these two groups was found when taking into consideration the defined average gait bout speed ($p = 0.29$). Furthermore, a considerable inequality was found in average gait speed within defined gait bouts between the groups ($p < 0.01$) with higher values for non-fallers ($\mu = 0.84 \pm 0.16$ m/s versus $\mu = 0.80 \pm 0.15$ m/s for non-fallers and acute fallers, respectively). To summarize, non-fallers have walked faster than acute fallers and moreover have performed smaller amounts of bouts shorter than 30 seconds.

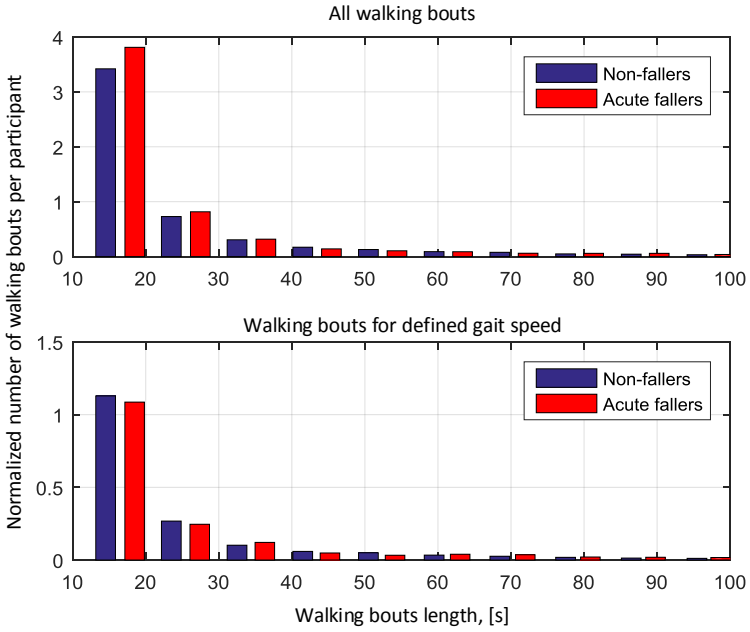

Figure 36 Distribution of the gait bouts length for acute fallers and non-fallers

6.1.1.2 Six-months FRA

In the six-months based analysis, 8088.1 hours of validated recording were used. From that, non-fallers generated 6157.5 hours (76.1%) of recording or 54.5 hours/per participant. In the same time period, fallers generated 1930.5 hours (23.9%) of validated recordings or 55.2 hours/per participant. Non-fallers generated 27383 walking bouts (77.6%) that were satisfying defined exclusion criteria (chapter 5.1), whereas 7906 walking bouts (22.4%) were detected within fallers' recordings. Consistently with the quantitative analysis for acute FRA, selected gait bout length included 34.4% of all walking bouts detected for non-fallers and brought clearly lower percentage (28.6%) walking bouts detected for fallers. This strongly indicates that fallers achieve a greater number of gait bouts shorter than 10 seconds compared to non-fallers, which follows well current literature findings in this field (Brodie, 2015).

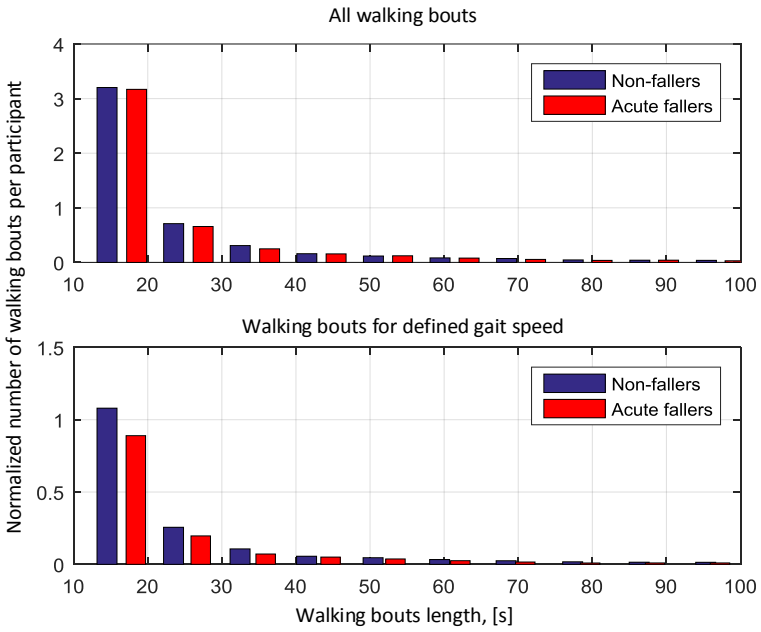

Figure 37 Distribution of the gait bouts length for 6-months based fallers and non-fallers

Similar to the previous chapter (6.1.1.1), a normalized distribution of the gait bout length for all and speed-limited bouts is shown (Figure 37). These findings are comparable to the analysis for acute FRA. Fallers have predominantly ($p < 0.01$) performed shorter walking bouts than

non-fallers (μ = 20.6 ± 15.6 versus μ = 21.2 ± 16.1 for fallers and non-fallers, respectively). Moreover, they have also walked with slower average gait speed ($p < 0.01$) than non-fallers (μ = 0.88 ± 0.17 m/s versus μ = 0.90 ± 0.17 m/s for fallers and non-fallers, respectively). Comparing only the average gait speed, six-months based fallers have walked much faster than acute fallers (0.08 m/s faster, or in other words with 10% higher average gait speed).

6.1.2 Feature analysis

6.1.2.1 Acute FRA

The feature analysis for acute FRA by means of the inter-limb features described in chapters 5.1.5 and 5.1.6, the results shown in the figures below (Figure 38 and Figure 39) were derived. The Figure 38 demonstrates the difference between acute fallers and non-fallers for features describing the bimanual coordination (STV and SPV). The STV feature has shown no difference between these two groups ($p = 0.790$), rather just an extremely high variability within the fallers group reflected throughout the wide confidence interval (95% CI = 0.117-0.127) in comparison to the non-fallers group (95% CI = 0.123-0.126). Despite that, the SPV feature was significantly higher ($p = 0.003$) for fallers than for non-fallers (μ = 0.036 s, 95% CI = 0.036-0.037 and μ = 0.034 s, 95% CI = 0.032-0.036, respectively).

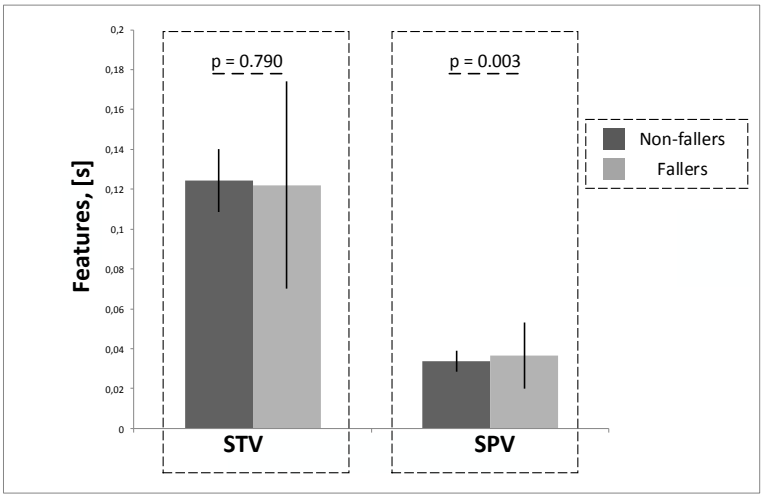

Figure 38 Bimanual coordination features for the acute FRA

The Figure 39 shows relation between IC, CC and YC features for the two defined groups respectively. The most significant difference between the groups was for the IC feature ($p < 0.001$), which was clearly higher for fallers than for non-fallers ($\mu = 0.333$ s, 95% CI = 0.331-0.336 and $\mu = 0.309$ s, 95% CI = 0.301-0.318). While YC feature has shown no difference between the groups ($p = 0.535$), the CC feature has shown statistically significant difference ($p = 0.030$). Despite again the relatively wide confidence interval in the fallers groups (95% CI = 0.317-0.328 versus 95% CI = 0.283-0.319), the mean values could have been distinctly distinguished ($\mu = 0.322$ and $\mu = 0.301$ for fallers and non-fallers, respectively). Interestingly to note, results previously published in (Pozaic, 2015) on a considerably smaller population (N = 16) are consistent with the current ones and therefore confirm high robustness of the proposed approach.

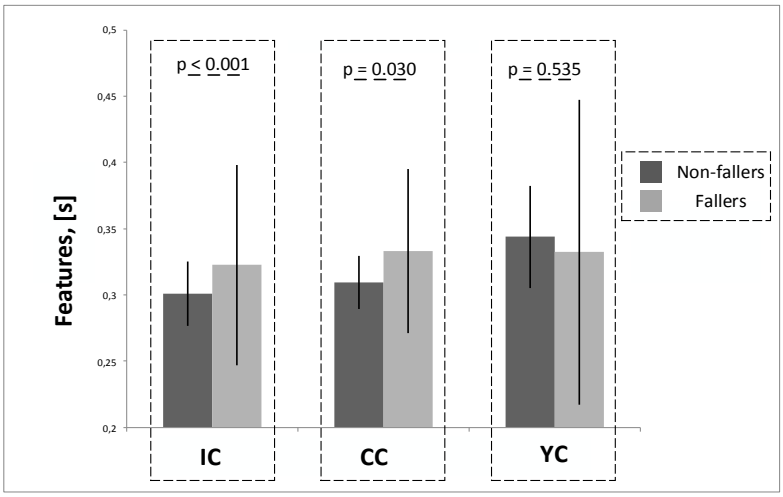

Figure 39 Features describing the upper to lower limb coordination for the acute FRA

6.1.2.2 Six-months FRA

The analysis performed on the six-months follow-up phase has revealed some further scientifically intriguing results, which are shown in the two-dimensional space by using the principal component analysis in the figure below (Figure 40). Namely, the defined five-dimensional space is orthogonally projected on two dimensions allowing a visual interpretation of extracted features. The blue dots in the figure depict non-fallers,

while fallers are depicted with the red dots. Additionally, the Gaussian contours are plotted for each group showing the probability distribution of the orthogonal feature projection.

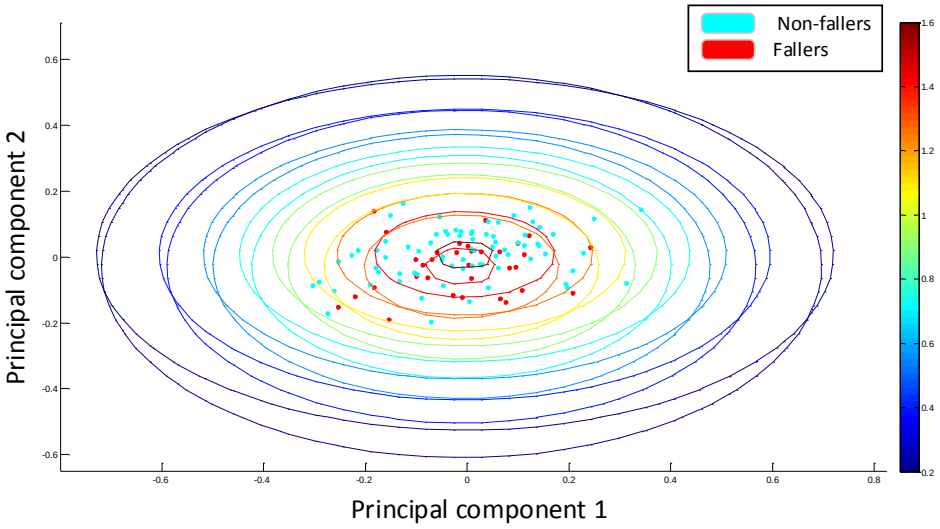

Figure 40 Gaussian contours for the two-dimensional projection of the inter-limb features

Quantitatively, the results have shown significant difference between the groups for four features ($p < 0.001$, $p < 0.001$, $p = 0.049$ and $p = 0.003$ for SPV, STV, IC and YC features, respectively). Both features describing the bimanual coordination were significantly higher for fallers ($\mu = 0.037$ s, 95% CI = 0.036-0.038 versus $\mu = 0.035$ s, 95% CI = 0.034-0.036 for the SPV and $\mu = 0.131$ s, 95% CI = 0.128-0.134 versus $\mu = 0.109$ s, 95% CI = 0.107-0.111 for the STV feature). Furthermore, IC feature's good performance has stayed consistent with the acute FRA (chapter 6.1.2.1) and it kept showing significantly higher values for fallers ($\mu = 0.327$ s, 95% CI = 0.323-0.332 versus $\mu = 0.322$ s, 95% CI = 0.319-0.326). Although in the acute FRA the YC feature has shown no difference between the groups, for the six-months based FRA it shows significantly higher average time delays between the heel strikes and corresponding arm swing for fallers ($\mu = 0.327$ s, 95% CI = 0.311-0.342 versus $\mu = 0.305$ s, 95% CI = 0.292-0.318). Interestingly, the CC feature does not show such a good performance ($p = 0.095$), but presents similar tendencies as in the previous analysis regarding acute fallers and non-fallers (chapter 6.1.2.1).

6.2 Gait analysis

Results for the local dynamic stability assessed throughout the Lyapunov exponent from the wrist-worn sensor data are shown in this chapter. In the first subchapter, the implemented algorithm validated on the Lorenz attractor is presented. The result of an analysis for acute and 6-months based FRA are reported in the following subchapter. The implemented feature (Lyapunov exponent) was tested when considering all participants as one group, as well as when considering participants regarding on which hand the sensor node was placed (dominant or non-dominant hand).

6.2.1 Algorithm validation

The algorithm described in the chapter 5.2.1 was firstly validated by using the Lorenz attractor. Lorenz attractor is a set of solutions of the chaotic Lorenz system, which is defined with three ordinary differential equations (Lorenz, 1963). The value of the largest Lyapunov exponent λ for the Lorenz system was previously calculated for the parameters $\sigma = 16.00$, $\rho = 45.92$ and $\beta = 4.00$ (Viswanath, 1998) and the result is shown in the figure below (Figure 41). This widely applied value of the largest Lyapunov exponent ($\lambda_{REF} = 0.91$) was used for validation purposes of the developed algorithm, where the output $\lambda_L = 0.92$ (relative error $\varepsilon = 1\%$) considerably well approximates distance between trajectories in the defined state space.

The in-house developed arm swing detector described in chapter 5.1.1 was used for an identification of arm swings during walking in ADL. Reliable estimation of the average gait speed within particular gait bout in ADL has shown good performance for the waist-worn device, whereas this estimation for the wrist-worn devices does not satisfy the standards of clinically relevant results. Therefore, due to the focus being set only on the wrist-attached sensor, the gait bouts used in the further feature analysis were defined by a single exclusion criterion – their temporal duration. The exclusion criterion, as suggested in the literature (Brodie, 2015), was set to 10 seconds. Lyapunov exponent, as defined in the

chapter 5.2.1, was calculated based on the Wolf's algorithm. Calculation was based in the state space constructed from the number of embedding dimensions determined by the false nearest neighbour algorithm and with time delay constant τ defined by the mutual information algorithm. The Lyapunov exponent was investigated for the selected gait bouts from the data from the FRA study (chapter 3.1.2).

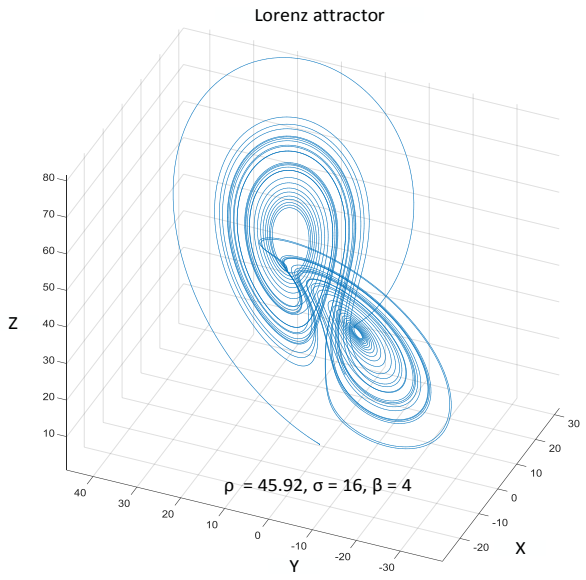

Figure 41 Lorenz attractor with defined parameters

6.2.2 Statistical analysis

The statistical analysis of the extracted largest Lyapunov exponent was performed by tools described in the chapter 5.4.1. In this thesis, only results for the acceleration sensor are shown since gyroscope and magnetometer sensor at the wrist have not brought any added value in distinguishing between fallers and non-fallers. Accordingly to the previous chapter with inter-limb coordination assessment, statistical analysis of this gait feature was independently performed for acute and 6-months based FRA.

Irrelevantly whether one is analysing this feature in terms of the acute or the 6-months based FRA, the λ_L feature shows consistently higher values for the participants at risk of falling (Table 3). Statistical significance

in this feature cannot be found by implementing it on particular sensor axes, but rather looking at the full acceleration contribution while walking (i.e. analysing this feature on the signal vector magnitude). For the magnitude of the acceleration signal significantly higher dynamics in the arm movement was present ($p = 0.045$) for acute fallers. The reliability of this assessment for the studied population was also assessed with high values (ICC = 0.750, 95% CI = 0.696-0.802).

Taking into consideration Lyapunov exponent from the acceleration signal vector magnitude ($\lambda_{L,\ ACC\_SVM}$) in 6-months based FRA, the fallers, compared to non-fallers, continued to achieve significantly higher values ($p = 0.025$). Nevertheless, these non-fallers have shown comparable results for $\lambda_{L,\ ACC\_SVM}$ as the ones defined in the first month of the follow-up phase, whereas acute fallers are still showing slightly higher values (i.e. instability) than regular fallers. In this experimental setup the reliability of this measure continued to be high (ICC = 0.753).

In order to further broaden the spectrum of understanding the Lyapunov exponent's performance in terms of FRA, acquired data was analysed separately for participants that wore the sensor node on their dominant hand (Table 4) and non-dominant hand (Table 5). Higher instability in the dominant arm swings while walking was profoundly found in all sensor axes, whereas only their joint contribution has shown significant and reliable difference between 6-months based fallers and non-fallers ($p = 0.015$, ICC = 0.758). Contrary, the non-dominant hand for acute FRA could clearly distinguish between participants at risk of falling and non-fallers, whereas 6-months based FRA has delivered confusing results suggesting deeper analysis of this case. In both cases, fallers have shown more instability during walking at the dominant than at the non-dominant hand ($p = 0.006$ and $p = 0.022$, for acute and 6-months based fallers respectively). These findings for fallers demonstrated poor normal distribution. Contrary to fallers, non-fallers have more normal distribution of performance between dominant and non-dominant hand.

Table 3 Statistical analysis of the Lyapunov exponent for all participants

		All gait bouts						
Domain	**Feature**	Mean		95% CI		p-value	ICC[4]	
		Non-fallers	Fallers	Non-fallers	Fallers		Mean	95% CI
Acute FRA	λ_{L,Acc_AP}[3,1]	0.664	0.676	0.641-0.687	0.559-0.793	0.532	0.757	0.704-0.808
	λ_{L,Acc_ML}	0.535	0.574	0.510-0.559	0.466-0.683	0.627	0.836	0.796-0.873
	λ_{L,Acc_VT}	0.625	0.629	0.598-0.652	0.513-0.746	0.654	0.811	0.767-0.853
	λ_{L,Acc_SVM}[2]	0.378	0.405	0.365-0.392	0.368-0.442	0.045*	0.750	0.696-0.802
6-months FRA	λ_{L,Acc_AP}	0.666	0.656	0.642-0.691	0.601-0.711	0.528	0.754	0.701-0.806
	λ_{L,Acc_ML}	0.544	0.515	0.518-0.569	0.452-0.578	0.647	0.834	0.794-0.872
	λ_{L,Acc_VT}	0.621	0.641	0.597-0.645	0.555-0.727	0.637	0.812	0.769-0.854
	λ_{L,Acc_SVM}	0.377	0.391	0.365-0.390	0.356-0.426	0.025*	0.753	0.699-0.805

[1]VT depicts X axis of the local coordination system of the sensor, AP is the Y axis, while ML is the Z axis; [2]SVM = Signal Vector Magnitude on which the feature was calculated; [3]Acc = Acceleration; [4]ICC = Intra-class correlation coefficient

Table 4 Statistical analysis of the Lyapunov exponent for the dominant hand

		All gait bouts						
Domain	**Feature**	Mean		95% CI		p-value	ICC[4]	
		Non-fallers	Fallers	Non-fallers	Fallers		Mean	95% CI
Acute FRA	λ_{L,Acc_AP}[3,1]	0.689	0.729	0.653-0.725	0.621-0.837	0.490	0.795	0.725-0.861
	λ_{L,Acc_ML}	0.533	0.517	0.502-0.565	0.411-0.622	0.667	0.719	0.633-0.804
	λ_{L,Acc_VT}	0.654	0.680	0.615-0.692	0.505-0.856	0.271	0.645	0.549-0.744
	λ_{L,Acc_SVM}[2]	0.396	0.419	0.378-0.414	0.345-0.494	0.896	0.540	0.438-0.655
6-months FRA	λ_{L,Acc_AP}	0.682	0.709	0.635-0.729	0.678-0.740	0.513	0.791	0.718-0.858
	λ_{L,Acc_ML}	0.530	0.536	0.491-0.570	0.494-0.577	0.093	0.700	0.610-0.789
	λ_{L,Acc_VT}	0.634	0.714	0.595-0.673	0.625-0.803	0.113	0.649	0.553-0.749
	λ_{L,Acc_SVM}	0.392	0.418	0.371-0.413	0.387-0.449	0.015*	0.758	0.679-0.834

[1]VT depicts X axis of the local coordination system of the sensor, AP is the Y axis, while ML is the Z axis; [2]SVM = Signal Vector Magnitude on which the feature was calculated; [3]Acc = Acceleration; [4]ICC = Intra-class correlation coefficient

Table 5 Statistical analysis of the Lyapunov exponent for the non-dominant hand

		All gait bouts						
Domain	**Feature**	Mean		95% CI		p-value	ICC[4]	
		Non-fallers	Fallers	Non-fallers	Fallers		Mean	95% CI
Acute FRA	λ_{L, Acc_AP}[3,1]	0.645	0.605	0.616-0.675	0.191-1.019	0.116	0.721	0.644-0.797
	λ_{L, Acc_ML}	0.535	0.651	0.499-0.572	0.308-0.994	0.986	0.879	0.836-0.916
	λ_{L, Acc_VT}	0.603	0.561	0.566-0.641	0.235-0.887	0.101	0.872	0.828-0.912
	λ_{L, Acc_SVM}[2]	0.365	0.385	0.346-0.383	0.337-0.434	0.026*	0.829	0.773-0.880
6-months FRA	λ_{L, Acc_AP}	0.655	0.593	0.628-0.682	0.482-0.704	0.606	0.721	0.644-0.797
	λ_{L, Acc_ML}	0.553	0.491	0.519-0.586	0.350-0.631	0.047*	0.879	0.837-0.917
	λ_{L, Acc_VT}	0.612	0.554	0.581-0.643	0.398-0.711	0.397	0.872	0.828-0.912
	λ_{L, Acc_SVM}	0.367	0.359	0.351-0.383	0.289-0.428	0.822	0.829	0.773-0.880

[1]VT depicts X axis of the local coordination system of the sensor, AP is the Y axis, while ML is the Z axis; [2]SVM = Signal Vector Magnitude on which the feature was calculated; [3]Acc = Acceleration; [4]ICC = Intra-class correlation coefficient

6.3 Sit-to-stand transition detection

6.3.1 Waist to wrist algorithm transfer

The algorithm proposed in the chapter 5.3.1.1 was tested on the data acquired in the pilot study described in the chapter 3.1.1. The study included in total 321 transitions assessed with the wrist- and waist-worn sensor nodes. Thereof, seven transitions were excluded from further analysis since their duration was longer than four seconds, which is maximum duration detectable with the proposed algorithm. Moreover, seven further transitions were excluded for the waist-based analysis because the algorithm could not detect the defined extrema (5.3.1.1). For the same reason, 23 transitions were excluded from the wrist-based analysis.

In another words, the algorithm's sensitivity for the waist-worn data was 97.8%, while for the wrist-worn data the sensitivity was 92.8%. The

specificity was not calculated for the proposed method, since only parts of the signal containing the transition were taken as input data (i.e. algorithm was not designed to automatically segment transitions from ADL but rather just estimate their duration). The mean transition duration derived from the labelled data was 1.73 ± 0.78 seconds.

Analysis on the whole defined spectrum of transition durations has shown that video-labelled durations were moderately associated with the waist sensor estimates (Pearson's $r = 0.56$, $p < 0.001$) while for the wrist sensor estimates a poor correlation was shown (Pearson's $r = 0.44$, $p < 0.001$). As a measure of accuracy of prediction, the standard error of estimate (SEE), defined as the sum of squared deviations of estimates, was introduced. For the waist estimates it was SEE = 0.75 seconds, while for the wrist estimates was slightly higher (SEE = 0.81 seconds).

If an imaginary line throughout the mean transition duration would be drown, the results change considerably in favour of the waist-worn sensor node. The transitions shorter than 1.73 seconds have shown for the waist sensor good linear correlation with the reference duration ($r = 0.79$, $p < 0.001$) with the considerably lower SEE = 0.32 seconds. At the same time, the wrist sensor shows moderate correlation ($r = 0.63$, $p < 0.001$) with similar SEE = 0.31 seconds. The scatter plot in Figure 42 shows estimation of the transition duration with the cut-off point between short and long transitions at 1.73 seconds (mean reference transition duration), indicating poor to moderate performance for the STST durations characteristic for the targeted population (elderly at risk of falling).

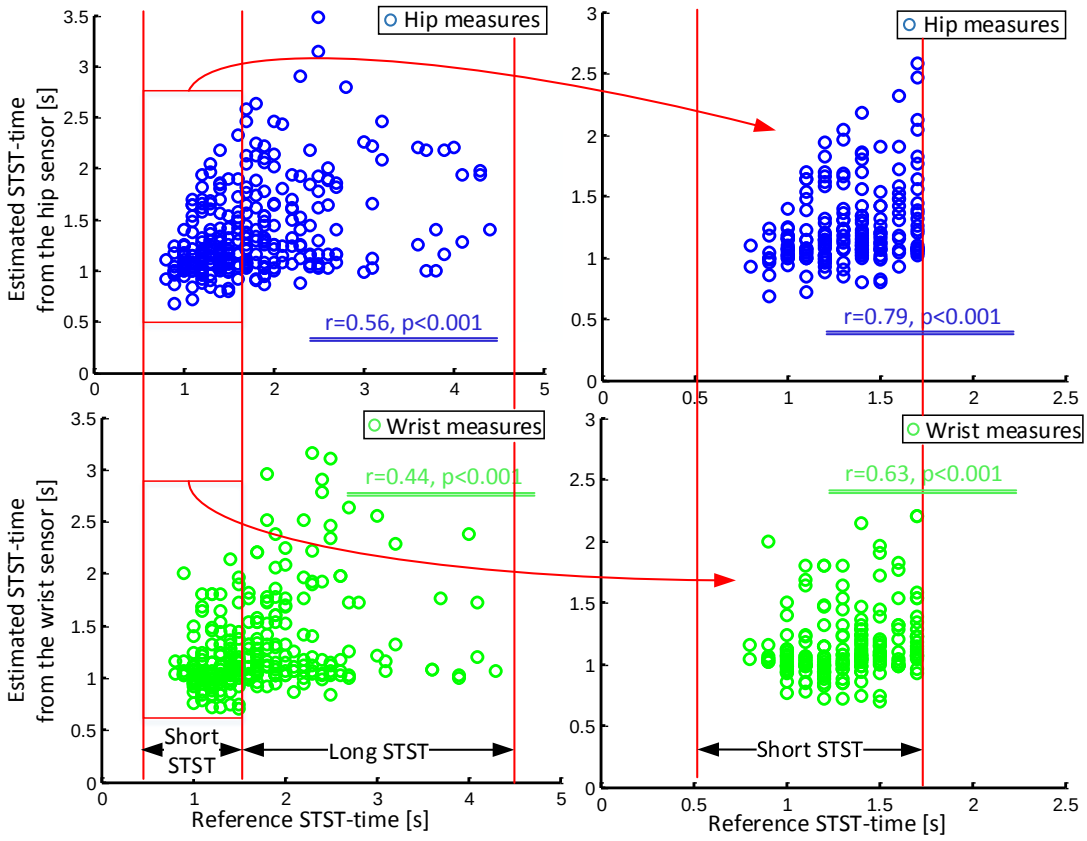

Figure 42 Waist and wrist sensor estimates in comparison to the reference values

Wrist and waist sensor estimates were further tested for eight groups defined in the chapter 3.1.1. Additionally to that, these eight groups were sorted into six following groups and corresponding SEE was shown for them as well in the Figure 43:

- Chairs with armrests;
- Chairs without armrests;
- Standing up by using hands;
- Standing up without using hands;
- Supervised transition;
- Unsupervised transition.

Generally speaking, waist sensor estimates have shown considerably better results in terms of SEE for nine out of 14 analysed groups. In all analysed groups, except one (standing up from a chair without armrests by using hands), the SEE is in the interval between half and one second.

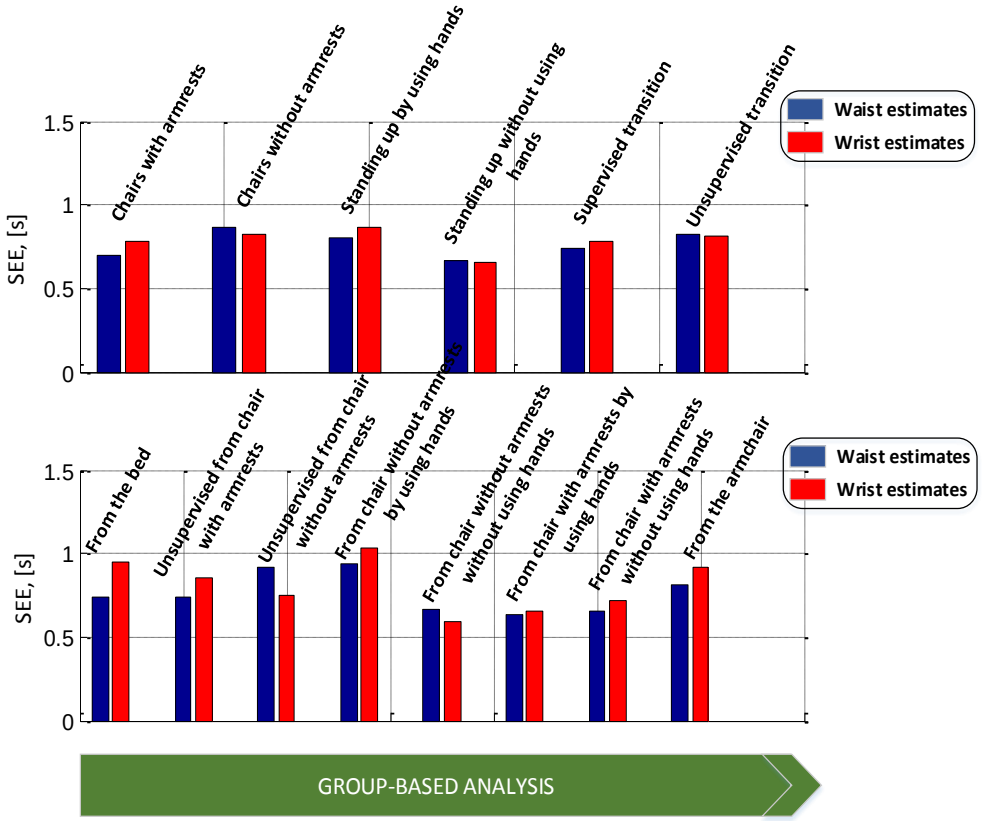

Figure 43 Group-based analysis of the SEE for the wrist and waist sensor estimates

6.3.2 Wrist perspective

The proposed algorithm was developed on a pilot study described in the chapter 3.1.1, which included eight different types of the sit-to-stand transitions in a controlled environment (i.e. camera-supervised laboratory setting) as part of the protocol that simulated activities of daily living. A hyper-parameter optimization was performed for a set of parameters defined in chapter 5.3.1.2. The parameters were optimized for the algorithm with and without the light-sensor feature and independent optimization was performed for the dominant and non-dominant hand. Due to relatively small number of parameters, as well as highly computationally inexpensive model (function) that has to be optimized, a computationally exhaustive grid-search method for hyper-parameter optimization explained in chapter 5.4.1 was used. The set of values used in the grid-search method are shown in the table below (Table 6).

Table 6 Parameter sets for the hyper-optimization process by the grid-search method

Parameter	*Minimum value*	*Maximum value*	*Step*
C1, [g]	*0.003*	*0.005*	*0.0005*
C2, [g]	*-0.005*	*-0.003*	*0.0005*
C3, [s]	*1.0*	*3.0*	*0.5*
C4, [°]	*70*	*90*	*5*
C5, [s]	*2.0*	*4.0*	*0.5*
C6, [°]	*40*	*60*	*5*

C_1 – threshold for maximum positive acceleration deviation; C_2 – threshold for maximum negative acceleration deviation; C_3 – minimum dormancy phase duration; C_4 – angle rotation; C_5 – standing interval; C_6 – standing angle

The defined parameters were optimized in terms of the algorithm's precision. The overall color-coded performance of the grid-search method for the proposed method without the light feature can be seen for the dominant and non-dominant hand in the Figure 44 and with the light feature in the Figure 45. Abscissas in the figure have parameters C_1, C_2 and C_3, while ordinates have the remaining parameters. Their values are distributed in the figures in the block order, meaning C_1 and C_4 parameters have continuous values for five consecutive blocks throughout the figure (5^2 values), values for the parameters C_2 and C_5 parameters change within each of these block for each 5^1 values, while parameters C_3 and C_6 change continuously. In this way, all possible parameter combination are shown in the two-dimensional space. Color-coded precision values are described with the colour bar, where dark red depicts the highest values. Part that is in both figures shown in dark blue colour depicts the lowest values. Namely, for the highest value of C_4 parameter ($C_4 = 90°$), algorithm's precision drops to zero (i.e. no transitions are detected) since derivative of the angle rotation from equations (30) and (31) is limited with definition of *atan* function limited on the interval from $\langle -\frac{\pi}{2}, \frac{\pi}{2} \rangle$.

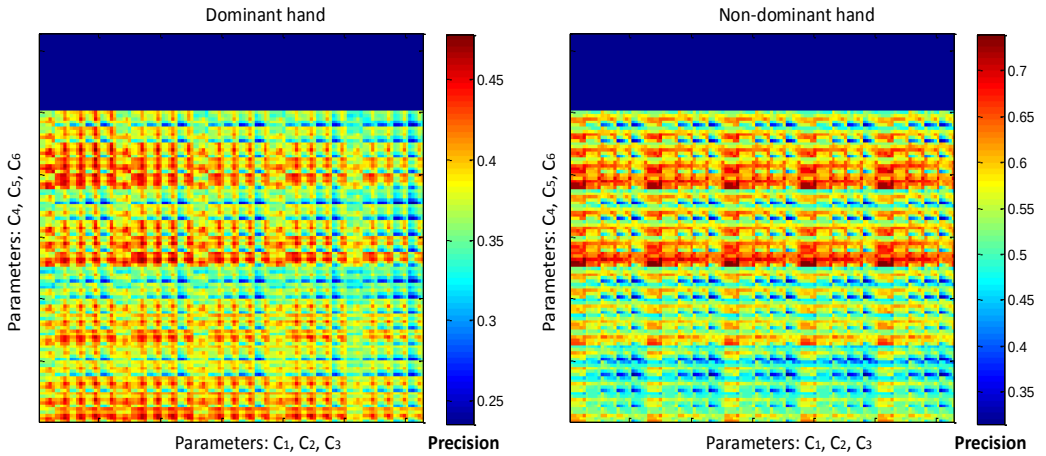

Figure 44 Algorithm performance without the light feature for parameter variation (C_1-C_6)

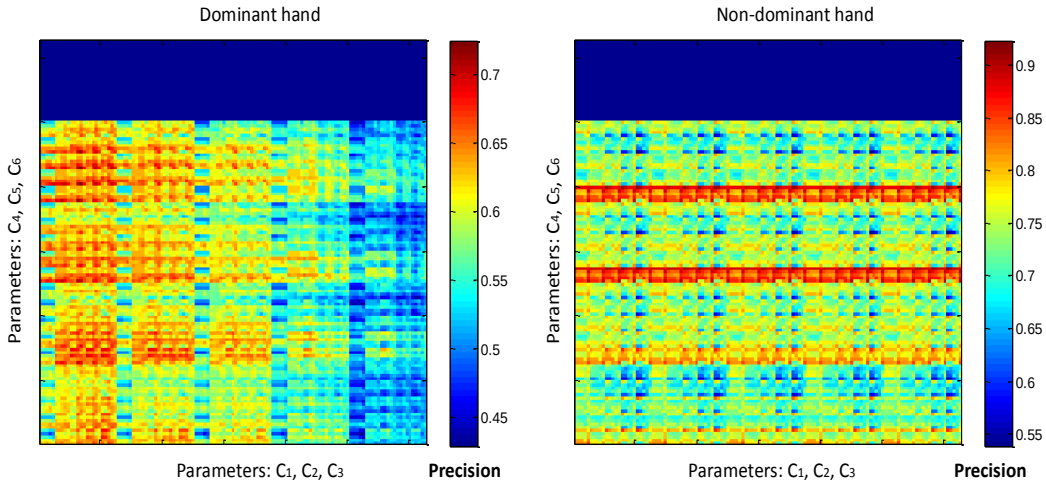

Figure 45 Algorithm performance with the light feature for parameter variation (C1-C6)

The precision or positive predictive value was defined as the ratio between the number of correctly detected transitions and total number of detected transitions. The transition is considered as correctly detected in cases when the trigger point defined in chapter 5.3.1.2 falls within the video-labelled transition interval including the 0.5 seconds deviation added to avoid possible human mistakes during labelling.

The best shown performance (i.e. highest algorithm precision) for the proposed method without the light feature was 47.8% and 73.9%, for the dominant and non-dominant hand respectively. By adding the light feature in the proposed method with a fixed parameter C_7 = 20 lux/s, the

algorithm's precision improves considerably. More precisely, the overall precision was 76.8%, for the dominant hand was 72.5% (improvement of 51.7%), while for the non-dominant hand was 92.3% (improvement of 24.9%). As a trade-off, this improvement in the precision yielded slightly lower sensitivity, but due to the high number of transitions in ADL enough data for clinically relevant interpretation of one's performance will still be ensured.

Different sets of parameters have shown the optimal performance for the dominant and non-dominant hand for the proposed method with and without the light feature. The Hausdorff distance h_D, as a measure of similarity of two metric spaces (in this case the metric spaces are precision matrixes for the algorithm performance at the dominant and non-dominant hand with the light feature), showed a low similarity between them ($h_D = 0.19$), thus suggesting different parameter sets for each hand.

6.4 Sit-to-stand transition assessment

The STST assessment is shown in separate subchapters for acute and 6-months based FRA. Each subchapter comprises of quantitative and feature analysis. Quantitative analysis includes the amount of validated recording time, number of detected STST and their distribution across different groups (fallers, non-fallers). Feature analysis shows statistical analysis of features proposed in chapters 5.3.2.1 and 5.3.2.2. In addition to that, a detail statistical analysis of a novel AS feature (chapter 5.3.2.3) for acute and 6-months based FRA is shown in the last subchapter. While quantitative analysis is performed on all participants disregarding on which hand the sensor node was placed on, feature analysis is performed on all participants taken as one group, as well as on participants wearing the sensor node on their dominant or non-dominant hand.

6.4.1 STST assessment for acute FRA

6.4.1.1 Quantitative analysis

The optimal set of parameters for the method including the light feature was applied for the detection of transitions in the study described in chapter 3.1.1. Only validated data that satisfies the defined exclusion criteria (explained in 3.1.2.3) was used for further analysis. In the FRA study 5934 hours of validated recordings were created, from which 588 hours (32.6 hours per participant per week of recording) for the acute fallers and 5346 hours for non-fallers (33.0 hours per participant per week). The algorithm detected 427 transitions in total for fallers (30.5 transitions per participant per week). From that number, 64 transitions were STW (15.0%), 357 (83.6%) were STSA and only 6 were STSP (1.4%). In the same time, the algorithm detected 6587 transitions for non-fallers (39.7 transitions per participant per week) from which 989 were STW (15.0%), 5488 were STSA (83.3%) and 110 were STSP (1.7%). Due to the rare occurrence of the STSP in ADL, these transitions were analysed together with the STSA.

Although non-fallers performed in average more transitions, solely the number of transitions could not distinguish between the groups ($p = 0.465$). Moreover, the transition patterns (share of each transition type) were similar in both groups from the macro perspective. A high variability in the number of detected transitions was present for both groups (30.5 ± 32.2 and 39.7 ± 45.9 transitions in average for fallers and non-fallers respectively). Nevertheless, the number of detected transitions followed the exponential distribution for the groups of fallers (Figure 46), while for the group of non-fallers this feature was bimodal (a mixture distribution was present).

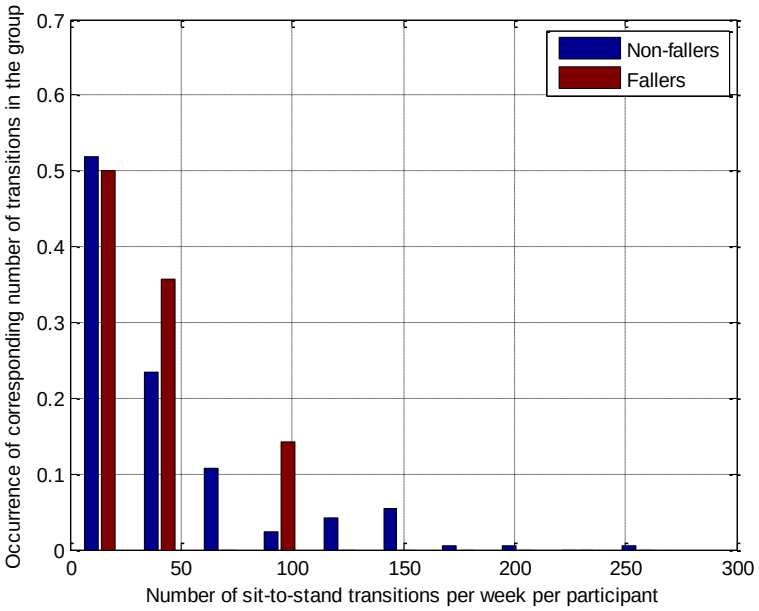

Figure 46 The distribution of the number of transitions for acute fallers and non-fallers

6.4.1.2 Feature analysis

The feature analysis was performed independently for the acute FRA and 6-months FRA. The results were analysed in both cases for all transitions, as well as separately for dominant and non-dominant hand. For each participant and each extracted feature, a mean value based on the all transitions within the participant's measurement period was derived and was further used in the statistical analysis. In total, for both FRA analyses 17 time and frequency domain features were tested.

For the acute FRA, the Benjamini-Hochberg correction for multiple comparison defined $p = 0.050$ as the critical p-values for all transitions, dominant and non-dominant hand. The one-sample Kolmogorov-Smirnov test rejected a null hypothesis that extracted features have a standard normal distribution at 5% significance level, thus a non-parametric Wilcoxon-Mann-Whitney test was applied.

After the correction for the multiple comparison, the test applied on all detected transitions has shown significant difference between the groups for in total five features and some further prominent results for

two more time domain features (Table 7). From that number, one feature was in the time domain and four were in the frequency domain. The only time domain feature showing the statistically significant difference between acute fallers and non-fallers was median value calculated on the signal vector magnitude of the transition (p = 0.026) with higher values in favour of the non-fallers (μ = 1.007, 95% CI = 1.003-1.011 versus μ = 1.003, 95% CI = 0.986-1.022). Despite, as already mentioned, promising results in previous studies (chapter 5.3.2), the peak value has shown no significant difference between the groups (p = 0.054). Nevertheless, considerable higher peak values in the ML and AP direction for acute fallers indicate more instability (side movement) while standing up and more pushing forward alongside armrests during transfers characteristic for people with lower limb weakness. From the feature concept, the jerk feature looked like a good feature based on the study mentioned in the chapter 5.3.2, but it has shown surprisingly poor performance for acute FRA, particularly due to very wide confidence intervals.

Table 7 Feature analysis for acute FRA for all detected transitions

		All detected transitions					
Domain	**Feature**	Mean		95% CI		p-value[11]	ICC
		Non-fallers	Fallers	Non-fallers	Fallers		
Time	Peak_VT[1]	0.789	0.756	0.769-0.808	0.686-0.827	0.224	0,821
	Peak_AP[1]	0.917	0.982	0.899-0.934	0.915-1.051	0.054	0,910
	Peak_ML[1]	0.855	0.903	0.841-0.869	0.845-0.962	0.108	0,874
	RMS_SVM[2,3]	1.023	1.019	1.019-1.028	1.001-1.037	0.054	0,855
	Median_SVM[2]	1.007	1.003	1.003-1.011	0.986-1.022	0.026*	0,872
	TTFS[4]	1.816	1.646	1.764-1.869	1.439-1.853	0.118	0,852
	AFS[5]	1.103	1.132	1.072-1.134	0.935-1.328	0.915	0,862
	SD[6]	0.155	0.158	0.152-0.158	0.149-0.167	0.103	0,841
	Jerk (10^{-3})	0.266	0.305	0.232-0.301	0.076-0.535	0.915	0,709
Frequency	Entropy_VT[1]	5.218	5.125	5.196-5.241	5.029-5.222	0.003*	0,789
	Energy_VT[1]	0.653	0.561	0.642-0.665	0.519-0.604	0.002*	0,854

FF_SVM[8]	1.253	1.240	1.234-1.272	1.175-1.305	0.915	0,714
AO_ML[1,9] (10^{-2})	0.279	0.250	0.250-0.317	0.201-0.302	0.104	0,854
AO_VT (10^{-2})	0.243	0.182	0.212-0.278	0.130-0.235	0.224	0,781
AO_AP (10^{-2})	0.564	0.508	0.519-0.613	0.398-0.629	0.164	0,780
RatioEnergy	12.03	12.56	11.86-12.23	11.62-13.50	0.621	0,804
IH_VT[1,10]	29.20	22.81	24.84-33.55	18.93-26.70	0.026*	0,821

[1]VT depicts X axis of the local coordination system of the sensor, AP is the Y axis, while ML is the Z axis; [2]SVM = Signal Vector Magnitude on which the feature was calculated; [3]RMS = Root Mean Square; [4]TTFS = Time to First arm Swing; [5]AFS = Amplitude of the First Step; [6]SD = Standard Deviation; [7]AS = Amount of applied Support; [8]FF = Fundamental Frequency; [9]AO = Amount of Oscillation; [10]IH = Index of Harmonicity; [11]Adjusted for multiple comparison

Overall speaking for the acute FRA, the frequency domain features have shown noticeably better performance. More precisely, entropy in the VT direction, energy in the VT direction and IH in the VT direction were all significantly higher for the non-fallers ($p = 0.003$, $p = 0.002$ and $p = 0.026$, respectively) conforming to previous literature findings and starting hypothesis (chapter 5.3.2.2). Once again, the fallers were presented with more than twice wider confidence intervals (95% CI = 5.029-5.222 versus 95% CI = 5.196-5.241 for entropy and 95% CI = 0.642-0.665 versus 95% CI = 0.519-0.604 for energy) despite the considerably smaller number of participants. Although the IH was significantly higher for non-fallers depicting the dominance of the first harmonic over the following five harmonics in the VT direction of the acceleration signal while standing up, the energy ratio could not distinguish between the groups. FF was on average also higher for non-fallers but without any significance ($p = 0.915$).

The analysis of the transitions detected in data acquired only at the dominant hand has revealed different features as significant fall risk predictor in terms of the sit-to-stand transitions. In total six features, from which four time and two frequency domain features, have shown statistically significant difference at significance level $\alpha = 0.05$ between the groups (Table 8). The peak values in the AP and ML direction have

consistently followed the results from the previous case with even higher difference between the groups (μ = 0.498, 95% CI = 0.472-0.525 and μ = 0.902, 95% CI = 0.786-1.018 for AP and μ = 1.017, 95% CI = 0.992-1.042 and μ = 0.901, 95% CI = 0.805-0.998 for peak values in ML direction). The results have also shown significantly higher peak values in the ML direction than in the AP direction for non-fallers ($p < 0.001$), whereas for fallers the movement was equally distributed ($p = 0.737$) yielding more unstable transition patterns while standing up. Both, median and RMS values were significantly higher for acute fallers ($p = 0.003$ and $p = 0.004$, respectively) with correspondingly wide confidence intervals (95% CI = 0.962-1.018 and 95% CI = 0.978-1.036, respectively). Interestingly, although the TTFS was slightly higher for non-fallers than for acute fallers, the amplitude of the first arm swing following the transfer reflected throughout the AFS feature was higher in fallers but without any statistical significance ($p = 0.296$ for both features).

Table 8 Feature analysis for acute FRA for transitions detected at the dominant hand

		Dominant hand transitions (7 fallers, 82 non-fallers)					
Domain	**Feature**	Mean		95% CI		p-value[11]	ICC
		Non-fallers	Fallers	Non-fallers	Fallers		
Time	Peak_VT[1]	0.631	0.739	0.597-0.665	0.624-0.853	0.172	0,796
	Peak_AP[1]	0.498	0.902	0.472-0.525	0.786-1.018	< 0.001*	0,806
	Peak_ML[1]	1.017	0.901	0.992-1.042	0.805-0.998	0.044*	0,845
	RMS_SVM[2,3]	1.003	1.007	0.995-1.011	0.978-1.036	0.004*	0,841
	Median_SVM[2]	0.988	0.991	0.980-0.995	0.962-1.018	0.003*	0,870
	TTFS[4]	1.686	1.554	1.591-1.780	1.264-1.846	0.296	0,875
	AFS[5]	1.012	1.214	0.955-1.068	0.853-1.575	0.296	0,888
	SD[6]	0.153	0.164	0.148-0.158	0.148-0.181	0.172	0,782
	Jerk (10^{-3})	0.075	0.540	0.018-0.131	0.076-0.104	0.142	0,635
Frequency	Entropy_VT[1]	5.142	5.043	5.099-5.183	4.886-5.199	0.034*	0,782
	Energy_VT[1]	0.577	0.546	0.558-0.595	0.480-0.612	0.419	0,785

FF_SVM[7]	1.255	1.276	1.221-1.289	1.167-1.385	0.375	0,681
AO_ML[1,8] (10^{-2})	0.344	0.317	0.285-0.402	0.231-0.409	0.172	0,907
AO_VT (10^{-2})	0.317	0.234	0.246-0.391	0.120-0.355	0.172	0,748
AO_AP (10^{-2})	0.686	0.635	0.580-0.796	0.407-0.862	0.427	0,752
RatioEnergy	12.15	12.77	11.77-12.55	11.17-14.38	0.727	0,791
IH_VT[1,9]	27.12	18.44	24.86-29.39	16.20-20.70	0.030*	0,796

[1]VT depicts X axis of the local coordination system of the sensor, AP is the Y axis, while ML is the Z axis; [2]SVM = Signal Vector Magnitude on which the feature was calculated; [3]RMS = Root Mean Square; [4]TTFS = Time to First arm Swing; [5]AFS = Amplitude of the First Step; [6]SD = Standard Deviation; [7]FF = Fundamental Frequency; [8]AO = Amount of Oscillation; [9]IH = Index of Harmonicity; [11]Adjusted for multiple comparison

In contrary to the feature analysis performed on all detected transitions, analysis only on the dominant hand has shown lower number of features in the frequency domain that can significantly separate acute fallers from non-fallers. More precisely, only entropy and IH in the VT direction has shown good performance in this particular case (Table 8). This just repeats the findings from previous analysis (Table 7). Both features were significantly higher ($p = 0.034$ and $p = 0.030$ for entropy and IH, respectively) for non-fallers than for fallers ($\mu = 5.142$, 95% CI = 5.099-5.183 versus $\mu = 5.043$, 95% CI = 4.886-5.199 and $\mu = 27.12$, 95% CI = 24.86-29.39 versus $\mu = 18.44$, 95% CI = 16.20-20.70 for entropy and IH, respectively). As the most noticeable change in comparison to the previous analysis, the FF feature was slightly higher ($p = 0.375$) for fallers than for non-fallers, but without any significance, which can mainly be ascribed to high variability (i.e. wide confidence intervals) in the feature values.

Table 9 Feature analysis for acute FRA for transitions detected at the non-dominant hand

		Non-dominant hand transitions (7 fallers, 84 non-fallers)					
Domain	**Feature**	Mean		95% CI		p-value[11]	ICC
		Non-fallers	Fallers	Non-fallers	Fallers		
Time	Peak_VT[1]	0.878	0.770	0.855-0.902	0.681-0.859	0.045*	0,807

Peak_AP[1]	1.155	1.045	1.136-1.174	0.964-1.126	0.274	0,901
Peak_ML[1]	0.763	0.905	0.747-0.778	0.833-0.977	< 0.001*	0,863
RMS_SVM[2,3]	1.035	1.028	1.031-1.040	1.005-1.052	0.332	0,835
Median_SVM[2]	1.019	1.0147	1.014-1.023	0.992-1.038	0.159	0,849
TTFS[4]	1.889	1.738	1.828-1.951	1.434-2.041	0.473	0,824
AFS[5]	1.154	1.049	1.117-1.190	0.876-1.222	0.614	0,808
SD[6]	0.156	0.154	0.152-0.159	0.144-0.164	0.332	0,888
Jerk (10^{-3})	0.376	0.125	0.332-0.419	0.068-0.318	0.331	0,773
Entropy_VT[1]	5.262	5.189	5.237-5.287	5.067-5.311	0.092	0,799
Energy_VT[1]	0.697	0.573	0.683-0.712	0.518-0.629	< 0.001*	0,882
FF_SVM[7]	1.252	1.213	1.229-1.274	1.133-1.292	0.424	0,775
AO_ML[1,8] (10^{-2})	0.242	0.198	0.212-0.270	0.142-0.256	0.473	0,756
AO_VT (10^{-2})	0.201	0.142	0.175-0.233	0.115-0.176	0.614	0,807
AO_AP (10^{-2})	0.495	0.409	0.457-0.538	0.329-0.491	0.332	0,823
RatioEnergy	11.96	12.40	11.72-12.19	11.29-13.51	0.613	0,824
IH_VT[1,9]	30.38	26.18	23.66-37.09	19.53-32.83	0.422	0,806

Frequency

[1]VT depicts X axis of the local coordination system of the sensor, AP is the Y axis, while ML is the Z axis; [2]SVM = Signal Vector Magnitude on which the feature was calculated; [3]RMS = Root Mean Square; [4]TTFS = Time to First arm Swing; [5]AFS = Amplitude of the First Step; [6]SD = Standard Deviation; [7]FF = Fundamental Frequency; [8]AO = Amount of Oscillation; [9]IH = Index of Harmonicity; [11]Adjusted for multiple comparison

Another perspective on the sit-to-stand transitions was provided by the analysis of features extracted from the non-dominant hand (Table 9). The peak-based features show good performance as for the dominant hand, whereas RMS and median features show no significant difference between acute fallers and non-fallers. The peak values in the VT direction show significantly higher values for non-fallers ($p = 0.045$), while in the ML direction the findings are consistent with the dominant hand. The TTFS is for the non-dominant hand significantly higher than for the dominant hand ($p < 0.001$ for both, fallers and non-fallers). Moreover,

for the non-dominant hand both, TTFS and AFS are slightly higher for non-fallers. In the frequency domain only energy in the VT direction shows significant difference between two defined groups. Hence, the entropy also shows tendencies as for the dominant hand with higher values for the non-fallers ($\mu = 5.262$, 95% CI = 5.237-5.287 versus $\mu = 5.189$, 95% CI = 5.067-5.311).

6.4.2 STST assessment for 6-months based FRA

6.4.2.1 Quantitative analysis

The quantitative analysis for 6-months based FRA was performed under same conditions as for the acute fallers (chapter 6.4.1). In total 5301 hours of recordings were analyzed, from which 1546 hours of data was generated by fallers and 3755 hours by non-fallers. Compared to the acute FRA, decreased number of participants was included into analysis due to insufficient number (less than six) of submitted fall diaries. The algorithm detected in total 6482 sit-to-stand transitions. Fallers performed in total 1678 transitions or 35.7 transitions per participant per week, whereas non-fallers performed considerably more ($p = 0.109$) transitions (4804 transitions in total or 49.0 transitions per participant per week). Looking at the transition types, their distribution resembles one in acute FRA (Figure 47). Namely, for non-fallers the most of transitions belongs to STSA type (4003 or 83.3%), minimal amount to STSP (88 or 1.8%) and as in acute FRA similar amount to STW (713 or 14.8%). The analysis for fallers brought 1429 STSA (85.2%), 20 STSP (1.2%) and 229 STW (13.6%).

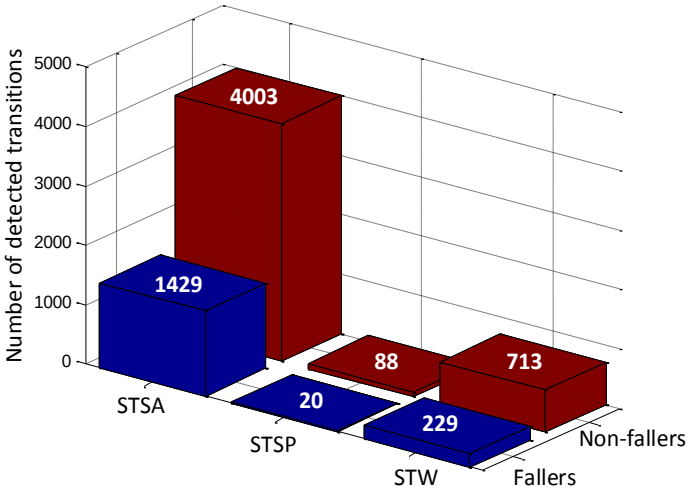

Figure 47 Distribution of transition types for 6-months based fallers and non-fallers

Occurrence of the transition types was similar between the groups, as well as in the acute FRA. High variability in the number of detected transitions was also present here. The distribution of the number of detected transitions per participant per week followed again an exponential distribution for fallers, whereas in the group of non-fallers this distribution was bimodal ($p < 0.001$ in both cases) as shown in the figure below (Figure 48).

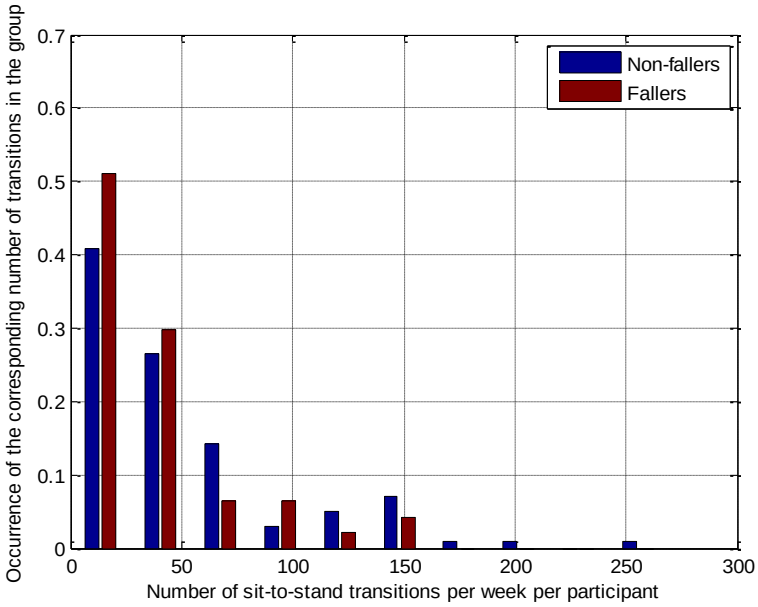

Figure 48 The distribution of the transition occurrence for 6-months based FRA

6.4.2.2 Feature analysis

The 6-months based FRA analysis of extracted features is shown in this chapter. Firstly, all participants, disregarding on which hand they wore the sensor node, were considered for the analysis. The results are shown consistently with the results for the acute FRA in chapter 6.4.1.2. After the correction for the statistical type I error in total seven features have shown significant difference between the fallers and non-fallers, from which four features derived in the time domain and two in the frequency domain. Peak values for all detected transitions show consistency with finding for acute fallers (6.4.1.2), where peak values in AP direction are significantly lower for fallers ($p < 0.001$), whereas peak values in the ML direction are significantly higher for the same group ($p = 0.003$). Moreover, median value calculated over the signal vector magnitude is significantly higher for non-fallers ($p = 0.024$), showing the remarkable consistency with previous findings for acute fallers. In this case the Wilcoxon-Mann-Whitney test has also shown difference for the SD feature ($p = 0.009$) (Table 10).

Analysis of the features implemented in the frequency domain has also shown good performance. Both, energy and entropy were significantly higher for the non-fallers than for the fallers ($p = 0.049$ and $p = 0.048$, respectively). The IH in the VT direction was, on the other hand, significantly higher for fallers ($\mu = 37.36$, 95% CI = 15.02-59.72 versus $\mu = 27.44$, 95% CI = 26.13-28.74 with $p = 0.020$), which is opposing previous findings (chapter 6.4.1.2). Although, the FF feature has not shown significant difference between the groups, it was again slightly higher for non-fallers. On top of that, all significant features have been shown as robust measures in terms of the FRA with high intra-test reliability (ICC > 0.750).

Table 10 Feature analysis for 6-months FRA for all detected transitions

		All detected transitions (35 fallers, 110 non-fallers)					
Domain	**Feature**	Mean		95% CI		p-value[11]	ICC
		Non-fallers	Fallers	Non-fallers	Fallers		
Time	Peak_VT[1]	0.797	0.772	0.775-0.819	0.729-0.814	0.698	0.807

Peak_AP[1]	0.949	0.839	0.930-0.969	0.801-0.879	< 0.001*	0.917
Peak_ML[1]	0.844	0.892	0.829-0.860	0.860-0.923	0.003*	0.864
RMS_SVM[2,3]	1.028	1.020	1.023-1.032	1.010-1.030	0.315	0.843
Median_SVM[2]	1.012	1.004	1.008-1.016	0.994-1.014	0.024*	0.860
TTFS[4]	185.3	176.1	1.796-1.911	1.634-1.888	0.368	0.832
AFS[5]	1.126	1.109	1.092-1.161	1.028-1.190	0.776	0.822
SD[6]	0.153	0.157	0.150-0.157	0.151-0.163	0.009*	0.871
Jerk (10^{-3})	0.270	0.230	0.232-0.308	0.147-0.313	0.181	0.692
Entropy_VT[1]	5.246	5.197	5.223-5.269	5.144-5.250	0.049*	0.750
Energy_VT[1]	0.661	0.629	0.648-0.674	0.602-0.655	0.048*	0.842
FF_SVM[7]	1.257	1.215	1.235-1.279	1.177-1.253	0.315	0.633
AO_ML[1,8] (10^{-2})	0.282	0.235	0.249-0.315	0.200-0.270	0.204	0.860
AO_VT (10^{-2})	0.253	0.171	0.216-0.290	0.149-0.193	0.341	0.786
AO_AP (10^{-2})	0.560	0.484	0.514-0.606	0.422-0.546	0.699	0.815
RatioEnergy	12.03	12.25	11.80-12.27	11.78-12.72	0.311	0.801
IH_VT[1,9]	27.44	37.36	26.13-28.74	15.02-59.72	0.020*	0.835

Frequency

[1]VT depicts X axis of the local coordination system of the sensor, AP is the Y axis, while ML is the Z axis; [2]SVM = Signal Vector Magnitude on which the feature was calculated; [3]RMS = Root Mean Square; [4]TTFS = Time to First arm Swing; [5]AFS = Amplitude of the First Step; [6]SD = Standard Deviation; [7]AS = Amount of applied Support; [8]FF = Fundamental Frequency; [9]AO = Amount of Oscillation; [10]IH = Index of Harmonicity; [11]Adjusted for multiple comparison

Secondly, the results for the dominant hand have shown that only three features can distinguish between fallers and non-fallers (Table 11). More precisely, two features in time domain (peak amplitude in the VT and AP direction) and one feature in the frequency domain (IH in the VT direction) have shown significant difference (all three with significance factor p = 0.047). Lastly and surprisingly, for the participants wearing the sensor node on the non-dominant hand, only IH in the VT direction has been shown as significant (p = 0.013) and reliable (ICC = 0.830) feature in terms of the six-months FRA.

Table 11 Feature analysis for 6-months FRA for transitions detected at the dominant hand

		Dominant hand transitions (16 fallers, 52 non-fallers)					
Domain	**Feature**	Mean		95% CI		p-value[11]	ICC
		Non-fallers	Fallers	Non-fallers	Fallers		
Time	Peak_VT[1]	0.608	0.696	0.567-0.649	0.634-0.759	0.047*	0,773
	Peak_AP[1]	0.474	0.529	0.442-0.506	0.479-0.579	0.047*	0,835
	Peak_ML[1]	1.023	0.984	0.992-1.054	0.936-1.032	0.972	0,837
	RMS_SVM[2,3]	1.002	1.009	0.993-1.012	0.994-1.024	0.815	0,814
	Median_SVM[2]	0.987	0.994	0.979-0.996	0.979-1.008	0.972	0,818
	TTFS[4]	1.674	1.748	1.560-1.788	1.534-1.961	0.586	0,854
	AFS[5]	1.033	1.037	0.963-1.102	0.907-1.168	0.972	0,908
	SD[6]	0.151	0.154	0.145-0.157	0.146-0.162	0.082	0,757
	Jerk (10^{-3})	0.063	0.774	0.009-0.135	0.026-0.181	0.586	0,583
	Entropy_VT[1]	5.153	5.184	5.104-5.203	5.106-5.262	0.712	0,702
	Energy_VT[1]	0.584	0.560	0.562-0.606	0.523-0.598	0.503	0,749
Frequency	FF_SVM[7]	1.273	1.182	1.229-1.317	1.127-1.237	0.389	0,584
	AO_ML[1,8] (10^{-2})	0.383	0.261	0.299-0.472	0.198-0.320	0.357	0,912
	AO_VT (10^{-2})	0.367	0.183	0.265-0.465	0.140-0.236	0.357	0,760
	AO_AP (10^{-2})	0.729	0.504	0.607-0.853	0.413-0.598	0.357	0,794
	RatioEnergy	11.95	12.77	11.46-12.44	11.96-13.59	0.147	0,781
	IH_VT[1,9]	28.51	24.25	25.52-31.50	20.10-28.39	0.047*	0,773

[1]VT depicts X axis of the local coordination system of the sensor, AP is the Y axis, while ML is the Z axis; [2]SVM = Signal Vector Magnitude on which the feature was calculated; [3]RMS = Root Mean Square; [4]TTFS = Time to First arm Swing; [5]AFS = Amplitude of the First Step; [6]SD = Standard Deviation; [7]AS = Amount of applied Support; [8]FF = Fundamental Frequency; [9]AO = Amount of Oscillation; [10]IH = Index of Harmonicity; [11]Adjusted for multiple comparison

Table 12 Feature analysis for 6-months FRA for transitions detected at the non-dominant hand

		Non-dominant hand transitions (19 fallers, 58 non-fallers)					
Domain	**Feature**	Mean		95% CI		p-value[11]	ICC
		Non-fallers	Fallers	Non-fallers	Fallers		
Time	Peak_VT[1]	0.881	0.835	0.855-0.906	0.778-0.892	0.811	0.801
	Peak_AP[1]	1.160	1.102	1.139-1.181	1.051-1.152	0.207	0.891
	Peak_ML[1]	0.765	0.813	0.748-0.782	0.773-0.853	0.286	0.846
	RMS_SVM[2,3]	1.039	1.029	1.034-1.044	1.016-1.043	0.811	0.812
	Median_SVM[2]	1.023	1.013	1.018-1.027	0.999-1.026	0.811	0.838
	TTFS[4]	1.934	1.770	1.869-1.998	1.610-1.930	0.290	0.811
	AFS[5]	1.169	1.158	1.130-1.207	1.054-1.261	0.811	0.809
	SD[6]	0.155	0.159	0.151-0.158	0.152-0.167	0.080	0.881
	Jerk (10^{-3})	0.362	0.359	0.318-0.406	0.235-0.484	0.900	0.717
	Entropy_VT[1]	1.475	1.461	1.465-1.485	1.436-1.487	0.811	0.799
	Energy_VT[1]	0.695	0.686	0.680-.0711	0.649-0.724	0.811	0.876
Frequency	FF_SVM[7]	1.250	1.242	1.225-1.274	1.191-1.294	0.958	0.702
	AO_ML[1,8] (10^{-2})	0.237	0.213	0.207-0.276	0.176-0.254	0.900	0.755
	AO_VT (10^{-2})	0.202	0.161	0.173-0.232	0.142-0.181	0.811	0.806
	AO_AP (10^{-2})	0.485	0.468	0.448-0.528	0.383-0.559	0.811	0.845
	RatioEnergy	12.07	11.81	11.81-12.33	11.27-12.34	0.901	0.705
	IH_VT[1,9]	23.90	23.75	23.12-24.68	21.02-26.47	0.013*	0.830

[1]VT depicts X axis of the local sensor system, AP is the Y axis, while ML is the Z axis; [2]SVM = Signal Vector Magnitude on which the feature was calculated; [3]RMS = Root Mean Square; [4]TTFS = Time to First arm Swing; [5]AFS = Amplitude of the First Step; [6]SD = Standard Deviation; [7]AS = Amount of applied Support; [8]FF = Fundamental Frequency; [9]AO = Amount of Oscillation; [10]IH = Index of Harmonicity; [11]Adjusted for multiple comparison

6.4.3 Novel feature analysis

Preceding the analysis of the novel feature in the FRA study, its validation was performed on transitions in the pilot study. In this manner, only parts of the signal that correspond to actual transitions performed by participants were extracted and AS feature was derived from them. The start and end points of all performed sit-to-stand transitions were defined based on the clinically defined points from perspective of the participant's torso. These points were detected in the recorded videos and correspondingly marked in the signals. The transitions were not analysed separately based on the type (movement pattern) but rather they were divided into transitions performed by fallers and non-fallers. The definition of fallers is in this case different from the one used in the FRA study (chapter 3.1.1), more precisely a specialized neurologist performed a classification of all participants based on their video recordings (i.e. performance during the study protocol).

The figure below shows an exemplary set of randomly selected 18 different sit-to-stand transitions (nine performed by fallers and nine by non-fallers). An FFT analysis of the wrist-acquired acceleration signal during these transitions was performed and the oscillation spectrum analysis for the AS feature between seven and 40 Hz is shown (Figure 49). The blue lines depict fallers, whereas the red lines depict non-fallers. On the first sight it is apparent from the picture the dominance of high amplitudes in this spectrum from transition performed by non-fallers. In order to give this observation a numerical description, a statistical Mann-Whitney test was applied on the AS feature derived from all transitions for fallers and non-fallers. AS feature was significantly higher ($p = 0.031$) for non-fallers than for fallers ($\mu = 0.0052$ and $\mu = 0.0028$ for non-fallers and fallers, respectively).

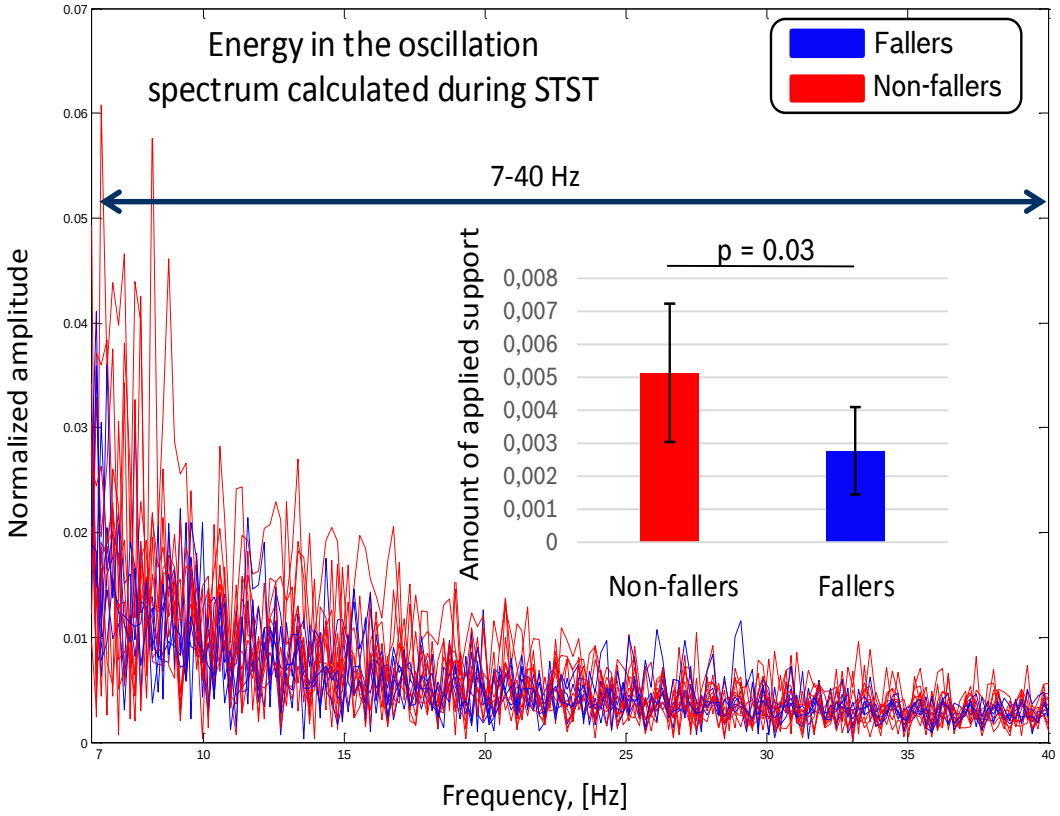

Figure 49 AS feature derived from the transitions performed within the pilot study

The newly proposed feature showed significant difference between the groups for all detected transitions ($p = 0.034$), as well as only for the non-dominant hand ($p < 0.001$), whereas for the dominant hand it showed no statistically significant distinction ($p = 0.251$) (Table 13). The AS feature was higher for non-fallers for all analysed transitions ($\mu = 0.512$ versus $\mu = 0.472$) and especially for the non-dominant hand ($\mu = 0.476$ versus $\mu = 0.351$), while for the dominant hand it was higher for fallers ($\mu = 0.629$ versus $\mu = 0.574$) but without any significance. Further analysis of this feature shows significantly more applied support at the dominant hand than at the non-dominant hand (Figure 50) for both, fallers ($p = 0.091$) and non-fallers ($p = 0.014$). In the most extreme cases the fallers have applied twice as much support at the dominant hand than at the non-dominant. The test retest reliability of the implemented feature has shown credible values between the days (ICC > 0.750 for all three cases).

Table 13 Acute FRA analysis of the AS feature for all three cases

Feature	Hand	Mean		95% CI		P-value	ICC
		Non-fall-ers	Fallers	Non-fall-ers	Fallers		
AS[1]	All (10^{-2})	0.512	0.472	0.474-0.550	0.312-0.632	0.034	0.819
	Dominant (10^{-2})	0.574	0.629	0.487-0.663	0.265-0.991	0.251	0.776
	Non-dom-inant (10^{-2})	0.476	0.351	0.445-0.508	0.302-0.400	< 0.001	0.830

[1]Amount of applied Support

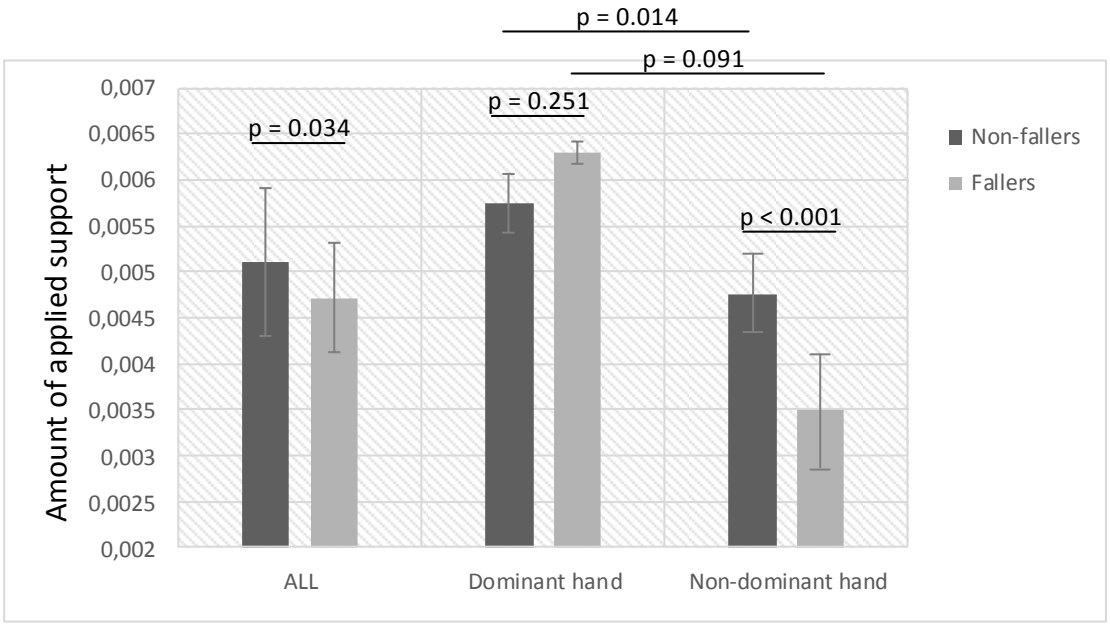

Figure 50 Analysis of the AS feature in terms of the acute FRA

The AS feature proposed in the chapter 5.3.2.3 shows no significance between the groups in 6-months based FRA, despite very good performance for the acute FRA (Table 14). Nevertheless, it was still slightly increased for non-fallers in all three cases (while analysing all transitions, as well as only for the transitions analysed at dominant and non-dominant hand) with considerably high reliability throughout the measurement week (ICC > 0.800), even slightly higher than for the acute FRA. While for the group of fallers has shown uniform distribution between applied support from the dominant and non-dominant hand (p = 0.344), non-fallers have applied significantly more support at their

dominant hand while standing up ($p < 0.001$). These results consistently follow the findings for the acute FRA for the novel feature.

Table 14 Six-months based FRA analysis of the AS feature for all three cases

Feature	Hand	Mean		95% CI		P-value	ICC
		Non-fallers	Fallers	Non-fallers	Fallers		
AS[1]	All (10^{-2})	0.524	0.411	0.479-0.570	0.380-0.442	0.090	0.823
	Dominant (10^{-2})	0.633	0.404	0.508-0.758	0.353-0.456	0.800	0.807
	Non-dominant (10^{-2})	0.477	0.417	0.442-0.511	0.379-0.454	0.509	0.832

[1]Amount of applied support

6.5 Fall risk assessment - classification

The final FRA for both, acute assessment as well as for 6-months based assessment, was performed throughout classification step by using the support vector machine with configuration described in the chapter 5.4.2. The classification was performed independently for the inter-limb features (FRA based on two sensors, wrist- and waist-worn) and for the sit-to-stand features (FRA based on only wrist-worn sensor).

The statistical tests in the chapters 6.1 and 6.3 have yielded the most significant features from which only the following ones were chosen throughout the forward feature selection process for classification purposes:

- Acute FRA
  - Inter-limb features: SPV, IC, CC;
  - Gait features: λ_{L,Acc_VT};
  - Sit-to-stand features: energy_SVM;
- Six-months FRA
  - Inter-limb features: STV, CC;
  - Gait features: λ_{L,Acc_AP}, λ_{L,Acc_SVM};
  - Sit-to-stand features: IH_VT, FF_SVM.

Classification was also analyzed for all extracted features, but with significantly lower results, thus these findings are not shown in the thesis. Furthermore, other machine learning techniques such as Random Forest and Naïve Bayes were tested for these purposes, but with lower performance, so these results are also not published here.

The AUC for the acute FRA based only on the selected inter-limb features was $AUC_{IL} = 0.76$, for the gait feature it was $AUC_G = 0.84$, whereas for the sit-to-stand features the results were slightly lower with $AUC_{STS} = 0.75$ (Figure 51). Comparing other statistical measures of the developed machine learning model, the results were considerably higher for sensitivity, specificity and accuracy for the inter-limb features in comparison to sit-to-stand features (Table 15). The model based on the gait dynamics has shown astonishingly high results. The PPV was high in all three cases ($PPV_{IL} = 0.98$, $PPV_G = 0.97$ and $PPV_{STS} = 0.97$), while F1-score has shown lower performance for the inter-limb features ($F1\text{-}score_{IL} = 0.76$) and considerably high results for other two models ($F1\text{-}score_G = 0.93$ and $F1\text{-}score_{STS} = 0.91$).

In comparison with the figures shown in available literature (Ihlen, 2015, Schooten, 2015, Schooten, 2012 and Cattelani, 2015), the latter results are exceeding them in good portions. Namely, AUC_G of the model for gait features is for 0.20 percentage points higher than the questionnaire-based FRAT-up score in (Cattelani, 2015). Furthermore, it is for 0.13 percentage points higher than the model based on the features extracted from the waist-worn device (Schooten, 2012). It also exceeds considerably (for 0.03 percentage points) the model based on combination of sensor-based and questionnaire-based features (Schooten, 2015), as well as it slightly outperforms (for 0.01 percentage points) the highest literature results in classification of participants at higher risk of falling (Ihlen, 2015). Results of other two proposed model based on the sit-to-stand and inter-limb features relates accordingly to these literature findings.

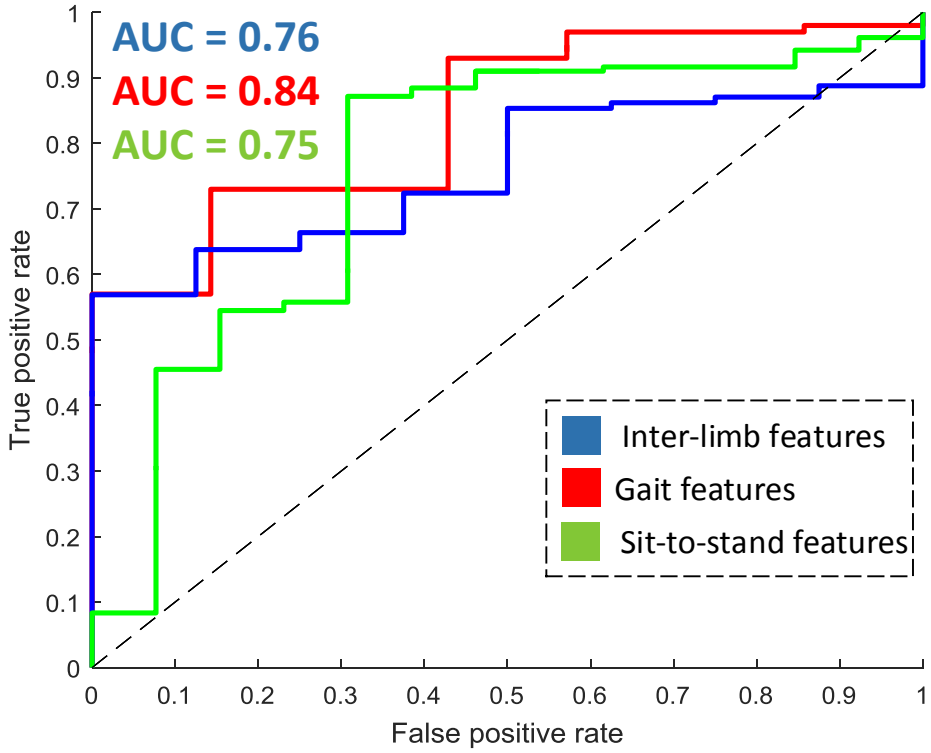

Figure 51 ROC analysis for acute FRA

Table 15 Classification results for the acute FRA

Feature / *Measure*	Inter-limb	Gait	Sit-to-stand
Sensitivity	0.65	0.90	0.86
Specificity	0.79	0.57	0.70
Accuracy	0.65	0.88	0.85
NPV[1]	0.16	0.42	0.38
PPV[2]	0.98	0.97	0.97
F1-score	0.76	0.93	0.91
AUC[3]	0.76	0.84	0.75

[1]NPV = Negative predictive value; [2]PPV = Positive predictive value; [3]AUC = Area under curve

Six-months based FRA, on the other hand yields results that are by all means worse than classification for acute FRA (Table 16). As in the previous case, the AUC is the highest for the gait feature (AUCG = 0.72) and intermediate good for the inter-limb and sit-to-stand features (AUC_{IL} = 0.69 and AUC_{STS} = 0.64) (Figure 52). The F1-score diverged

throughout the models ($F1\text{-}score_G = 0.86$ versus $F1\text{-}score_{IL} = 0.72$ versus $F1\text{-}score_{STS} = 0.77$). The biggest drop in comparison to the acute FRA can be seen in classification specificity ($specificity_G = 0.20$, $specificity_{IL} = 0.55$ and $specificity_{STS} = 0.33$, for the gait, inter-limb and STST features respectively) and in the number of correctly identified fallers ($PPV_G = 0.80$, $PPV_{IL} = 0.78$ and $PPV_{STS} = 0.72$). On the other hand, sensitivity is similar for 6-months based analysis and the acute FRA, whereas accuracy of developed models decreased ($accuracy_{IL} = 0.64$, $accuracy_G = 0.77$ and $accuracy_{STS} = 0.66$). In general, there is a clear tendency for good results in the gait-based model, with promising performance of the model based on the sit-to-stand features.

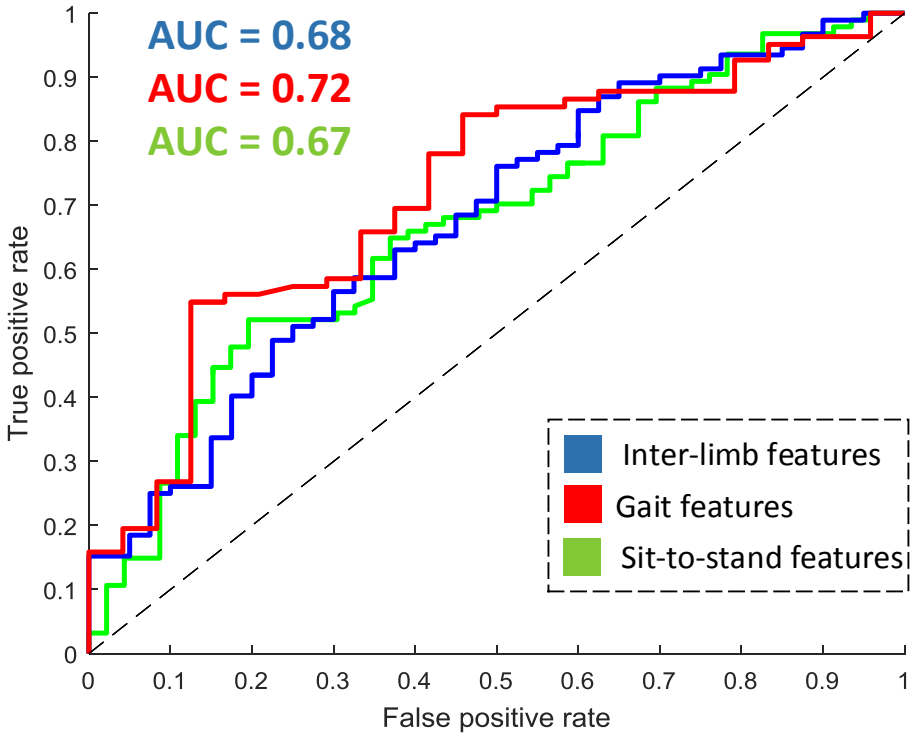

Figure 52 ROC analysis for 6-months FRA

Table 16 Classification results for the 6-months FRA

Feature / *Measure*	**Inter-limb**	**Gait**	**Sit-to-stand**
Sensitivity	0.68	0.93	0.83
Specificity	0.55	0.20	0.33
Accuracy	0.64	0.77	0.66

NPV[1]	0.44	0.50	0.51
PPV[2]	0.78	0.80	0.72
F1-score	0.72	0.86	0.77
AUC[3]	0.68	0.72	0.67

[1]NPV = Negative predictive value; [2]PPV = Positive predictive value; [3]AUC = Area under curve

6.6 Summary

The results performed on large scale of participants in the cross-sectional FRA study are clearly showing that the proposed methods do not just offer an alternative solutions for non-stigmatized assessment of the fall risk in the home setting, but also they fully overcome limitations of clinical tests and propose a reliable clinical application of wrist-bands in terms of highly acute and 6-months based FRA in the geriatric population. Moreover, the findings further boost the understanding of human movement from the wrist perspective and offer first descriptive measures for clinically novel group of acute fallers.

The chapter 6.1 confirms the previous knowledge about the reduced inter-limb coordination in the population at risk of falling, but in broader spectrum of movement (i.e. uncontrolled home environment) and with significantly reduced number of sensors. Despite the high variability in one's performance throughout the measurement week, SPV, IC and CC features have shown robustness and high reliability in terms of acute FRA. As already noted in the pilot study, YC feature due to reduced hip rotation could not identify highly acute fallers in ADL. Nevertheless, in a more relaxed environment (6-months based FRA), this feature (i.e. proposed approach with the gyroscope sensor) shows remarkable results. Confirmation of set up hypotheses (chapter 5.1) was found in all other features that assess lower-limb, as well as upper- to lower-limb coordination, which emphasizes the importance of the multi-sensor approach in critical evaluations. The findings also stress the need for additional investigations of inter-limb coordination in ADL, with focus on both, dominant and non-dominant hands.

Purely gait dynamics assessed on the wrist (6.2) offers exceptional results for potential clinically relevant applications in terms of highly acute and 6-months based FRA. Higher local dynamics for participants at risk of falling can be seen independently on which body side the sensor node was worn, suggesting correlation of performance from the macro perspective.

Hyper-parameter optimization by using the exhaustive grid-search method has yielded outstanding results in terms of the algorithm's precision (6.3.2). An overview of various time and frequency domain features has revealed numerous crucial factors for better quantitative and qualitative understanding of transition performance from the wrist perspective (6.4.1 and 6.4.2). Choice of the hand for this application was relevant and has to be taken with caution. Importance of the meaningful hand-crafted features above solely statistic features or symbolic context recognition based on the deep learning techniques is obvious in required computational power, but also in keeping interpretation of given results possible for technical and non-technical disciplines. These features due to their simplicity are possible for implementation in real-time systems and offer a wide palette of possibilities for all proposed applications. The results for the novel acute fall risk predictor (amount of applied support in the oscillation spectrum) have two significant perspectives (6.4.3). From the engineering side it offers a measure for easy determination of participants at high risk of falling, whereas from the clinical perspective it reveals a new area of research and broadens the existing knowledge about the stand-up strategies.

ROC analysis has shown for acute FRA remarkable results for all three proposed models, whereas in the 6-months based FRA it has shown comparable results with state-of-the-art findings based on the models with waist-derived measures and questionnaire assessments (6.5). The models were performing well for the approach on the periodic gait movements, as well as for the approach on solely assessment of non-recurrent patterns (i.e. transitions). These findings add value to the debate

about the wrist-worn devices in terms of the clinically relevant applications and open further questions regarding capturing specific movements far from the origin (e.g. translation of movement, cognitive component in the whole process, trade-offs and their relevance).

7 Discussion

7.1 Inter-limb coordination assessment

7.1.1 Quantitative analysis

Non-fallers have performed 30.4% more walking bouts that were satisfying the exclusion criteria from chapter 5.1.2 per participant per week than acute fallers. The previous studies have already confirmed slower gait speed as an excellent fall risk predictor (Verghese, 2009), which was just further confirmed with the findings in this thesis for acute FRA, where acute fallers have shown significantly lower average gait speed within defined gait bouts than non-fallers. Furthermore, this average gait speed was higher for both groups than the one determined for the population in the nursing homes (Peel, 2013). Hence, one should not disregard the possible error of estimation of the gait speed in the way proposed in chapter 5.1.4, which might have influenced the final results. There are certainly another methods for the gait speed estimation based on the inertial sensors (Song, 2007, Li, 2010 & Hartmann, 2009), as well as better sensor position for these purposes (Yang, 2012), so it would be also advisory to validate the proposed method with state-of-the-art methods in order to eliminate or at least better understand possible influences on the final results.

Additionally, a considerable number of short gait bouts (shorter than defined exclusion criteria) should also not be disregarded. These bouts were not analysed since previous studies have suggested to avoid them in ADL due to high variability and low certainty of correct step detection within them (Schooten, 2014 & Brodie, 2015). Thus, choice of only particular gait bouts that are defined as clinically relevant in terms of the FRA from perspective of the total length, as well as from the perspective of the average gait speed yields reliable results but also leaves space for improvement.

Despite the precaution steps implemented, based on the recent findings from the literature, analysis of all gait bouts longer than 10 seconds might have included some other activities during the day, like walking up or down the hill or taking the stairs, as these events are difficult to differentiate based on the accelerometer data (Kwapisz, 2010) used in the proposed step detector (5.1.1). Usage of the pressure sensor in these cases could have helped to distinguish these events as proposed in (Moncada-Torres, 2014), but then this again opens a debate whether it would be more indicative to analyse gait bouts only during these more fall-prone activities or during normal walking. Some research has already tried to address this issue but without clear suggestions (Rispens, 2015).

Estimation of the gait speed within each walking bout have one major limitation. Namely, the filter used for estimation of the absolute orientation based on the quaternion calculus and inertial sensor outputs (Madgwick, 2011) assumed that the accelerometer and magnetometer would measure only the gravity and the earth's magnetic field. As already experimentally shown in chapter 4.1, these sensor outputs (especially the magnetometer) can potentially be corrupted with local magnetic distortions, but in most applications these disturbances are present for only short period of times. Thus, with appropriate filter gains as proposed in (Madgwick, 2011) it is possible to minimize the influence of environmental distortions on accelerometer and magnetometer, i.e. their influence on the estimated orientation during these problematic periods is reduced. As a trade-off the filter outputs need certain time to converge, so parts of the walking bouts influenced by this divergence have to be eliminated from further analysis.

For the statistical analysis a mean value of the particular feature above all gait bouts for particular participant was used, thus averaging the extremes. The finding in (Rispens, 2015) argue that these extremes might be more indicative (but noisy) for high risk of falling (or in this case for acute FRA), so the further investigation should address this issue. In order to enable this kind of analysis, a further improvement in the step

detection, as well as in gait speed estimation should be performed to ensure a high reliability needed for clinically relevant interpretation of the results.

When talking about assessment of one's inter-limb coordination in ADL, approach with continuous activity monitoring during seven consecutive days seems reasonable because it covers participant's leisure, as well as work hours (when applicable). Moreover, previous studies have confirmed that this period reflects well one's physical performance as well as it offers a reliable statistical analysis. Nevertheless, the sensor system used in the study (3.1.2.2) is able to monitor one's activity for up to 10 hours. Corresponding to the study design, where the participants start wearing the sensor system in the morning after they wake up, the late afternoon hours are mostly missing in recordings. This fact can especially influence participants that are more physically active in the later hours (e.g. due to sedentary work obligations or while doing long afternoon walks). The problem was addressed by prolonging the battery life-time by usage of the low-power microcontrollers in the sensor nodes, as well as real-time operating system optimized in terms of the energy consumption.

The study covered the full year, including all four seasons and weather conditions. Walking during different weather conditions can be influenced in its duration and intensity as shown in (Klenk, 2011), but on a chosen large data set and monitoring period the influence is minimized. Also during certain seasons a probability for extreme weather conditions is higher (e.g. iced or slippery ground), but the influence that this has on one's performance was in this study disregarded due to inability of reliable estimation of the weather conditions with provided sensor systems. Thus, the importance of the environmental context on the inter-limb coordination in terms of the fall risk assessment should be evaluated throughout further studies since the influence of the external parameters on the fall risk is not negligible and might explain why current clinical prediction models provide only poor to fair predictive ability (Schooten, 2015).

7.1.2 Feature analysis

Although, numerous previous studies have found significant differences in the STV between fallers and non-fallers on both, 6-months (Schooten, 2015) and 12-month bases (Brodie, 2015 & Rispens, 2014), the analysis for the acute FRA yielded no differences between the groups, particularly due to wide confidence interval of this gait feature. The first assumption for the reason for such a high variability between the participants, and thus no significant difference between the groups, might be in still insufficient long enough gait bouts, as well as in the influence of the external factors and activity misclassification as already discussed in the chapter 7.1.1. Anyhow, STV has been surprisingly shown as a not significant fall risk predictor for acute FRA in ADL, while the same features shows considerable changes for the 6-months based FRA.

Another feature describing the bimanual coordination, SPV, has shown good performance in both cases. Therefore it just confirms the hypothesis that due to focus on more variable and more affected swing phase of the human gait cycle this feature will show more significant difference between the groups (Verghese, 2009), especially in more critical assessment of acute fall risk. While usage of the SPV in 6-months FRA is not new in the scientific community (Plotnik, 2007), it is a great novel acute fall risk predictor. Moreover, the method for SPV calculation proposed in chapter 5.1.5 based on the flat foot phase detection shows robustness for elderly population with wide level of physical performance.

While the steps within defined gait bouts were relatively easy to detect, the real challenge was to detect the corresponding arm swings in order to enable inter-limb coordination assessment. There are numerous reasons for these concerns. The long lasting debate about counting step (i.e. arm swing) at the wrist shows that there are definitely some deviations between this sensor position and the one at the waist (Tudor-Locker, 2015), especially in the uncontrolled environment (i.e. in ADL). More precisely, while the wrist-worn devices have shown consistently less detected steps for all selected gait speeds on the treadmill, in

the free-living conditions it has shown significantly more detected steps, but with high variability within the studied population (Tudor-Locke, 2015). Hence, the study in (Korpan, 2015) has shown that even the waist is not the best sensor placement for step detection in older adults so these results should be interpreted critically.

A logical train of thoughts opens a question regarding the reasons for such findings. Starting from physiological perspective, an arm swing can be seen as an integral part of human bipedal walking and in normal gait serves for reduction of energy expenditure (Meyns, 2013). Arm swing in the normal gait is well correlated with steps (i.e. upper body movement is primarily powered by lower body movement), in which the arms act as passive mass dampers that reduce torso and head rotation (Pontzer, 2009). However the arm swing detection is in ADL further affected with external variables (such as holding hands somewhere, carrying or holding something in hands, with different environmental conditions that affect balance and visual sense) that can cause either reduced arm swing or additional swings while walking. Exact influence of these external variables on the arm swing still has to be investigated, although it has already been shown that the absence of the arm swing causes no significant changes in step width or step frequency (Ortega, 2008).

On other hand, various upper extremity dysfunctions could additionally affect the reliable arm swing detection in the elderly population. Reduced and asymmetrical arm swing is characteristic for PD (Roggendorf, 2012), which is then further associated with fall risk (Deandrea, 2010) and due to reduction in the signal amplitude causes lower sensitivity in the arm swing detection (i.e. less detected arm swings). Additional fall-prone groups such as post stroke participants (Ford, 2007) and participants affected with other diseases (neurodegenerative diseases) or medical conditions (e.g. hip and arm fractures) would have reduced arm swing and therefore can influence the final assessment. Essentially important for the elderly population, reduced arm swing has

been shown as a sign of the early frailty (Nakakubo, 2014), which is also well correlated with the fall risk.

The approach proposed in chapter 5.1.6 for detection of the highest points in the arm swings while walking with trade-off of rather ignoring uncertain swings and corresponding steps than analysing wrong movements throughout the features for upper- to lower-limb coordination assessment seems to deliver reliable results. Nevertheless, the results should be interpreted with extra caution since the study in (Tudor-Locke, 2015) has shown that even small changes in the filter choice can influence significantly detection of steps in ADL. Filter choice for the arm swing detector was already discussed in previous publication as with its maximally flat response in the band pass area attenuates frequencies that do not correspond to dominant frequency components of the human arm swinging while walking (Pozaic, 2015 & Pozaic, 2016).

Mapping the detected steps to the corresponding arm swings is also a critical point here which was successfully overcome by choosing adaptable and robust thresholds able to adjust on different gait speed, as well as on high time delays between arm swings and corresponding heel strikes (i.e. on high upper- to lower-limb imbalance). This is also the only point in the algorithm where a search-backward loop was used in order to enable detection of the corresponding arm swing prior and after the heel strikes (i.e. detection of imbalance in both ways), as this is of high importance shown in the previous studies of inter-limb coordination (Stephenson, 2009). A search-backward loop is performed within a one-dimensional buffer of total length of one second (corresponding to 100 samples at the chosen sampling frequency), which still yields no extra memory load even for embedded devices.

The added value of this mapping approach was reflected throughout the IC feature for both, acute and 6-months based FRA where a significant difference between the defined groups was found. The results show considerably higher imbalance for the fallers in ADL and within defined gait bouts. Very little studies have previously addressed upper- to lower-limb coordination in ADL particularly due to obtrusive technical

solutions inconvenient for ubiquitous usage (Wagenaar, 2000, Debaere, 2001 & Stephenson, 2009), but higher time delays between arm swings and corresponding heel strikes (i.e. higher imbalance) is well correlated with instable (less smoother) gait which is directly related to higher risk of falling (Schaafsma, 2003). Thus, it can be concluded that this fall risk predictor follows consistently the current findings in the literature for both use cases. Important to notice, this feature is still not affected with hip rotation (i.e. method based on the gyroscope signal for discernment between left and right steps), but rather focused only on acceleration-based analysis. Narrow confidence intervals for non-fallers just further confirm this hypothesis, since variability within their gait bouts for this feature is significantly smaller than by fallers, and especially than by acute fallers.

The effects of the rotation in the hip while taking a specific step and its variability within studied population has been already shown in the algorithm development section (Figure 23). It is already empirically obvious from this picture that, although dominant rotation can be seen in the hip while taking the ipsilateral step, the amplitude varies a lot. This effect should be analysed from perspective of the lower-limb and hip muscle weakness, which is not only altered in the elderly population but it is also shown as a significant fall risk predictor (Moreland, 2004). A strong evidence has been found for a deficit in hip external rotation (i.e. the one occurring while taking the ipsilateral step), abduction and hip extension strength (directly influencing the signal amplitude) directly related to the muscle weakness (Prins, 2009). Certainly, the lower-limb and hip muscle weakness can be improved with different exercise programs such as strength trainings (Seguin, 2003) or Tai-Chi (Woo, 2007), but till then a robustness of the proposed method will be challenged and thus influence the final outcomes.

Except the degenerative muscle weakness characteristic in the older age, another reason for absence or reduced hip rotation can be history of hip fractures, frequent in elderly population (Orwoll, 2009). Furthermore, empirically observed in the pilot study (chapter 3.1.1), a reduced

hip rotation was present also in participants with walking aid (particularly walking frame), where also absence or reduction of the arm swing occurs. Despite indicated reasons that influence the hip rotation while walking, which is critical for discernment between left and right step, a clinically relevant and significant results could be extracted from the derived features for the ipsilateral and contralateral upper- to lower-limb coordination.

Contralateral coordination index shows significantly higher time delays, as well as more variability in these time delays for acute fallers than for non-fallers. In terms of the acute FRA, the YC index shows no significance between the groups which can be attributed to lack of reliability in hip rotation detection, from reasons listed above. On other hand, YC shows significant difference between the groups for the 6-months based FRA. This just further supports the latter thesis about hip rotation because, while acute fallers due to more significant hip and lower-limb muscle weakness show poor performance throughout this feature, fallers identified on a 6-months basis have enough muscle power to reflect the real added value of the YC feature. The CC feature does not show significant difference between the groups, but still points in the right direction. Reasons for absence of the clearer difference might also lie in the choice of the side where the sensor system was worn. One can here only speculate that participants have predominantly chosen less affected (stronger) side to wear the sensor system, thus time delays in the contralateral coordination are smaller between the groups than they would be in the other situation.

With that said, a limitation of the proposed method for upper- to lower-limb coordination assessment comes to surface. Namely, although the method makes enormous steps in the user-friendliness of the sensor system by reducing the number of sensor nodes to only two, it still can only evaluate one upper limb. This can be critical in specific situation such as PD or stroke, where only one side of the body is usually dominantly affected with the disease. Nevertheless, the choice of this

trade-off yielded negligible influence on the FRA, since the assessment spans over both lower limbs.

Worthy mentioning, when looking at the statistical significance of particular inter-limb features, a remarkable consistence is shown between 6-months FRA and results from the sample population published in (Pozaic, 2015), despite different reference and size of the analysed population in that publication. Nevertheless, this further supports the high reliability of the FRA based on extracted features.

Additional features (e.g. frequency domain features) or features assessed on daily or even walking bout basis from the macro perspective as proposed in (Del Din, 2015), could give added value in distinguishing between the groups but in this thesis were not tested since already proposed time domain features yielded satisfying results in terms of both, acute and 6-months FRA.

7.2 Gait analysis

7.2.1 Local dynamic stability

The proposed method for assessment of acute risk of falling in ADL with the wrist-attached sensor node shows statistically significant differences for the λ_L independently on which side the device was worn, as well as only for the non-dominant hand. On other hand, for the 6-months based FRA the same feature applied on the acceleration signal shows differences for the dominant hand and independently on which side the sensor node was worn. The λ_L has been noted as a reliable feature throughout the measurement period (seven consecutive days) in all applications of the wrist-worn acceleration sensor.

When analysing these two cases separately, it is interestingly to note how particular sensor axes could not distinguish between acute fallers and non-fallers, whereas their joint contribution (signal vector magnitude) has been showing a significant difference between the corre-

sponding groups. The reason for that could lie in the fact that small perturbations in faller's kinematics throughout the walking bouts are equally distributed in all three directions. Support for this hypothesis can be found in presented tables since acute fallers were consistently showing more instability in arm swings while walking than non-fallers (in particular sensor axes, as well as in the magnitude). The findings have also shown how dominant hand movement is unclear or more precisely, larger variability is present, thus suggesting focus of analysis of λ_L on the non-dominant hand.

Critical points such as hand movements that can be misclassified as walking or reduced arm swings would lead to decreased number of detected steps, should also be taken into account although in this uncontrolled environment within the scope of this work were not separately analysed. Situations with walking aid, where arm swings are prevailingly diminished and have nothing or very little to do with actual walking pattern would disrupt the proposed model. Solution for these situations can be proposed in detection of the walking aid and inclusion of it as an additional external factor in the FRA model.

The scope of this thesis included also other inertial sensors (gyroscopes and magnetometers), but no difference could be found between the groups in them. Gyroscope sensor is depicted with less sensitivity, i.e. high frequency components of linear movement are less represented in the total sensor output. Magnetometer sensor in the current realization is too affected with extrinsic magnetometer disturbances, so λ_L would rather be represented with noise than with actual perturbations in human kinematics.

Decision to focus only on particular gait bouts (as in inter-limb coordination assessment in 6.1) is inspired by the will for higher step detection reliability (especially from the wrist perspective) and more stable meaningful gait. Nevertheless, once the arm swing detectors reach beyond current performance it would be definitely of interest to focus also on the shorter gait bouts or even on gait initialization in ADL since these

events despite high variability could contain hidden pearls of one's physical performance for particular diseases or use cases.

Short Lyapunov exponent is by default something more sensitive since it is focused on the start of a walking phase, but even under these circumstances it can reliably distinguish between designated groups. Its long version proposed in previous studies (Schooten, 2015) could reduce the noise and it that case maybe even show possible significant differences not only in the magnitude but also in particular sensor axes. Disadvantage of this approach is in computational power, but with constant improvement in this field for specific medical applications it might be worthwhile.

Further limitations influenced by the data acquisition that were discussed in previous chapter 7.1, should not be disregarded but won't be further addressed in this manner. The results extracted from the wrist for the λ_L, despite above mentioned limitations, correspond quantitatively with current findings in the literature (Ihlen, 2015 and Schooten, 2012) and thus show possible applications of this feature in acute and 6-months based FRA.

7.3 Sit-to-stand transition detection

7.3.1 Waist to wrist algorithm transfer

The algorithm proposed in 5.3.1 was based on the transition time estimation previously used in (Bidargaddi, 2007), where it has shown promising results for the sensor node attached at the sternum. The solely detection of the transitions in provided data with both, wrist- and waist-worn sensors, was very high, but it is also a critical point, since specificity of the proposed algorithm could not be tested. Namely, automatic segmentation of transitions from the signals from ADL was in this case not implemented, since pattern used for estimation of transition duration (Figure 26) can be found also in numerous other activities (e.g. walking, turning, sitting down, housework activities). Nevertheless, the

proposed method causes a trade-off between elimination of the movement artefacts (especially present at the wrist-worn devices) prior and directly after the transitions (see chapter 4.2) and the loss of information for the transition parts outside local extremes interval.

The population on which the algorithm was tested corresponds by the age very well with the target groups in previous studies (Rispens, 2015, Schooten, 2014 & Ihlen, 2015). Moreover, the average reference transition duration derived from the labelled data is similar to previously tested populations in terms of the FRA (Zijlstra, 2012). When looking at the whole spectrum of transition durations, moderate association between both sensor estimates and reference duration is predominantly caused by longer transition durations. Estimation of these long transition durations deviates more from the actual duration than by the short transitions due to the increasing transition parts outside extremes interval. In other words, linear relation between phases within extrema interval and outside that interval, as proposed in (Bidargaddi, 2007), is not preserved anymore so well in these cases. Even non-linear relations between these two parts have not yielded considerably better results due to high variability in duration of different phases as well as high instability during these long transitions (Millor, 2014). As expected, the waist sensor estimates have shown slightly better results than the wrist sensor estimates for all transition durations since this sensor is closer to the centre of mass where biggest portion of movement during transition can be caught.

The proposed method on the other hand shows considerably better performance for transitions shorter than 1.73 seconds (both in the correlation between sensor estimates, as well as in SEE). Moreover, the difference in SEE for the waist and wrist sensor estimates for short transitions is smaller, showing similar algorithm performance independently on the sensor position. The previous studies (Doheny, 2013) identified differences in transition duration between the fallers and non-fallers that are in case of the whole transition spectrum smaller than provided SEE. Moreover, the transition duration especially in the group of fallers aims

more for durations that have shown poor performance with this algorithm (Doheny, 2013 & Zijlstra, 2012). Thus, although the method enables estimation of duration of various types of transitions characteristic also for the daily life activities, it is appropriate only for assessment of well performing persons.

Nevertheless, the proposed method revealed three key points that steered further development of the algorithm for transition detection in ADL. Firstly, the time estimation, especially on the wrist, is not appropriate in uncontrolled settings. This is reflected in even higher SEE for unsupervised transitions, as well as in transitions from the bed and armchair (Figure 43). The main reason for that is hidden in inability to detect the actual start and end points of the transitions due to overwhelming noisy movement directly prior and after the transitions. Transitions that are rather unnatural (from the chair without armrest by using hands for support) have also yielded high SEE due to the hesitation at the start of the transition, while common transitions (from the chair with armrests by using hands) (Dolecka, 2015) have yielded almost 50% lower SEE. Whether this directly means that more common transition patterns are smoother and less influenced by other movement still has to be further investigated. Most importantly, these findings have clearly shown that analysis of the whole transitions is a rather challenging task, as well as detection of dominant points in the transfer pattern depicted with local extremes in the signal, such as seat-off event, should be performed on the well prepared datasets (i.e. further filters for noisy movement are necessary).

Secondly, the analysis of the transition duration has just confirmed previous findings, which showed significantly longer transitions in the elderly population and especially for fallers (Najafi, 2002). Moreover, fall risk was well correlated with less steadiness in the ML direction while standing up (Millor, 2014), as well as already particular phases of the transition movement have shown difference in this elderly population (Zijlstra, 2012). Latter mentioned findings are important for support of the hypothesis that for assessment of the transitions in the ADL does not

necessary has to be performed on the whole duration in order to detect participants at risk of falling.

Lastly, similar performance of the proposed method was found for both sensor estimates which further support the hypothesis of the implementation of the transition detector on the wrist, despite suggestions in the previous studies (Mannini, 2013). Furthermore, looking at the group-based analysis (Figure 43) the transitions performed without using hands for support have yielded surprisingly slightly lower SEE for the wrist estimates than for the waist sensor estimates. One can also argue here that in these cases wrist follows the whole body movement better than the waist.

A comprehensive analysis of different transitions had a limitation in inability to analyse the transitions independently for fallers and non-fallers, but these issue was then further addressed in the FRA study. Moreover, other algorithms for transition detection (Najafi, 2002, Zijlstra, 2012, Rodriguez-Martin, 2013 & Lugade, 2014), as well as for its duration estimation (Giansanti, 2006), were not further tested on the data from this pilot study since already proposed method yielded clear guidelines for the transition detection in ADL from the wrist acquired datasets.

7.3.2 Wrist perspective

The focus of the proposed method is on the algorithm precision (i.e. correct detection of the performed transitions in ADL) rather than on the sensitivity (i.e. positive hit rate). The hyper-optimization of the available parameters was performed with a robust, but time consuming grid-search method in terms of the algorithm precision because of already explained reasons for the sturdy method for wide physical performance of the study population. Thus, although only a portion of the total number of performed transition in ADL is detected, findings in (Dall, 2010) still enable detection of enough transitions for further analysis even with low algorithm sensitivity. Dormancy and step detectors explained in chapters 5.3.1.2 and 5.1.1 have made this high precision

possible, but the influence of the false positives in the analysis should not be disregarded. This effect is particularly visible in the comparison of the results for the dominant and non-dominant hand already from the perspective of the number of features that show significant differences between the groups. Lower precision for the dominant hand, caused by more chaotically movement that in acceleration signal look like sit-to-stand transitions (e.g. writing, cooking, cleaning, turning), has consequently caused lower performance of the extracted features. The limitation of this approach is in inability to detect the exact extreme points of the transfer (as defined in the clinical practice), but approach with various different features has overcome this problem. Nevertheless, further quantitative assessment of the whole transitions from the wrist perspective should be addressed in a controlled setting in order to confirm the presented finding in the daily life environment.

In the above mentioned circumstances, the proposed method has revealed some profoundly interesting research results from the non-ambulatory acquired data. Non-fallers have performed more transitions than acute and 6-months based fallers, which can be supported with the predominantly sedentary behaviour characteristic for the individuals at high risk of falling (Thibaud, 2012). Although the macro perspective of the transition patterns offers no significant discernment between the groups, different phases of specific transitions and their temporal characteristics can already distinguish between various groups and possible pathologies (Dolecka, 2015), once they can be reliably detected in ADL. Further micro-analysis of different types of transitions, their occurrence as well as their influence and correlation with proposed features should be addressed in future work since it can further extend the knowledge about the group-specific transfer techniques in ADL.

Taking into consideration that the number of detected transitions is well correlated with the number of actually performed transitions since no pattern-specific performances in transition detection were found in the conducted pilot study (chapter 3.1.1), distribution of the detected number of transitions shows interesting, but also similar results for both,

acute and 6-months based FRA. Namely, non-fallers in both cases have bimodal distribution of the number of detected transitions, with further peaks between 100 and 150 transitions which fits with clinical findings in (Dall, 2010), whereas exponential distribution for fallers shows rapid decline in the number of performed transitions suggesting again more sedentary behaviour for the groups at risk of falling. Moreover, acute fallers were limited with maximum of 100 detected transitions, whereas 6-months based fallers with 150 or more transition are rather an exception (i.e. outliners) than a rule. This suggests actually that a solely number of transitions, or more precisely their distribution, can serve as a novel fall risk predictor which reliability should be tested in controlled conditions to confirm these preliminary findings.

7.4 Sit-to-stand transition assessment

7.4.1 Quantitative and feature analysis

The quantitative analysis, was performed independently for acute and 6-months FRA (important for the execution of the statistical type I error compensation process). Quantitative analysis can be also understood as an evaluation process of numerous extracted features. A number of these features both, time- and frequency-domain based, indicated the significant difference between acute fallers and non-fallers, as well as between 6-months based fallers and non-fallers. The differences were found independently of the side of the body (dominant or non-dominant hand) where the sensor system was worn.

When looking strictly on the acute FRA, despite the poor performance of the clinical tools that are currently used in assessment of the fall risk (habitual gait speed (Stone, 2015), 30 seconds chair rise test (Jones, 1999 & Millor, 2013) and history of falls), the proposed method based on the assessment of the wrist performance during sit-to-stand transitions has overcome this highly complex multifactorial challenge. The reason for that lies in the analysis of not only macro perspective of

the sit-to-stand transitions but rather on its detailed quantitative assessment enabled throughout different implemented features. From the perspective of the statistical analysis, the presented results for the assessment of highly acute fall risk have shown similar significant differences between the defined groups as the previous studies assessing the fall risk either based upon detailed quantitative evaluation of the clinical characteristics (stride variability (Hausdorff, 2007)) or features derived from the waist-worn devices (local dynamic stability (Schooten, 2012)).

The differences, although not statistically significant, in the peak amplitudes in the AP and ML direction suggest that findings in the transfer techniques between healthy elderly and elderly with dementia (more movement and pushing through the armrest while standing up) (Dolecka, 2015) could also be applied for detecting of the acute fall-prone population. Despite higher peak values in the AP and ML direction, the median value of the acceleration signal indicates overall higher acceleration for non-fallers which actually fits with previous findings of shorter transition duration for this group (i.e. intensity and time are inversely proportional). Moreover, this further means smoother transitions for non-fallers, whereas fallers perform these transitions with variable movement influenced by sudden twitches in the AP and ML directions. In addition to that, the IH feature just confirms the dominance of the first harmonic in the relationship to the following five for non-fallers, thus showing that oscillations in the acceleration signal for non-fallers are smaller than for fallers (i.e. movement during transfer is smoother).

Other time-domain features could not differentiate between the defined groups (i.e. have shown poor performance). Furthermore, opposite from expected, TTFS feature was slightly higher in non-fallers than fallers. From strictly pathological perspective there might be two main reasons for this kind of feature behaviour. Firstly, as already shown in the analysis of video recording in the pilot study, as well as in the previous studies of the transfer patterns (Dolecka, 2015 & Zijsltra, 2012), hands were very often used as support while standing up especially when the

armrests were provided. Usage of hands for support entails that less forward trunk rotation is needed in preparation for standing up and as a further consequence the end of backward trunk rotation may occur earlier in the sequence of events and therefore affect transition duration (i.e. time to first arm swing in STW transitions). Secondly, due to less imbalance in transitions for fallers as shown throughout the IH feature and consequently less stabilizing trunk movements, shorter TTFS can be explained with the need for arm swing in order to regain the balance right after the transition.

Significantly more energy for the non-fallers can be explained with more lower and upper limbs strength. This also means that total energy invested in the transition is higher for this group despite the shorter time period (i.e. power of transition would depict even higher differences between the groups). Complexity of the movement, as measured throughout the entropy from the waist-attached sensor, while standing up was significantly higher for groups at higher risk of falling (Fatmehsari, 2011). The results for the wrist-worn device show quite the opposite behaviour indicating more complex movement patterns for non-fallers from the wrist perspective. This would suggest that non-fallers are actually use their hands while standing up more often which can be supported with higher rigidity characteristic for elderly at higher risk of falling. Second theory is that fallers simply need more support from the armrests (or chair itself) so their hands are skin-tight attached to the chair, whereas in non-fallers the hands are overwhelmingly firmly loosen up next to the body.

The same features show good performance for the 6-months based FRA as for the acute FRA with addition of the SD feature. This shows remarkable similarity in the transition patterns from the wrist perspective between acute fallers and 6-months based fallers. Does this consequently means that the proposed method based on the implemented feature would not be able to differentiate between acute and regular faller is still not sure, but what has been already shown in the chapter 3.3 is that

being an acute fallers does not automatically means being a recurrent faller.

For investigating whether this novel method shows adequate results for discrimination of other specific pathologies in elderly population with impaired transitioning (e.g. PD population), the studied population might not be entirely suitable for that purposes since there can be significant difficulties while standing up as already shown in (Zijlstra, 2012). Nevertheless, the robustness of the proposed method is obvious throughout the number of features that have shown the difference between defined groups, as well as throughout more than satisfactory performance in both studied use cases.

7.4.2 Novel feature assessment

The novel feature described in the chapter 5.3.2.3, AS, indicates that the energy of the applied support while standing up is highly beneficial for distinguishing between acute fallers and non-fallers. To emphasize the importance of this feature and in the same time avoid the influence of other artefacts in the analysis (e.g. false positives detected by the algorithm), the additional experiment performed on the transitions from the pilot study have just confirmed the significance of the findings in the FRA study (chapter 6.4.3). Namely, when the AS feature is derived only from the actual transitions, it still shows significantly more applied support while standing up for the group of participants that were classified as non-fallers by a specialized neurologist, independently on the type of the standing up pattern. In one hand, this analysis shows robustness of the proposed feature to different types of the sit-to-stand transitions, as well as remarkable consistency between the values of the AS feature in the pilot and FRA study. Furthermore, these findings also show that the influence of false positives on the proposed feature (i.e. its values) is negligible, especially for the non-fallers group.

Motivated by these findings, a further analysis of the upper-limb role in a well-known and widely used 5-times-sit-to-stand test, where the arms

should be folded across chest (Buatois, 2008), would be considered reasonable. More precisely, the accepted proposal of not using hands while standing up, especially during the clinical applications, should be reconsidered since from this feature is clearly visible the importance of hand support and its influence on the transfer patterns, as well as on the transfer performance.

These findings further supplement the knowledge about the transfer strategies in elderly population, showing that non-fallers that have more available upper and lower limb strength (Kang, 2012) will apply more energy for support while standing up, while being a faller does not automatically imply more applied support. The findings could be even further elaborated by combining the proposed method with the force plates in which case the lower-limb weakness can be directly brought into relationship with the amount of applied support (i.e. energy in the oscillation spectrum) while standing up.

From the perspective of the wrist, AS feature shows significant difference in applied support between hands only for non-fallers suggesting more uniformly distribution of the applied support in both hands in acute fallers (i.e. in people with upper and lower limb weaknesses). This is also an important factor for the fall prevention implications since some of the strategies have been shown to affect only those parts receiving interventions (Cadore, 2013), thus suggesting further personalized and target-orientated trainings and exercises. Furthermore, wearing the sensor at the non-dominant hand provides more distinguishing features in terms of the acute FRA, which suggests possible combination of the proposed method within a watch (or similar wrist-worn device) in further applications for a highly non-stigmatized medical use.

The 6-months based analysis revealed no significant discernment between the groups based on this feature despite the fact that non-fallers have again consistently showed more applied support than fallers. In one hand, this limits the AS feature only as an acute fall risk predictor, while on the other hand opens further research questions that could ex-

plain such behaviour in ADL. If acute fallers can be considered predominantly, but not necessarily, as recurrent fallers (chapter 3.3), the lower-limb weakness is thus more emphasized which then consequently means less possibility for applied support while standing up.

But why is the difference between 6-months based fallers and non-fallers so weak? It is possible that from one side reason for that simply lies in the human physical behaviour in the home environment or more precisely, in the fact that participants are simply not keen enough to apply all available power for support while standing up. For sure one can also speculate that the reasons for that may lie in the insufficiently high precision of the algorithm for transition detection that includes then other movements (e.g. turning, start of walking, specific household activities) from the ADL in the statistical analysis. Occurrence of the hand support while standing up in ADL can also play an important role here (both, absolute to the total number of transitions as well as relative ratio between fallers and non-fallers). Additionally, the challenges mentioned in chapter 3.1.2.1 (question of a reliable reference) that affect statistical analysis of all features, as well as classification of participants, can have influence also on this novel feature. Possibility for another compensation movements (e.g. hand swinging in the flexion phase) during transfer would also make the border between fallers and non-fallers in terms of the AS feature fuzzier.

7.4.3 Dominant versus non-dominant hand

Very little information is currently available in the literature regarding side-dependent analysis of algorithm's performance in ADL. In one hand, that would require inclusion of a large scale of participants or application of multi-sensor systems in ADL, which as discussed before is impropriate for daily usage. On the other hand, previous findings in the literature have always marked wrist as a sensor position with poor or low performance. Conventional approaches have been focused on the centre of mass, while limbs depicting body extremes were unfairly dis-

regarded. Encouraged with positive findings in chapter 6.4, in both applications, an additional sub-chapter was dedicated only to analysis of dominant and non-dominant hand on the proposed measures.

As shown in 6.3.2, choice of hand has significant influence on the algorithm's performance and consequently on the feature analysis (6.4). Just the opposite from the gait feature, the precision for STST detection is higher for the non-dominant hand and thus the influence of FP on the feature analysis, or more precisely, situations that can be misclassified as transitions (such as turning or different house works), is lower than for the dominant hand. This fact should be kept in mind when analysing the obtained results.

Nevertheless, more features could reliably distinguish between the groups for the dominant than for the non-dominant hand suggesting better reflection (or transfer) of the full body capabilities in the dominant hand (and consequently their correct detection), despite higher influence of noise. These results were consistent for both, acute and 6-months based FRA (6.4.1 and 6.4.2). Influence of the more distinguished group of acute fallers in terms of physical performance was also consistently visible in this analysis.

The question that pops out here is whether the same algorithm can be used independently on which side the sensor node is worn. Conventional features does not offer a solution in this case, but AS feature for acute FRA sounds as a perfect match. This suggest that not just the level of noise in extracted signal parts is high, but also the source of this noise is different for the dominant and non-dominant hand. In the non-dominant hand the source comes from less reflection of full body performance, whereas in the dominant hand the source of this noise could be found in transition's posteriori movements (i.e. additional signal dynamics). The question is also whether some components in this behaviour have a direct link with the brain and further with cognitive functionality, which would be definitely interesting to investigate in the next steps. Importantly to add, similar features were found as significant for acute and 6-months based FRA for the dominant hand, as well as for the

non-dominant hand (with emphasize of clearer difference in acute FRA). The findings would thus suggest a positive answer on the question from the beginning of this section.

Previously it was also briefly mentioned how different diseases that mostly affect one side of the body would be critical for this application, especially when considering the geriatric population. Understanding the correct source of noise in the transition detection that affects feature analysis and correct selection of features could potentially lead to possible reliable application of this algorithm even in extreme cases, but this has to be further confirmed in additional explorative study.

7.5 Fall risk assessment – classification

The classification of the acute and 6-months based fallers was performed by using the SVM with RBF kernel and in order to avoid overfitting a 10-fold CV was included in the process. Based on the provided results in chapter 6.5 it can be concluded that inter-limb coordination, non-linear quantitative gait features and sit-to-stand transition assessment in ADL contribute to the prediction of fall risk in both, acute and 6-months based analysis. The predictive values of the developed machine leaning models can be compared with the state-of-the-art fall risk models (Schooten, 2015 & Ihlen, 2015), especially when looking at the acute FRA. Although the results suggest that analysis of the transitions in daily life from the wrist perspective provides information on behavioural characteristics and although it is likely for that to have a bearing on fall risk, it is not necessarily superior over inter-limb coordination assessment based on waist and wrist attached sensor or gait assessments in the laboratory setting in terms of the fall risk prediction.

For the fall prediction models for transition features, a lower values might be also explained by limiting the number of implemented features in order to ensure lower significance values for feature addition. With the ability of many fall risk related features, the exact selection is sensitive to subtle differences. In addition, subjective parameters (such as fall

risk questionnaire) could increase the predictive values of the model (Schooten, 2015), but are in this case avoided in order to keep the focus on unobtrusiveness and objectiveness of the measured features. Moreover, backwards feature selection process (or any other process) can be tested in the future work for the model since in this work they were not tested due to limited number of features.

Precision of the developed models might slightly vary since not exactly the same population was used for the model training. Namely, due to the long-lasting process of the follow-up phase after the measurement week, the number of participants in the 6-months based prediction model is lower than for the acute FRA. Thus, although the performance of the fall prediction models explained in chapter 6.5 are expressed by the AUC as well as with other statistical measures associated to the model evaluation, the 6-months FRA would need another update once the study (i.e. follow-up phase) is completely finished.

The classification techniques used for fall prediction models vary study-wise but as long as the reference for them follow the same guidelines with additional Gaussian noise for deviations in fall reporting, a possibility for comparison of the prediction values is justified. In the thesis the same technique was used for acute and 6-months FRA, although in the acute FRA a problem of imbalanced classes, where presence of one class is prevailing (i.e. acute fallers) (Kubat, 1997), is present. The number of acute fallers is expected to be below 10% for the elderly population above 65 years old (Li, 2005). The SVM algorithm works well on such datasets since class weighting is designed in that way that it deals with unbalanced data by assigning higher misclassification penalties to training instance of the minority class (He, 2009). Decision trees algorithms perform well on such imbalanced datasets since the splitting rules that look at the class attributes can force both classes to be addressed (He, 2009), but as previously mentioned due to limited number of extracted features these techniques were not used in the thesis. The importance of the evaluation of the predictive performance of the model is important to emphasize as well, since solely investigation of the

model's accuracy is not appropriate measure for imbalanced datasets (Nitesh, 2010) and another measures (such as F1-score and AUC) as proposed in chapter 5.4.2 are needed.

The features that were used for modelling were sampled with 100 Hz thus covering 99% of frequency components of human movement (Karantonis, 2006). The question of lower sampling frequency that reduces the energy consumption of the sensor node and thus extends its life-time was addressed in the work by applying the features on limited frequency spectrums as well as averaging them within small time windows. Nevertheless, the work in (Schlaegel, 2016) argues that the robustness of some prediction model regarding the sampling frequency and its effects on statistical inference is satisfactory, but still a systematic mathematically founded framework for the analysis should be applied.

In this work only accelerometer-based features were used for model training as accelerometry is applicable in large scale studies and widely accepted also in the clinical practice, as well as it contributes to the low-energy performance of the sensor node. As signal characteristics differ throughout various activities in daily life (e.g. angular velocity during turning), reliability of the prediction models might be improved when deriving additional features from other sensors.

From strictly pathological perspective regarding the differences in model performances, more precisely why the model for acute FRA shows better results, two theories are possible to the best of the author's knowledge. Firstly, acute fallers are depicted with more distinct behaviour (parameters) in terms of both, inter-limb coordination, gait and sit-to-stand transition assessment, as presented in the statistical analysis (chapters 6.1, 6.2 and 6.4). This is contributed with emphasized differences in physical conditions (such as upper and lower limb weakness), daily behaviour (increased time spent in the sedentary activities) and cognitive impairment (Muir, 2012). Acute fallers should also be differentiated from recurrent fallers since the direct reliable association

between these two groups was not obvious (chapter 3.3). Second possibility lies in the environmental conditions, in which case participant's behaviour is significantly influenced by extrinsic factors during longer period of time within monitored interval. In the analysed study, the presence of such situations was noted (e.g. hiking). While there is no or very little evidence for acute falling (excluding the extrinsic fall risk factors), the proposed model offers a valuable insight in this problem throughout the upper to lower limb coordination as well as throughout the way of standing up in ADL.

7.6 Summary

In this chapter a thorough discussion about each point of the work, from data acquisition, over algorithm development to validation of proposed methods, was presented. All three domains of the algorithm development (inter-limb coordination, gait and transitions) were addressed firstly separately and afterwards discussed as integral parts of developed SVM models. In each domain, special attention was given to consideration of presented results in terms of clinical relevance. Questions regarding the uncontrolled environment in which the data acquisition was performed and numerous unobservable factors that influenced it were addressed as well for both, quantitative evaluation and classification.

The global structure of the discussion chapter corresponds to the previous chapters. In 7.1 a macro analysis of the walking class, as detected with proposed step detector, was critically analysed in terms of acute and 6-months based FRA. Furthermore, feature performance and critical points addressing novel approaches (in particular reduction of the sensor nodes, detection of the hip rotation and gait speed estimation) were addressed. The chapter 7.2 supplements the previous one with additional feature assessing local dynamic stability in walking, but with focus only on the wrist-worn sensor node. Additional macro analysis of walking was not given for this feature, but rather just a side-dependent analysis of feature performance was discussed. Following chapter (7.3)

covers topics about waist to wrist algorithm transfer and different transition detection approaches applied in the work, as well as influence of various extrinsic factors on their performance (environmental luminance, transition's posteriori hand movements, frailty). Throughout the chapter 7.4 a quantitative assessment of extracted features was discussed in terms of dominant and non-dominant hand, which yields a new perspective of understanding one's performance in the home setting. Application of these findings on the existing clinical tools was considered in this chapter as well. The chapter 7.5 analyses developed models, their correlations with currently available state-of-the-art models and influence of study limitations on them.

8 Scientific contribution

The scientific contribution of this research work, as presented in the above listed chapters, can be split into two main fields – clinical and engineering. Validation of the developed novel assessment methods and cost-effective algorithms, as well as machine learning models on a large scale of data acquired in a clinical study enabled immediate objective and reliable confirmation of relevance of the proposed approach. Nevertheless, clinical significance of these results for the fall prevention strategies with the goal of reduction of fall rate, as well as the number of fallers, still has to be confirmed in an additional prospective study.

8.1 Clinical perspective

The contribution of this thesis to the clinical community from the author's point of view was significant in the few points that will be emphasized here accordingly. All highlighted findings were performed on studies with clinically relevant numbers of participants providing a firm support for presented interpretations and conclusions. In the work, a novel fall risk predictor (amount of applied support in the oscillation spectrum for standing up, AS) for identification of acute fallers was presented, extending the knowledge about the current STST strategies and suggesting further consideration of well-known and widely used clinical tests.

Performed video analysis has broaden the understanding of the STST strategies in the elderly population, as well as their definition from the wrist perspective. Furthermore, a concise definition of different STST types from the wrist perspective was given, which opens a completely new field for further investigations.

A remarkable performance of the gait feature λ_L has showed its robustness in reliable assessment of elderly population by using only the wrist-attached sensor node. Investigation of this feature for dominant

and non-dominant hand suggested that, despite increased uncertainty when detecting walking from sensor data acquired from the wrist, small perturbations in the human kinematics can still reliably distinguish between non-fallers and fallers, both in acute and 6-months based study.

Clear contribution was made by proposing and identifying a group of acute fallers. Their relationship to other groups, as well as characteristic performance that they have shown are novel in the field of FRA. Using the model for acute FRA it is not just possible to act even faster and target critical subjects, but also it is enabled to monitor a short-term (on a monthly basis) progress of these subjects and influence of proposed fall prevention strategies on them. In addition to that, model based on the SVM with the RBF kernel confirmed non-linear connection between the defined groups (in acute FRA, as well as in 6-months based FRA), as well as it has proposed means for their identification based on all three domains (inter-limb, gait and transitions).

8.2 Engineering perspective

The engineering community has benefited considerably from the findings of this thesis as well. More precisely, significant optimization of the number of sensor nodes for reliable evaluation of the inter-limb coordination in ADL in terms of the FRA was suggested by using the multi-sensor (accelerometer, gyroscope and pressure sensor) fusion approach. This approach enabled new tools for various other applications, such as assessment of upper- to lower-limb coordination in PD or other motor disorders. It is especially worth to highlight added value of the gyroscope sensor in combination with accelerometer for contralateral and ipsilateral coordination assessment by using only two sensor nodes. Additionally, synchronization of physically distant sensors without network connection or RTC by means of temperature-compensated filtered pressure signal with high offset stability has shown very promising results and it can find its application in numerous other systems affected by erroneous sensor readings (in healthcare and industry).

Proposed methods for detection of non-recurrent movements, such as STST, in the noisy environments, such as ADL, by using combination of movement filters (dormancy detectors), extreme analysis (rotation detector) and conventional signal processing techniques has moved the boundaries in algorithm development for another step forward. Inclusion of the analysis of the environmental context (luminance) was proposed not to necessary directly understand one's physical performance, but to rather set one's behaviour in the situational setting and add supplementary information as an input to the algorithm. This novel approach has shown importance of the situational awareness when analysing someone's movement and added value to the algorithm's performance by using something that is already provided at the hand reach (without significant increase in the system costs or size).

Machine learning models based on the SVM have just confirmed an expected non-linear relationship between the groups suggesting a further consideration for mapping of current low-dimensional linear models to higher dimensional space with perspective of increased performance. Finally, the developed models have shown a possible detection of subjects at risk of falling, independently of the domain of assessment (gait, inter-limb coordination or transitions), which suggests their close correlation, enables additional reduction in size of the feature space and opens possibility for increase in cost-effectiveness, reliability and consequently clinical applications.

9 Conclusion and outlook

In this chapter, the work carried out in the thesis is summarized. Additionally, the conclusion is provided by reflecting what was set out to achieve and what has been accomplished. At the end, an outlook about possible application of the proposed models is given. The main focus of the work was on designing SVM-based models with features derived from wrist-attached sensor nodes worn in ADL, with emphasize on a highly unobtrusive and non-stigmatized approach for FRA. Verily, falls are a burning problem in a continuously aging society and means that would offer a widely acceptable solution for their prevention are eminently desirable. Additional multi-sensor approach for evaluation of the inter-limb coordination was investigated as well, but further consideration of the conventional waist-attached sensor node would not be recommended since it has not shown added value in terms of the FRA. Nevertheless, findings in this area have yielded scientifically worth mentioning results that can find its application also in other areas, such as motor disorder progression monitoring or long-term gait and postural transition assessment.

9.1 Conclusion

To this end, the crux of the thesis lies in two main points that will be separately discussed further below:

- Concepts for assessment of inter-limb coordination, gait and STST in ADL;
- Validation of derived features and developed models in terms of statistical significance, accuracy and robustness.

The first point corresponds prevailingly to the algorithm development part (chapter 5). The novel tools that were proposed in all three investigated domains, despite their limitations elaborated in the discussion,

offer not just reliable solutions for the FRA, but also open a broad spectrum of new possibilities in other areas.

In the inter-limb coordination domain, a solution for the precisely clock synchronized multi-sensor approach based on the cross-correlation of temperature compensated pressure signals of physically distant sensor nodes has shown incredible dominance above the currently used method with the magnetometer sensor, especially for magnetic-prone environments. Moreover, sensor fusion based on the quaternions for the actual horizontal gait speed estimation within longer gait bouts, as well as further usage of the gyroscope as an added value to the accelerometer for the hip rotation detection and consequently step selection were presented.

Gait feature short Lyapunov exponent with an optimized step (i.e. arm swing) detector was presented. Furthermore, its performance was evaluated separately for the participants wearing the sensor node on their dominant and non-dominant hand. Although a gait speed estimation for analysed gait bouts was not possible with the wrist-attached sensor due to poor correlation between arm swings and steps, the local dynamic stability was applied on the gait bouts that by their temporal duration correspond to the literature.

Wrist perspective in the STST strategies to the best of the author's knowledge is a novel study that should be further investigated in terms of different diseases, but it already gives remarkable insights in the postural transfers of geriatric population. Proposed combined filter approach for detection of non-recurrent movements such as STST in ADL enhanced with the understanding of the environmental context has shown significant improvements against the approach based only on the inertial (movement) data. Moreover, performance of such an approach was investigated for both, dominant and non-dominant hand.

Importantly to add, simulation of ADL in a controlled setting with the goal of reliable and robust algorithm development of inter-limb coordi-

nation, gait and STST assessment was presented. This kind of experimental and observational study gave a valuable insight and broaden the needed understanding about the investigated topic.

Second point concerning the validation of derived features and developed methods is mostly summarized in the chapter 6. The conducted analysis on a clinically relevant number of participants has yielded a novel fall risk predictor for acute FRA in terms of the STST assessment. Furthermore, additional basic features (such as peak amplitude or complexity of the signal expressed as the signal entropy) were identified as FRA predictors for the wrist-attached sensor. Robustness of the implemented features via ICC was tested and it has shown a high reliability for all features that can considerably distinguish between fallers and non-fallers. The findings regarding the side-dependence contribute to better understanding and definition of the upper-limb role in the elderly population, as well as improve disreputableness of the wrist-worn devices. On top of that, they open a broad spectrum of new additional options that could be investigated in further studies (e.g. different transfer strategies, correlation with other sensor positions, additional sensors for better understanding of the environmental context, possible applications in neurodegenerative diseases that affect motor performance).

The proposed machine learning models based on the SVM have shown high performance for acute FRA that exceeds state-of-the-art results in this area. Six-months based FRA models still consistently follow the best sensor-based results in the literature, but with slightly reduced performance, particularly due to the improper definition of falls and questionable reliability of ground truth (fall-diaries-based reference). Nevertheless, the study may be especially worthwhile for clinicians, as it provides tools for better adjustment of the fall prevention strategies, as well as for tracking their progress on a regular/monthly basis. Cost-effective multifactorial interventions that reduce the rate of falls and the number of fallers in hospital setting, could benefit from the proposed models since they are orientated on the individually-designed prevention programs based on the previous assessments.

9.2 Outlook

Except the evident motivation for the work, a reasonable amount of acceptance of the proposed approach should be present for both, consumer and medical sector. On the one hand, the fact of rapidly rising number of wearables, especially in the consumer (non-medical) sector, while on the other hand the emphasized desirability for tracking of physical performance in both sectors (Figure 53) justify the conducted work. In addition to these preliminary findings a brief market research was conducted regarding possible applications of the FRA models.

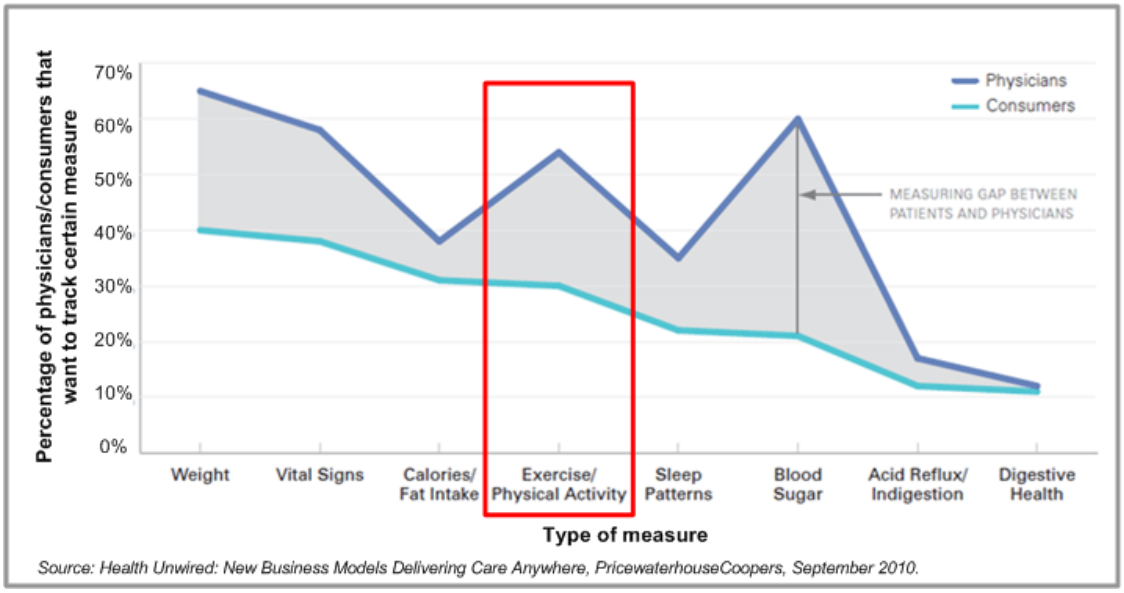

Figure 53 What consumers and clinicians would like to track in ADL

As a final result of the thesis six different machine learning models (from which four are only wrist-based) for acute and 6-months based FRA were developed. Their implementation in wrist bands as part of existing (e.g. Apple's iWatch or Fitbit's fitness wristband) or solely based products seems like a reasonable decision. The user-orientated study focused on the targeted population has revealed a surprisingly low desire for FRA products as solely-based solutions. However, as part of the existing trackers or more precisely as an additional feature that would be supported by a call service centre in case of an emergency rises its acceptance rate and desirability significantly.

To sum up, the proposed unobtrusive non-stigmatized approach for FRA can imply crucial changes in the fall prevention strategies such as:

- Optimization of balance and strength trainings;
- Avoidance of home hazards and shoe modifications;
- Drug related modifications and interventions.

The possible impact of these changes was briefly analysed for the figures in Germany (Figure 54). Twenty-one percentage of population in Germany is above 65 years, from which one third is at risk of falling. The recent findings have shown that 10% of all falls end up with an injury that requires medical attention or even longer hospitalization. Generally speaking, average costs for these kind of falls go up to € 32000. Taking into account that fall prevention strategies can decrease fall rate for in average 35%, a market of approximately € 500 million can be reached by the proposed solutions only in Germany.

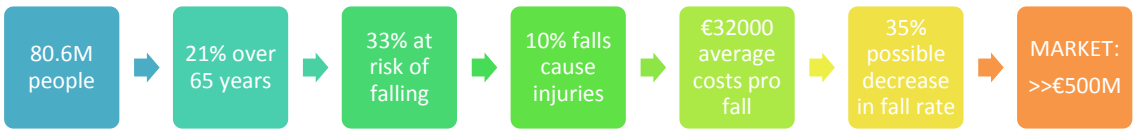

Figure 54 Market analysis for the FRA

Bibliography

Balzer, K. *et al.* (2012). *Sturzprophylaxe bei älteren Menschen in ihrer persönlichen Wohnumgebung.* Health Technology Assessment in Germany.

Barry, E. *et al.* (2013). *Is the timed up and go test a useful predictor of risk of falls in community dwelling older adults: a systematic review and meta-analysis.* BMC Geriatrics. 14: 1.

Bidargaddi, N. *et al.* (2007). *Wavelet based approach for posture transition estimation using a waist worn accelerometer.* 29th International Conference of IEEE Engineering in Medicine and Biology Society. Lyon, France.

Biderman, A. *et al.* (2002). *Depression and falls among community dwelling elderly people: a search for common risk factors.* Journal of Epidemiology & Community Health. 56: 631-636.

Becker, C. *et al.* (2013). *Stürze in der Geriatrie.* Der Internist. 52(8): 939-945.

Blake, A. J. *et al.* (1988). *Falls by elderly people at home - prevalence and associated factors.* Age and Aging. 17(6): 365-372.

Brodie, M. A. *et al.* (2015). *Eight-week remote monitoring using a freely worn device reveals unstable gait patterns in older adults.* IEEE Transactions on Biomedical Engineering. 62: 2588-2594.

Buatois, S. *et al.* (2008). *Five times sit to stand test is a predictor of recurrent falls in healthy community-living subjects aged 65 and older.* Journal of American Geriatrics Society. 56: 1575-1577.

Cadore, E. L. *et al.* (2013). *Effects of different exercise interventions on risk of falls, gait ability, and balance in physically frail older adults: A systematic review.* Rejuvenation Research. 16: 105-114.

Catellani, L. *et al.* (2015). *FRAT-up, a web-based fall risk assessment tool for elderly people living in the community.* Journal of Medical Internet Research. 17: e41.

CDC: Center for Disease Control and Prevention (2015). *Costs of falls among older adults.* http://www.cdc.gov/homeandrecreationalsafety/falls/fallcost.html.

Dall, P. M. *et al.* (2010). *Frequency of the sit-to-stand task: an observational study of free living adults.* Applied Ergonomics. 41: 58-61.

Deandrea, S. *et al.* (2010). *Risk factors for falls in community-dwelling older people: A systematic review and meta-analysis.* Journal of Epidemiology. 21: 658-668.

Debaere, F. *et al.* (2001). *Coordination of upper and lower limb segments: deficits on the ipsilesional side after unilateral stroke.* Experimental Brain Research. 141: 519-529.

Del Din, S. *et al.* (2015). *Accelerometer based free-living data: Does macro gait behavior differ between fallers and non-fallers with and without Parkinson's disease?* International Society for Posture & Gait Research. Sevilla, Spain.

Doheny, E. P. *et al.* (2013). *Falls classification using tri-axial accelerometers during the five-times-sit-to-stand test.* Gait & Posture. 38: 1021-1025.

Dolecka, U. E. *et al.* (2015). *Comparison of sit-to-stand strategies used by older adults and people living with dementia.* Archives of Gerontology and Geriatrics. 60: 528-534.

Ermes, M. *et al.* (2008). *Detection of daily activities and sports with wearable sensors in controlled and uncontrolled conditions. IEEE Transactions on Information Technology in Biomedicine. 12: 20-26.*

Fatmehsari, Y. R. *et al.* (2011). *Sit-to-stand or stand-to-sit: Which movement can classify better Parkinsonian patients from healthy elderly subjects?* 18th Iranian Conference on Biomedical Engineering. Teheran, Iran. 48-53.

Ford, M. *et al.* (2007). *Phase manipulation and walking in stroke.* Journal of Neurologic Physical Therapy. 31: 85-91.

Federal Office of Statistics (2007). *Krankheitskosten: Deutschland, Jahre, Geschlecht, Altersgruppen.* Wiesbaden, Germany. https://www.destatis.de/DE/Startseite.html.

Fraser, A. M. *et al.* (1986). *Independent coordinates for strange attractors from mutual information.* Physical Review A. 33(2): 1134.

Garcia-Sanchez, A. J. *et al.* (2010). *Wireless sensor network deployment for monitoring wildlife passages.* Sensors. 10: 7236-7262.

Giansanti, D. *et al.* (2006). *Physiological motion monitoring: A wearable device and adaptive algorithm for sit-to-stand timing detection.* Physiological Measurement. 27: 713.

Gill, T. M. *et al.* (2000). *Environmental hazards and the risk of nonsyncopal falls in the homes of community-living older persons.* Medical Care. 38(12): 1174-1183.

Gillespie, L. D. *et al.* (2012). *Interventions for preventing falls in older people living in the community.* Cochrane Database System Revision. 9(11).

Graafmans, W. C. *et al.* (1996). *Falls in the elderly: a prospective study of risk factors and risk profiles.* American Journal of Epidemiology. 143(11): 1129-1136.

Grewal, M. S. *et al.* (2001). *Kalman filtering: Theory and practice using MATLAB.* John Wiley & Sons. New York, USA.

Guralnik, J. M. S. *et al.* (1994). *A short physical performance battery assessing lower extremity function.* Journal of Gerontology. 49(2): 85-94.

Hamacher, D. *et al.* (2011). *Kinematic measures for assessing gait stability in elderly individuals: a systematic review.* Journal of the Royal Society Interface. 8(65): 1682-1698.

Hamalainen, W. *et al.* (2011). *Jerk-based feature extraction for robust activity recognition from acceleration data.* 11th International Conference on Intelligent Systems Design and Applications. Cordoba, Spain. 831-836.

Handsaker, J. C. *et al.* (2014). *Contributory factors to unsteadiness during walking up and down stairs in patients with diabetic peripheral neuropathy.* Diabetes Care. 37(11): 3047-3053.

Hartmann, A. *et al.* (2009). *Concurrent validity of a trunk tri-axial accelerometer system for gait analysis in older adults.* Gait & Posture. 29: 444-448.

Hausdorff, J. M. *et al.* (2001). *Gait variability and fall risk in community-living older adults: a 1-year prospective study.* Archives of Physical Medicine and Rehabilitation. 82 (8): 1050-1056.

Hausdorff, J. M. *et al.* (2007). *Gait dynamics, fractals and falls: Finding meaning in the stride-to-stride fluctuations of human walking.* Human Movement Science. 26: 555-589.

He, H. *et al.* (2009). *Learning from imbalanced data.* IEEE Transactions on Knowledge and Data Engineering. 21: 1263-1284.

Hegger, R. *et al.* (1999). *Improved false nearest neighbour method to detect determinism in time series data.* Physical Review E. 60(4): 4970.

Holford, N. H. G. *et al.* (2006). *Disease progression and pharmacodynamics in PD: evidence for functional protection with levodopa and other treatments.* Journal of Pharmacokinetics and Pharmacodynamics. 33: 281-311.

Hollman, J. H. *et al.* (2011). *Normative spatiotemporal gait parameters in older adults.* Gait & Posture. 34: 111-118.

Holt, S. *et al.* (2010). *Potentially inappropriate medications in the elderly: the PRISCUS list.* Detsches Ärzteblatt International. 107(31-32): 543-551.

Ihlen, E. A. F. *et al.* (2015). *The discriminant value of phase-dependent local dynamic stability of daily life walking in older adult community-dwelling fallers and non-fallers.* BioMed Research International.

Ilg, W. *et al.* (2009). *Intensive coordinative training improves motor performance in degenerative cerebellar disease.* Journal of Neurology. 73: 1823-1830.

Iluz, T. *et al.* (2015). *Can a body-fixed sensor reduce Heisenberg's uncertainty when it comes to the evaluation of mobility?* Journal of Gerontology Series A: Biological Sciences and Medical Sciences. 49.

Jones, C. J. *et al.* (1999). *A 30-s chair stand test as a measure of lower body strength in community-residing older adults.* Research Quarterly for Exercise and Sport. 70: 113-119.

Kang, H. C. *et al.* (2012). *Effect of lower limb strength on falls and balance of the elderly.* Annals of Rehabilitation Medicine. 36: 386-393.

Kannus, P. *et al.* (2007). *Alarming rise in the number and incidence of fall-induced cervical spine injuries among older adults.* Journal of Gerontology. 62 (2): 180-183.

Karantonis, D. M. *et al.* (2006). *Implementation of a real-time human movement classifier using a triaxial accelerometer for ambulatory monitoring.* IEEE Transactions on Information Technology in Biomedicine. 10: 156-167.

Katzman, R. *et al.* (1983). *Validation of a Short-Orientation-Memory-Concentration test of cognitive impairment.* The American Journal of Psychiatry. 140: 734-739.

Kerr, A. *et al.* (2007). *Timing phases of the sit-to-walk movement: Validity of a clinical test.* Gait & Posture. 26: 11-16.

Klenk, J. *et al.* (2011). *Walking on sunshine: effect of weather conditions on physical activity in older people.* Journal of Epidemiology & Community Health.

Korpan, S. M. *et al.* (2015). *Effect of ActiGraph GT3X+ position and algorithm choice on step accuracy in older adults.* Journal of Aging and Physical Activity. 23: 377-382.

Kubat, M. *et al.* (1997). *Addressing the curse of imbalanced training sets: One-sided selection.* 14th International Conference on Machine Learning. Nashville, Tennessee, USA. 97: 179-186.

Kuys, S. S. *et al.* (2014). *Gait speed in ambulant older people in long term care: a systematic review and meta-analysis.* Journal of the American Medical Directors Association. 15: 194-200.

Kwapisz, J. R. *et al.* (2010). *Activity recognition using cell phone accelerometers.* ACM SIGKDD Explorations Newsletter. 12: 74-82.

Landsiedel, O. *et al.* (2006). *Rat watch: using sensor networks for animal observations.* ACM REALWSN.

Larson, S. C. *et al.* (1931). *The shrinkage of the coefficient of multiple correlation.* Journal of Medical Psychology. 22: 45-55.

Li, F. *et al.* (2005). *Tai Chi and fall reductions in older adults: A randomized controlled trial.* Journal of Gerontology. 60: 187-194.

Li, Q. *et al.* (2010). *Walking speed estimation using a shank-mounted inertial measurement unit.* Journal of Biomechanics. 43: 1640-1643.

Lipsitz, L. A. *et al.* (1986). *Syncope in institutionalized elderly: the impact of multple pathological conditions and situational stress.* Journal of Chronic Diseases. 39(8): 619-630.

Lord, S. R. *et al.* (2003). *A physiological profile approach to falls risk assessment and prevention.* Journal of the American Physical Therapy Association. 83: 237-252.

Lord, S. R. *et al.* (2007). *Falls in older people: risk factors and strategies for prevention.* Cambridge University Press.

Lorenz, E. N. *et al.* (1963). *Deterministic nonperiodic flow.* Journal of the Atmospheric Sciences. 20: 130-141.

Lugade, V. *et al.* (2014). *Validity of using tri-axial accelerometers to measure human movement - Part I: Posture and movement detection.* Medical Engineering & Physics. 36: 169-176.

Luukinen, H. *et al.* (1994). *Incidence rate of falls in an aged population in northern Finland.* Journal of Clinical Epidemiology. 47: 843-850.

Madgwick, S. O. H. *et al.* (2011). *Estimation of IMU and MARG orientation using a gradient descent algorithm.* IEEE International Conference on Rehabilitation Robotics. Zurich. Switzerland. 1-7.

Mancini, M. *et al.* (2016). *Potential of APDM mobility lab for the monitoring of the progression of Parkinson's diease.* Expert Review of Medical Devices. 13: 455-462.

Mannini, A. *et al.* (2013). *Activity recognition using a single accelerometer placed at the wrist or ankle.* Medicine & Science in Sports & Exercise. 45: 2193-2203.

Masse, F. *et al.* (2016). *Wearable barometric pressure sensor to improve postural transition recognition of mobility-impaired stroke patients.* IEEE Transactions on Neural Systems and Rehabilitation Engineering. 99: 1.

Masud, T. *et al.* (2001). *Epidemiology of falls.* Age and Ageing. 30: 3-7.

Mayston, M. J. *et al.* (2001). *Physiological tremor in human subjects with X-linked Kallmann's syndrome and mirror movements.* Journal of Physiology. 3: 551-563.

Mazza, C. *et al.* (2004). *Association between subject functional status, seat height, and movement strategy in sit-to-stand performance.* Journal of the American Geriatrics Society. 52: 1750-1754.

Meyns, P. *et al.* (2013). *The how and why of arm swing during human walking.* Gait & Posture. 38: 555-562.

Milat, A. J. *et al.* (2012). *Prevalence, circumstances and consequences of falls among community-dwelling older people.* NSW Public Health Bull. 22(3-4): 43-48.

Millor, N. *et al.* (2014). *Kinematic parameters to evaluate functional performance of sit-to-stand and stand-to-sit transitions using motion sensor devices.* IEEE Transactions on Neural Systems and Rehabilitation Eng. 22: 926-936.

Moe-Nilssen, R. *et al.* (2002). *Trunk accelerometry as a measure of balance control during standing.* Gait & Posture. 16: 60-68.

Moncada-Torres, A. *et al.* (2014). *Activity classification based on inertial and barometric pressure sensors at different anatomical locations.* Physiological Measurement. 35(7).

Moreland, J. D. *et al.* (2004). *Muscle weakness and falls in older adults: A systematic review and meta-analysis.* Journal of the American Geriatrics Society. 52: 1121-1129.

Muir, S. W. *et al.* (2008). *Use of the Berg Balance Scale for predicting multiple falls in community-dwelling elderly people: A prospective study.* Journal of the American Physical Therapy Association. 88: 449-459.

Muir, S. W. *et al.* (2012). *The role of cognitive impairment in fall risk among older adults: A systemativ review and meta-analysis.* Age and Ageing. 41: 299-308.

Najafi, B. *et al.* (2002). *Measurement of stand-sit and sit-stand transitions using a miniature gyroscope and its application in fall risk evaluation in the elderly.* IEEE Transactions on Biomedical Engineering. 49: 843-851.

Nakakubo, S. *et al.* (2014). *Does arm swing emphasized delibarately increase the trunk stability during walking in the elderly adults?* Gait & Posture. 40: 516-520.

Nitesh, V. C. *et al.* (2010). *Data mining for imbalanced datasets: An overview.* Data Mining and Knowledge Discovery Handbook. 45: 875-886.

O'Connor, J. M. *et al.* (2013). *A method to synchronize signals from multiple patient monitoring devices through a single input channel for inclusion in list-mode acquisition.* Medical Physics. 40 (12).

Orendurff, M. S. *et al.* (2008). *How humans walk: Bout duration, steps per bout, and rest duration.* Journal of Rehabilitation Research & Development. 45: 1077-1090.

Ortega, J. D. *et al.* (2008). *Effects of aging and arm swing on the metabolic cost of stability in human walking.* Journal of Biomechanics. 41: 3303-3308.

Orwoll, E. S. *et al.* (2009). *Finite element analysis of the proximal femur and hip fracture risk in older men.* Journal of Bone and Mineral Research. 24: 475-483.

Pan, J. *et al.* (1985). *A real-time QRS detection algorithm.* IEEE Transactions on Biomedical Engineering. 32: 230-238.

Pasolini, F. and Binda I. (2007). *Pedometer device and step detection method using an algorithm for self-adaptive computation of acceleration thresholds.* Patent US 20070143068 A1. USA.

Peel, N. M. *et al.* (2013). *Gait speed as a measure in geriatric assessment in clinical settings: A systematic review.* Journals of Gerontology. 68: 39-46.

Pierobon, A. *et al.* (2013). *Sturzrisikofaktoren.* Sprache, Stimme, Gehör. 37(2): 83-88.

Plotnik, M. *et al.* (2007). *A new measure for quantifying the bilateral coordination of human gait: effects of aging and Parkinson's disease.* Experimental Brain Research. 181: 561-570.

Pontzer, H. *et al.* (2009). *Control and function of arm swing in human walking and running.* Journal of Experimental Biology. 212: 523-534.

Pozaic, T. *et al.* (2015). *Inter-limb coordination assessment and fall risk in ADL.* IFMBE International Conference on Biomedical and Health Informatics, Haikou, China.

Prins, M. R. *et al.* (2009). *Females with patellofemoral pain syndrome have weak hip muscles: a systematic review.* Australian Journal of Physiotherapy. 55: 9-15.

Prudham, D. *et al.* (1981). *Factors associated with falls in the elderly: a community study.* Age and Aging. 10(3): 141-146.

Punt, M. *et al.* (2015). *Effect of arm swing strategy on local dynamic stability of human gait.* Gait & Posture. 41: 504-509.

Rapp, K. *et al.* (2012). *Epidemiology of falls in residential aged care: Analysis of more than 70000 falls from residents of Bavarian nursing homes.* Journal of American Medical Directors Association. 13: 187.e1-187.e6.

Raiche, M. *et al.* (2000). *Screening older adults at risk of falling with the Tinetti balance scale.* The Lancet. 356: 1001-1002.

Rispens, S. M. *et al.* (2014). *Identification of fall risk predictors in daily life measurements.* Neurorehabilitation and Neural Repair.

Rispens, S. M. *et al.* (2015). *Do extreme values of daily-life gait characteristics provide more informaiton about fall risk than median values?* Journal of Medical Internet Research.

Riva, F. *et al.* (2013). *Orbital stability analysis in biomechanics: A systematic review of a nonlinear techniques to detect instability of motor tasks.* Gait & Posture. 37: 1-11.

Riva, F. *et al.* (2013). *Estimating fall risk with inertial sensors using gait stability measures that do not require step detection.* Gait & Posture. 38: 170-174.

Rodriguez-Martin, D. *et al.* (2013). *SVM-based posture identification with a single waist-located triaxial accelerometer.* Expert Systems with Applications. 40: 7203-7211.

Roggendorf, J. *et al.* (2012). *Arm swing asymmetry in Parkinson's Disease measured with ultrasound based motion analysis during treadmill gait.* Gait & Posture. 35: 116-120.

Rosenstein, M. T. *et al.* (1993). *A practical method for calculating largest Lyapunov exponents from small data sets.* Physica D: Nonlinear Phenomena. 65(1-2): 117-134.

Rubenstein, L. Z. *et al.* (1996). *Falls and fall prevention in the nursing homes.* Clinics in Geriatric Medicine. 12(4): 881-887.

Seguin, R. *et al.* (2003). *The benefits of strength training for older adults.* American Journal of Preventive Medicine. 25: 141-149.

Schaafsma, J. D. *et al.* (2003). *Gait dynamics in Parkinson's disease: relationship to Parkinsonian features, falls and response to levodopa.* Journal of the Neurological Sciences. 212: 47-53.

Schenkman, M. L. *et al.* (1990). *Whole-body movements during rising to standing from sitting.* Physical Therapy. 70: 638-648.

Schlaegel, U. E. *et al.* (2016). *A framework for analyzing the robustness of movement models to variable step discretization.* Journal of Mathematical Biology. 1-31.

Schooten, K. S. *et al.* (2012). *Assessing gait stability: The influence of state space reconstruction on inter- and intra-day reliability of local dynamic stability during over-ground walking.* Journal of Biomechanics. 46: 137-141.

Schooten, K. S. *et al.* (2014). *Assessing physical activity in older adults: Required days of trunk accelerometer measurements for reliable estimation.* Journal of Aging and Physical Activity.

Schooten, K. S. *et al.* (2015). *Ambulatory fall-risk assessment: Amount and quality of daily-life gait predict falls in older adults.* Journal of Gerontology. 1-8.

Shannon, C. E. *et al.* (1948). *A mathematical theory of communication.* Bell System Technical Journal. 27: 379-423.

Sharrington, C. *et al.* (2008). *Effective exercise for the prevention of falls: a systematic review and meta-analysis.* Journal of American Geriatric Society. 56(12): 2234-2243.

Shaw, F. E. *et al.* (2002). *Falls in cognitive impairment and dementia.* Clinics in Geriatric Medicine. 18(2): 159-173.

Shumway, C. A. *et al.* (2000). *Predicting the probability for falls in community-dwelling older adults using Timed Up & Go test.* Journal of American Physical Therapy Association. 80: 896-903.

Song, Y. *et al.* (2007). *Speed estimation from a tri-axial accelerometer using neural networks.* 29th Annual International Conference of the IEEE Engineering in Medicine and Biology Society. Lyon, France. 3224-3227.

Spain, R. I. *et al.* (2012). *Body-worn motion sensors detect balance and gait deficits in people with multiple sclerosis who have normal walking speed.* Gait & Posture. 35: 573-578.

Stalenhoef, P. A. *et al.* (2002). *A risk model for the prediction of recurrent falls in community-dwelling elderly: a prospective cohort study.*Journal of Clinical Epidemiology. 55(11): 1088-1094.

Stephenson, J. L. *et al.* (2009). *The coordinaiton of upper and lower limb movements during gait in healthy and stroke individuals.* Gait & Posture. 29: 11-16.

Stevens, J. A. *et al.* (2006). *The costs of fatal and nonfatal falls among older adults.* Injury Prevention. 12: 290-295.

Stone, E. *et al.* (2015). *Average in-home gait speed: investigation of a new metric for mobility and fall risk assessment of elders.* Gait & Posture. 41: 57-62.

Thibaud, M. *et al.* (2012). *Impact of physical activity and sedentary behaviour on fall risk in older people: A systematic review and meta-analysis of observational studies.* European Review of Aging and Physical Activity. 9: 5-15.

Tinetti, M. E. *et al.* (1988). *Risk factors for falls among elderly persons living in the community.* New England Journal of Medicine. 319 (26): 1701-1707.

Tinetti, M. E. *et al.* (1995). *The contribution of predisposing and situational risk factors to serious fall injuries.* Journal of American Geriatric Society. 43(11): 1207-1213.

Tinetti, M. E. *et al.* (2003). *Preventing falls in elderly persons.* New England Journal of Medicine. 348 (1): 42-49.

Toebes, M. J. P. *et al.* (2012). *Local dynamic stability and variability of gait are associated with fall history in elderly subjects.* Gait & Posture. 36: 527-531.

Tudor-Locke, C. *et al.* (2015). *Comparison of step outputs for waist and wrist accelerometer attachment sites.* Medicine and Science in Sports and Exercise. 47: 839-842.

Verburgh, L. *et al.* (2013). *Physical exercise and executive functions in preadolescent children, adolescents and young adults: A meta-analysis.* British Journal of Sports Medicine.

Verghese, J. *et al.* (2009). *Quantitative gait markers and incident fall risk in older adults.* Journal of Gerontology. 64: 896-901.

Viswanath, D. (1998). *Lyapunov exponents from random Fibonacci sequences to the Lorenz equations.* Ph.D dissertation, Cornell University, New York, USA.

Wagenaar, R. C. *et al.* (2000). *Resonant frequencies of arms and legs identify different walking patterns.* Journal of Biomechanics. 33: 853-861.

Walther, P. D. *et al.* (2008). *Schwindel und Stürze im Alter.* HNO. 56(8): 833-842.

Weiss, A. *et al.* (2010). *Can an accelerometer enhance the utility of timed up and go test when evaluating patients with Parkinson's Disease?* Journal of Medical Engineering and Physics. 32(2): 119-125.

Weiss, A. *et al.* (2011). *An instrumented timed up and go: The added value of an accelerometer for identifying fall risk in idiopathic fallers.* Physiological Measurement. 32 (12).

Weiss, A. *et al.* (2014). *Objective assessment of fall risk in Parkinson's Disease using a body-fixed sensor worn for 3 days.* PloS One. 9(5).

Whitney, S. L. *et al.* (2011). *Clinical measurement of sit-to-stand performance in people with balance disorders: validity of data for the Five-Times-Sit-To-Stand test.* Physical Therapy. 85(10): 1034-1045.

Wolf, A. *et al.* (1985). *Determining Lyapunov exponents from a time series.* Physica D: Nonlinear Phenomena. 16(3): 285-317.

Woo, J. *et al.* (2007). *A randomised controlled trial of Tai Chi and resistance exercise on bone health, muscle strength and balance in community-living elderly people.* Age and Aging. 36: 262-268.

Zhang, S. *et al.* (2012). *Physical activity classification using the GENEA wrist-worn accelerometer.* Ph.D dissertation, Lippincott Williams and Wilking.

Yang, S. *et al.* (2012). *Inertial sensor-based methods in walking speed estimation: A systematic review.* Sensors. 12: 6102-6116.

Yogev, G. *et al.* (2007). *Gait asymmetry in patients with Parkinson's disease and elderly fallers: when does the bilateral coordination of gait require attention.* Experimental Brain Research. 177: 336-346.

Zecevic, A. A. *et al.* (2006). *Defining a fall and reasons for falling: Comparison among the view of seniors, health care providers, and the research literature.* The Gerontologist. 46: 367-376.

Zhu, M. *et al.* (2001). *Feature extraction and dimension reduction with applications to classification and the analysis of co-occurrence data.* Ph.D dissertation, Dept. of Statistic, Stanford University, Stanford, CA, USA.

Zijlstra, A. *et al.* (2012). *Sit-stand and stand-sit transitions in older adults and patients with Parkinson's disease: event detection based on motion sensors versus force plates.* Journal of NeuroEngineering and Rehabilitation. 9: 75-84.

Supervised student research

Blaser Leonie (2016). *Aktigraphische Messung von Schlafqualität – Herleitung eines Studiendesigns zur Erhebung von Daten für die Entwicklung komplexer Algorithmen.* Bachelor Thesis, ID-244309. Medical Engineering, Faculty for Mechanical and Medical Engineering, Furtwangen University.

Föll Roman (2015). *Kernel perceptron für Distanzdaten.* Bachelor Thesis, ID-2424846. Institute for Applied Analysis und Numerical Simulation, University of Stuttgart.

Groß Caroline Elma Katharina (2016). *Situationsabhängige Sturzrisikobewertung mittels am Handgelenk angebrachter Inertialsensorik.* Master Thesis, ID-633576. Department of Medical Engineering and Biotechnology, Ernst-Abbe Jena University.

Publications

Pozaic T., Lindemann U., Grebe A.K., Stork W. (2016). *Sit-to-stand transition reveals acute fall risk in activities of daily living.* IEEE Journal of Translational Engineering in Healthcare and Medicine. 4: 1-11.

Pozaic T., Föll R., Grebe A.K., Stork W. (2016). *Wrist reveals the fall risk in activities of daily living.* 20th International Congress of Parkinson's Disease and Movement Disorders. 19-23rd June 2016, Berlin, Germany.

Pozaic T., Haeberlen N. (2016). *Method for precise clock synchronization of physically distant sensor nodes.* Patent Application. Official reference: 102016203338.7. Germany.

Pozaic T., Grebe A. K. (2016). *Method for sit-to-stand transition detection based on acceleration and light sensor.* Patent Application. Official reference: 102016203325.5. Germany.

Pozaic T., Grebe A.K., Lindemann U., Stork W. (2015). *Inter-limb coordination assessment and fall risk in ADL.* IEEE International Conference on Biomedical and Health Informatics. 8-10th Octobert, Haikou, China.

Pozaic T. (2015). *Method for assessment of upper limb weakness.* State-of-the-art. 10-14th August 2015. Feuerbach, Germany.

Pozaic T., Grebe A.K., Lindemann U., Klenk J., Stork W. (2015). *Sit-to-stand transition time estimation based on wrist and waist accelerometer sensor.* ISPGR World Congress. 28th June - 02nd July 2015, Sevilla, Spain.

Hayn H., Grebe A.K., Pozaic T., Wegend C. (2014). *Validation and verification of a medical activity monitor.* 5th Bosch Conference on Systems and Software Engineering. 12-15th Mai 2014, Ludwigsburg, Germany.